

**Ahr1-dependent regulation of *ECE1* and other core filamentation
response genes in *Candida albicans***

**Dissertation
zur Erlangung des akademischen Grades
„doctor rerum naturalium“ (Dr. rer. nat.)**

**vorgelegt dem Rat der Fakultät für Biowissenschaften
der Friedrich-Schiller-Universität Jena**

**von Master of Science
Sophia Irma Ruben
geboren am 10.04.1989 in Berlin**

Jena, April 2020



FRIEDRICH-SCHILLER-
UNIVERSITÄT
JENA

The following work was conducted at the Centre for Innovation Competence (ZIK) Septomics and the Leibniz Institute for Natural Product Research and Infection Biology - Hans Knöll Institute in the group Fungal Septomics under the supervision of Prof. Dr. med. Oliver Kurzai and Prof. Dr. Bernhard Hube.



The PhD project was supported by a scholarship from the International Leibniz Research School for Microbial and Biomolecular Interactions (ILRS).

Reviewers:

1. Prof. Dr. Oliver Kurzai
Research Group Fungal Septomics, Leibniz Institute for Natural Product Research and Infection Biology—Hans Knoell Institute, Jena, Germany
Institute for Molecular Infection Biology and Institute for Hygiene and Microbiology, University of Würzburg, Würzburg, Germany
2. Prof. Dr. Bernhard Hube
Department Microbial Pathogenicity Mechanisms, Leibniz Institute for Natural Product Research and Infection Biology—Hans Knoell Institute and Institute of Microbiology, Friedrich Schiller University, Jena, Germany
3. Prof. Dr. Julian Naglik
Mucosal and Salivary Biology Division, Dental Institute and Centre for Host-Microbiome Interactions, Faculty of Dentistry, Oral & Craniofacial Sciences, King's College London, London, United Kingdom

Date of public defense: 16th of December 2020

Content

I.	List of abbreviations	IV
II.	List of figures	VII
III.	List of tables	IX
IV.	Zusammenfassung	X
V.	Summary	XI
1.	Introduction	1
1.1.	<i>Candida</i> species as causative agents of fungal infections	1
1.2.	The human fungal pathogen <i>Candida albicans</i>	2
1.2.1.	The polymorphism of <i>C. albicans</i> and virulence	3
1.2.1.1.	Regulation of hyphal development in <i>C. albicans</i>	4
1.2.1.2.	Core filamentation response genes of <i>C. albicans</i>	7
1.2.2.	Filament-associated virulence factors of <i>C. albicans</i>	8
1.2.2.1.	Adhesion and biofilm formation	8
1.2.2.2.	Agglutinin-like sequence 3 - Als3	8
1.2.2.3.	Secreted aspartyl proteinases - Saps	9
1.2.2.4.	Superoxide dismutases - Sods	10
1.2.2.5.	Candidalysin	10
1.3.	Aim of this study	13
2.	Material and Methods	14
2.1.	Strains	14
2.2.	Plasmids	17
2.3.	Primers	18
2.4.	Strain maintenance and growth conditions	19
2.5.	Plasmid creation	20
2.6.	<i>E. coli</i> transformation and plasmid extraction	20
2.7.	<i>C. albicans</i> transformation	20
2.8.	Ribonucleic acid extraction	21
2.9.	Reverse transcriptase quantitative polymerase chain reaction	22
2.10.	Als3 staining	23
2.11.	Microscopy	23
2.12.	Measurement of secreted Candidalysin	24
2.13.	Lactate dehydrogenase (LDH) assay	24
2.14.	Invasion assay	25
2.15.	Chromatin Immuno Precipitation DNA Sequencing (ChIP-Seq)	25
3.	Results	27
3.1.	Ahr1 is a regulator of <i>ECE1</i> expression	27
3.1.1.	Identification of possible activators of <i>ECE1</i> expression	27
3.1.2.	Screen of activator mutants reveals that Ahr1 is necessary for high-level <i>ECE1</i> expression in hyphal morphology	27
3.2.	Ahr1 is important for Candidalysin secretion	29
3.3.	Hyperactive Ahr1 induces high-level <i>ECE1</i> expression	30

3.3.1.	Hyperactive Ahr1 induces <i>ECE1</i> expression in wild type and independent of Cph1 and Efg1 under yeast growth conditions	30
3.3.2.	Hyperactive Ahr1 increases Candidalysin secretion	31
3.3.3.	Hyperactive Ahr1 only leads to slight increase of cytotoxicity of the <i>ahr1</i> Δ and the <i>cph1</i> Δ / <i>efg1</i> Δ mutants	32
3.3.4.	Mutants lacking <i>AHR1</i> or <i>CPH1</i> and <i>EFG1</i> can still invade epithelial cells	33
3.3.5.	Hyperactive Ahr1 induces <i>ECE1</i> expression independent of Ume6, Tec1, Ndt80 and Brg1	34
3.3.6.	Hyperactive Ahr1 has no effect on <i>ECE1</i> expression in the <i>tup1</i> Δ mutant	36
3.4.	Ahr1 activates expression of core filamentation response genes	37
3.4.1.	Ahr1 is important for the expression of other core filamentation response genes in hyphae	37
3.4.2.	Hyperactive Ahr1 is able to induce the expression of other core filamentation response genes independent of Cph1 and Efg1	38
3.4.3.	Hyperactive Ahr1 relies on Tup1 for the induction of high-level <i>ALS3</i> expression	40
3.4.4.	Hyperactive Ahr1 induces Als3 localization on cell surface independent of Cph1 and Efg1	40
3.5.	ChIP-Seq analyses of hyperactive Ahr1	42
3.5.1.	Hyperactive Ahr1 binds upstream of <i>ECE1</i> , <i>ALS3</i> and other core filamentation response genes	42
3.5.2.	Hyperactive Ahr1 binds upstream of and activates the expression of hyphal regulators	43
3.5.3.	The hyperactive Ahr1 binds upstream of genes encoding for other cell wall proteins, hyphal regulators and virulence factors	47
3.5.4.	The binding motif of the hyperactive Ahr1	48
3.6.	The role of Mcm1 in the expression of <i>ECE1</i> and other core filamentation response genes	49
3.6.1.	<i>MCM1</i> overexpression induces expression of <i>ECE1</i> in a partly Ahr1-dependent manner	49
3.6.2.	The induction of <i>ECE1</i> expression via <i>MCM1</i> overexpression relies on Tup1 and partly on Cph1 and Efg1	51
3.6.3.	<i>MCM1</i> overexpression induces the expression of other CFR genes	52
3.6.4.	<i>MCM1</i> overexpression induces Als3 localization on cell surface	54
3.7.	The influence of a mutated <i>SSN3</i> allele on the expression of <i>ECE1</i> , <i>ALS3</i> and other CFR genes	55
3.7.1.	Mutated <i>SSN3</i> allele induces <i>ECE1</i> expression	55
3.7.2.	Mutated <i>SSN3</i> allele induces <i>ALS3</i> expression and Als3 localization on cell surfaces	57
3.7.3.	Mutated <i>SSN3</i> allele induces the expression of other CFR genes	58

3.7.4. Deletion of <i>SSN3</i> induces expression of <i>ECE1</i> and <i>ALS3</i> and other CFR genes	60
4. Discussion	63
4.1. The transcription factor Ahr1 is required for high-level expression of <i>ECE1</i> and Candidalysin secretion	63
4.2. A hyperactive Ahr1 induces high-level <i>ECE1</i> expression independent of Cph1 and Efg1	64
4.3. A hyperactive Ahr1 binds upstream of <i>ECE1</i> , <i>ALS3</i> and other core filamen- tation response genes and activates their expression	65
4.4. A hyperactive Ahr1 regulates other important transcriptional regulators . .	66
4.5. A mutated <i>SSN3</i> allele induces <i>ECE1</i> and <i>ALS3</i> expression independent of Ahr1 and Tup1	68
4.6. <i>MCM1</i> overexpression induces the expression of <i>ECE1</i> and <i>ALS3</i> in partly Ahr1-dependent manner	69
4.7. High-level expression of <i>ECE1</i> and <i>ALS3</i> relies on Tup1	69
4.8. Model for Ahr1-dependent transcription of <i>ECE1</i> and <i>ALS3</i> in <i>C. albicans</i> hyphae	69
VI. Literature	XII
VII. Appendix	XXVII
VIII. List of publications	XXXVII
IX. Acknowledgment	XXXIX
X. Ehrenwörtliche Erklärung	XLI

I. List of abbreviations

Abbreviation	Meaning
µl	micro liter
µM	micro molar
A	adenine
AIDS	acquired immune deficiency syndrome
a. M.	am Main
AMP	adenosine monophosphate
amp	ampicillin
ATP	adenosine triphosphate
bp	base pair(s)
C	cytosine
<i>C.</i>	<i>Candida</i>
cAMP	cyclic adenosine monophosphate
CDK	cyclin-dependent kinase
cf.	confer
CFR	core filamentation response
CO ₂	carbon dioxide
DAPI	4',6-diamidino-2-phenylindole
DIC	differential interference contrast
DNA	desoxyribonucleic acid
EDTA	ethylenediaminetetraacetic acid
e. g.	exempli gratia
FBS	fetal bovine serum
Fig.	Figure
FRET	Förster resonance energy transfer
G	guanine
GAD	Gal4 activator domain
GDP	guanosine diphosphate
GFP	green fluorescing protein
GlcNac	N-acetylglucosamine
GPI	glycosylphosphatidylinositol
GTP	guanosine triphosphate
h	hour
H ₂ O	dihydrogen monoxide, water
HCL	hydrochloric acid
HKI	Hans-Knöll-Institute
HS	human serum
IGB	Integrated Genome Browser
IgG	immunoglobulin G
K	lysine
l	liter(s)
LB	lysogeny broth
LC	liquid chromatography
LDH	lactate dehydrogenase
LiAc	lithium acetate
<i>MCM1</i> ^{OE}	<i>MCM1</i> overexpression

Abbreviation	Meaning
MAM	Molecular and Applied Microbiology
MAPK	mitogen-activated protein kinase
mg	milli gram(s)
min	minute(s)
MKP1	MAPK phosphatase 1
MOPSO	2-hydroxy-3-morpholinopropanesulfonic acid
MPM	Microbial Pathogenicity Mechanisms
mRNA	messenger RNA
ms	milli second(s)
MS	mass spectrometry
NEB	New England Biolabs
ng	nano gram(s)
nm	nano meter(s)
NTC	nourseothricin
OD ₆₀₀	absorbance measured at 600 nm wavelength
ORF	open reading frame
PBS	phosphate buffered saline
PCR	polymerase chain reaction
PEG	polyethylene glycol
PKA	proteinkinase A
PSM	peptide spectrum matches
RT-qPCR	reverse transcriptase quantitative polymerase chain reaction
R	arginine
ref. no.	reference number
resp.	respectively
RNA	ribonucleic acid
ROS	reactive oxygen species
rpm	rounds per minute
RPMI	Roswell Park Memorial Institute
RT	room temperature
Saps	secreted aspartyl proteinases
SDG	synthetically defined glucose
SDN	synthetically defined N-acetylglucosamine
Sec.	Section
<i>SSN3_m</i>	mutated <i>SSN3</i> gene
SNP	single nucleotide polymorphism
SOD	superoxide dismutase
spp.	species
Str.	strand
T	thymine
Tab.	Table
TE	Tris-EDTA
USA	United States of America
v/v	volume in volume
w/o	without
w/v	weight in volume
x g	times earth's gravitational force

I. List of abbreviations

Abbreviation	Meaning
YNB	yeast nitrogen broth
YNBS	YNB medium with sucrose
YPD	yeast extract peptone dextrose
VVC	vulvovaginal candidiasis

II. List of figures

1.	Regulation of hyphal development in <i>C. albicans</i>	5
2.	Schematic display of putative transcription factor binding sites in the 5' intergenic region of <i>ECE1</i>	27
3.	The transcription factor Ahr1 is important for <i>ECE1</i> expression in <i>Candida albicans</i> hyphae	28
4.	Ahr1 is important for Candidalysin secretion of <i>C. albicans</i>	29
5.	Hyperactive Ahr1 induces <i>ECE1</i> expression under yeast growth conditions and independent of Cph1 and Efg1	30
6.	Hyperactive Ahr1 increases Candidalysin secretion under hyphal-growth conditions in <i>C. albicans</i>	32
7.	Cytotoxicity of the wild type and the <i>ahr1</i> Δ and <i>cph1</i> Δ / <i>efg1</i> Δ mutants with and without hyperactive Ahr1	33
8.	Invasion capacities are not inhibited in the <i>ahr1</i> Δ and the <i>cph1</i> Δ / <i>efg1</i> Δ mutants	34
9.	Hyperactive Ahr1 induces <i>ECE1</i> expression independent of Ume6, Tec1, Ndt80 and Brg1	35
10.	Hyperactive Ahr1 depends on Tup1 for induction of high-level <i>ECE1</i> expression	37
11.	Ahr1 is important for the expression of core filamentation response genes in <i>C. albicans</i> hyphae	38
12.	Hyperactive Ahr1 induces expression of <i>ALS3</i> , <i>HWP1</i> and <i>IHD1</i>	39
13.	Hyperactive Ahr1 depends on Tup1 for induction of high-level <i>ALS3</i> expression	40
14.	Hyperactive Ahr1 induces Als3 localization on cell surface independent of Cph1 and Efg1	41
15.	Hyperactive Ahr1 binds to 5' intergenic regions of <i>ECE1</i> and <i>ALS3</i>	42
16.	Hyperactive Ahr1 binds to 5' intergenic regions of <i>HWP1</i> , <i>IHD1</i> , <i>HGT2</i> , <i>RBT1</i> and <i>DCK1</i> but not orf19.2457	43
17.	Hyperactive Ahr1 regulates <i>AHR1</i> , <i>BCR1</i> , <i>BRG1</i> and <i>EED1</i> expression	44
18.	Hyperactive Ahr1 regulates <i>EFG1</i> , <i>HGC1</i> , <i>SFL2</i> but not <i>NDT80</i> expression	45
19.	Hyperactive Ahr1 regulates <i>TCC1</i> , <i>TEC1</i> and <i>UME6</i> expression	46
20.	Binding site motif of hyperactive Ahr1 identified using MEME-ChIP	48
21.	Identified binding motifs coincide with local peak summits in 5' intergenic region of <i>ECE1</i>	49
22.	<i>MCM1</i> overexpression induces <i>ECE1</i> expression in partly Ahr1-dependent manner	50
23.	Induction of <i>ECE1</i> expression via <i>MCM1</i> overexpression (<i>MCM1</i> ^{OE}) relies on Tup1 and partly on Cph1 and Efg1	51
24.	<i>MCM1</i> overexpression induces the expression of some CFR genes but oftentimes depends on Ahr1, Tup1 or Cph1/Efg1	53
25.	<i>MCM1</i> overexpression induces Als3 localization on cell surface	54
26.	Mutated <i>SSN3</i> allele (<i>SSN3_m</i>) induces <i>ECE1</i> expression in the wild type and the <i>ahr1</i> Δ , the <i>tup1</i> Δ and the <i>cph1</i> Δ / <i>efg1</i> Δ mutants	56
27.	Mutated <i>SSN3</i> allele (<i>SSN3_m</i>) induces <i>ALS3</i> expression and Als3 localization on cell surface	58

II. List of figures

28. Mutated <i>SSN3</i> allele (<i>SSN3_m</i>) influences the expression of CFR genes	59
29. Deletion of <i>SSN3</i> induces expression of <i>ECE1</i> and <i>ALS3</i> and Als3 localisation on filament surface	61
30. Deletion of <i>SSN3</i> induces expression of <i>HWP1</i> and <i>IHD1</i>	62
31. Model for the regulation of <i>ECE1</i> and <i>ALS3</i> in <i>C. albicans</i> ' hyphae	70
32. Deletion of <i>SSN3</i> induces the expression of <i>ECE1</i> in SDG medium at 37°C . . .	XXXIV

III. List of tables

1.	<i>C. albicans</i> strains used in this study	14
2.	<i>E. coli</i> strains and plasmids used in this study	17
3.	Primers used for RT-qPCR analyses	18
4.	Primers used for plasmid generation	19
5.	Primers used for verification of <i>C. albicans</i> transformants	19
6.	Possible transcription factor binding sites upstream of the <i>ECE1</i> ORF	XXVII
7.	Secretion of Candidalysin	XXIX
8.	Identified binding motifs of hyperactive Ahr1 on intergenic regions of sought out genes	XXX

IV. Zusammenfassung

Candida albicans ist ein normalerweise harmloser, kommensaler Pilz und Teil des humanen Mikrobioms, wo er auf der Haut und den Schleimhäuten des Darms und der Mundhöhle gefunden werden kann. In immungeschwächten Patienten kann *C. albicans* jedoch Krankheiten mit unterschiedlichen Schweregraden auslösen. Diese erstrecken sich von oberflächlichen Infektionen des Oropharynx oder der Vagina zu lebensbedrohlichen systemischen Blutstrominfektionen. Weltweit gehört *C. albicans* zu den häufigsten Erregern von nosokomialen Pilzinfektionen. Eine seiner wichtigsten Virulenzfaktoren ist die Fähigkeit, in Abhängigkeit von der umgebenden Nische, reversibel von Hefen- zu Hyphenwachstum überzugehen. Die Hochregulierung sogenannter hyphenspezifischer Gene ist eng mit diesem morphologischen Übergang verbunden. Dieser Gruppe gehören einige virulenzassoziierte Gene, wie *ALS3* und *ECE1*, an. Das letztere ist eines der am höchsten exprimierten Gene in Hyphen und kodiert ein Vorgängerprotein des Peptidtoxins Candidalysin. Während der Invasion der Wirtszellen durch den Pilz wird Candidalysin von den Hyphen in Invasionstaschen sekretiert, wo es die Zytolyse von Wirtszellen vermittelt. Aufgrund der Bedeutung für die Virulenz des Pilzes hat die Erforschung der Regulation von *ECE1* einen großen Wert und trägt zum Verständnis der Pathogenitätsmechanismen von *C. albicans* bei.

Während der Untersuchung von Deletionsmutanten von Transkriptionsfaktoren wurde festgestellt, dass Ahr1 wichtig für die hohe Expression von *ECE1* ist. Eine Mutante, der dieser Transkriptionsregulator fehlt, zeigte eine mittelgradige *ECE1* Transkription, niedrige Candidalysinsekretion und eine abgeschwächte Virulenz in einem oralen Epithelzellmodell. Im Gegensatz dazu induzierte ein hyperaktives Ahr1 eine hohe Expression von *ECE1* sogar unter Hefenbedingungen und umging die Abwesenheit zahlreicher Transkriptionsfaktoren einschließlich Brg1, Efg1 und Ume6. Ein ähnliches Regulationsmuster konnte für das hyphenspezifische *ALS3* Gen beobachtet werden, welches für ein wichtiges Adhesin und Invasin kodiert. Chromatinimmunoprecipitation DNA Sequenzierung bewies, dass ein hyperaktives Ahr1 stromaufwärt von *ECE1*, *ALS3* und anderen hyphenspezifischen Genen bindet. Es wurde auch an den Promotoren von zahlreichen Regulatorgenen, inklusive *BRG1* und *UME6* gefunden. Diese Bindung ging mit der Hochregulierung dieser Transkriptionsfaktorgene einher. *MCM1* kodiert einen essentiellen Transkriptionsfaktor und Bindepartner von Ahr1. In einem teils Ahr1-abhängigem Prozess sorgte die Überexpression von *MCM1* für die Hochregulierung der *ECE1* und *ALS3* Expression. Interessanterweise zeigt diese Studie, dass Tup1, normalerweise ein globaler Repressor der Hyphenentwicklung und der assoziierten Genexpression, benötigt wird für den nützlichen Effekt des hyperaktiven *AHR1* Allels und der *MCM1* Überexpression. Dies deutet darauf hin, dass Tup1 nicht nur als Repressor arbeitet sondern auch für die hohe Expression von *ECE1* und *ALS3*, welche über Ahr1 und Mcm1 vermittelt wird, erforderlich ist. Zusätzlich wurde entdeckt, dass eine Punktmutation eines Allels des *SSN3* Gens, welches eine cyclin-abhängige Kinase kodiert, die Expression dieser beiden Gene unabhängig von Ahr1, Tup1, Efg1 und Cph1 aktivieren kann. Zusammenfassend betrachtet identifizierte diese Studie neue Mitwirkende im komplexen Regulatornetzwerk, welches die Transkription von virulenzassoziierten Genen in den unterschiedlichen Morphologien von *C. albicans* kontrolliert und betont die Rolle von Ahr1 und Tup1 in diesem Netzwerk.

V. Summary

Candida albicans is a normally harmless commensal fungus and part of the human microbiota where it can be found on the skin and mucosal surfaces of the gut and the oral cavity. However, in immunocompromised patients, *C. albicans* can cause diseases of different severity. These can range from superficial infections of the oropharynx or the vagina to life threatening systemic bloodstream infections. *C. albicans* is one of the most common causes for nosocomial fungal infections worldwide. A major virulence trait is its ability to undergo reversible yeast-to-hyphae transition depending on the environmental niche. The up regulation of so called hyphae-specific genes is tightly linked to this morphological transition. This group of genes includes several virulence-associated ones, like *ALS3* and *ECE1*. The latter is one of the most highly expressed genes in hyphae and encodes for a precursor protein of the peptide toxin Candidalysin. During fungal invasion of host cells, Candidalysin is secreted into invasion pockets by the hyphae where it mediates host cell cytolysis. Due to its importance for the virulence of the fungus, research on the regulation of *ECE1* is of great value and contributes to the understanding the pathogenicity mechanisms of *C. albicans*.

During a screen of transcription factor deletion mutants, Ahr1 was identified to be important for the high-level expression of *ECE1* in *C. albicans* hyphae. A mutant lacking this transcriptional regulator is characterized by intermediate *ECE1* transcription, low secretion of Candidalysin and attenuated virulence in an oral epithelial cell infection model. In contrast, a hyperactive *AHR1* allele induces high levels of *ECE1* expression even under yeast growth conditions. Furthermore, it can bypass the absence of several transcription factors, including Brg1, Efg1 and Ume6. A similar regulatory pattern could be observed for the hypha-specific *ALS3* gene, which encodes for an important adhesin and invasin. Chromatin immunoprecipitation DNA sequencing proved that a hyperactive Ahr1 binds upstream of *ECE1*, *ALS3*, and other hyphae-associated genes. It was also found on the promoters of several regulatory genes including *BRG1* and *UME6* and this binding correlated with an upregulation of these transcription factor genes. In a partially Ahr1-dependent process, overexpression of *MCM1*, which encodes an essential transcription factor and binding partner of Ahr1, led to the upregulation of *ECE1* and *ALS3*. Interestingly, it was found in this study that Tup1, which is normally a global repressor of hyphal development and associated gene expression, is required for the beneficial effects of the hyperactive *AHR1* allele as well as of *MCM1* overexpression. This indicates that Tup1 does not only work as a repressor but is also required for high-level expression of *ECE1* and *ALS3* mediated by Ahr1 and Mcm1. In addition, it was also found that a point-mutated allele of the *SSN3* gene, which encodes a cyclin-dependent kinase, could activate expression of the two genes without involvement of Ahr1, Tup1, Efg1 and Cph1. Overall, this study identifies novel contributors to the complex regulatory network which controls the transcription of virulence-associated genes in the different morphologies of *C. albicans* and underlines the central role of Ahr1 and Tup1 within this network.

1. Introduction

1.1. *Candida* species as causative agents of fungal infections

Species from the genus *Candida* are the world's second most common cause for invasive fungal infections (Brown *et al.*, 2012). According to estimates, 400,000 of these infections are inflicted by *Candida* species (spp.) each year with a mortality rate of 46-75% (Brown *et al.*, 2012). This is only exceeded by *Cryptococcus* spp., which account for approx. 1,000,000 infections worldwide. In Germany *Candida* spp. are the most prevalent cause of invasive and non-invasive fungal infections (Ruhnke *et al.*, 2015). In a nationwide surveillance study in the United States of America (USA), it was found that *Candida* spp. were the most commonly isolated fungi from nosocomial bloodstream infections (Wisplinghoff *et al.*, 2004). While coagulase-negative staphylococci, *Staphylococcus* spp. and *Enterococcus* spp. amounted to roughly 60% of bloodstream infections, *Candida* spp. were responsible for 9% of the cases (Wisplinghoff *et al.*, 2004). Similar numbers were reported from German intensive care units, where 6.5% of primary nosocomial laboratory-confirmed bloodstream infections were caused by *Candida* spp. (Meyer *et al.*, 2013).

There are approximately 200 *Candida* spp. but only few of them are known colonizers of the human body. Furthermore, only 16 species have already been isolated from infected patients (Pfaller and Diekema, 2007; Polke *et al.*, 2015; Yapar, 2014). From these, *C. albicans*, *C. glabrata*, *C. parapsilosis*, *C. tropicalis* and *C. krusei* were identified as pathogens in more than 90% of cases (Pfaller and Diekema, 2010, 2007; Yapar, 2014). Additionally, the new species *C. auris* has been described for the first time in 2009 (Sato *et al.*, 2009). In contrast to the other pathogenic *Candida* spp., *C. auris* is able to readily spread in health-care facilities from human to human and through other surfaces, causing nosocomial outbreaks. A review from Rhodes and Fisher (2019) summarizes the current knowledge on *C. auris*.

As already mentioned, several *Candida* spp. are able to colonize healthy individuals. They usually reside as benign members of human microbiota on the mucosa and skin without causing any disease symptoms. However, under certain conditions they are also able to cause infections in their hosts. Three groups of people are especially vulnerable to infections by *Candida* spp., called candidiasis. First of all, immunocompromised individuals for example, people in the extremes of age, organ transplant recipients receiving immunosuppressive therapy, patients with the acquired immunodeficiency syndrome (AIDS) or cancer patients receiving chemotherapy can develop candidiasis (Pfaller and Diekema, 2007; Arendrup, 2010; Viscoli *et al.*, 1999). Second of all, individuals with a disequilibrium of the host microbiome (e. g. through the use of antibiotics) are prone to opportunistic *Candida* infections (Pfaller and Diekema, 2007; Vincent *et al.*, 2009; Perlroth *et al.*, 2007). Thirdly, patients where disruption of mucosal and cutaneous barriers took place (e. g. through burn wounds, surgery or central venous catheters) can develop candidiasis (Moore *et al.*, 2010; Lortholary *et al.*, 2014; Ahlquist Cleveland *et al.*, 2015). In these cohorts, colonizing *Candida* can potentially proliferate on mucosal surfaces, invade tissues and possibly further disseminate via the bloodstream from where they can reach and infect other organs.

Candida infections range from superficial infections of the mucosa, such as vulvovaginal or oro-

pharyngeal candidiasis, to life-threatening systemic infections, like disseminated candidiasis and candidemia (infection of the bloodstream with *Candida*). Oral or esophageal candidiasis, also called thrush, is especially common in AIDS (Fidel, 2011) and cancer patients (Lalla *et al.*, 2010). Oral candidiasis is also associated with the use of dentures (Salerno *et al.*, 2011). At least 75% of all women will have one or more episodes of vulvovaginal candidiasis (VVC) in their life (Sobel, 1997). Five to eight percent of them are suffering from idiopathic recurrent infections (Sobel, 1997).

In immunocompromised people *Candida* species are able to reach the bloodstream through mucosal surfaces (e. g. in the colon) or via central venous catheters. In a population based study in the USA, 85% of 3,848 candidemia patients had a central venous catheter (Ahlquist Cleveland *et al.*, 2015). From the bloodstream the fungus can spread through the whole body, infecting virtually all organs leading to invasive candidiasis and even sepsis.

Over the recent decades, an increase in candidemia was visible in different parts of the world (Arendrup, 2010). A study, only focusing on patients in intensive care units in Germany, did not come to the same conclusion (Meyer *et al.*, 2013). Through advances in medical possibilities, more aggressive surgery and transplantations, the use of broad spectrum antibiotics and an increased survival of patients with severe illnesses, the amount of susceptible patients, especially in the nosocomial setting, has increased (Arendrup, 2010; Perlroth *et al.*, 2007). Due to this, it is not surprising that risk factors for the development of invasive candidiasis include long-term stays in intensive care units, central venous catheters and different kinds of abdominal surgery and organ transplantation (Kullberg and Arendrup, 2016; Ahlquist Cleveland *et al.*, 2015; Arendrup, 2010).

Additionally, several pathogenic *Candida* spp. have developed intrinsic resistances against the common antimycotics used for the treatment of candidiasis (Arendrup, 2010). Only three known classes of antimycotics are readily used for combating systemic *Candida* infections. First line treatment of invasive candidiasis includes Echinocandins, which inhibit 1,3- β glucan synthase and thus disrupt the cell wall composition (Denning, 2002). Azoles (e. g. Fluconazole, Itracozazole, Voriconazole and Posaconazole) fight *Candida* infections by inhibiting lanosterol 14 α -demethylase in the ergosterol pathway, thus negatively influencing membrane synthesis of the fungus (Maertens, 2004). Amphotericin B is a polyene that binds to ergosterol in the fungal cell wall, which results in pore formation and subsequent ion leakage and death (Lemke *et al.*, 2005; Gray *et al.*, 2012).

1.2. The human fungal pathogen *Candida albicans*

C. albicans is a colonizer of mucosa of the gastrointestinal tract, the genitalia, the lower respiratory tract, the oropharynx and the skin of 30-70% of healthy individuals (Polke *et al.*, 2015; Arendrup, 2010). It is the causative agent of 50-70% of invasive candidiasis (Arendrup, 2010; Perlroth *et al.*, 2007), which makes it the most clinically important *Candida* species. However, over the last decades the incidence of *C. albicans* infections has slightly decreased, while other, non-*albicans* species' prevalences have increased, e. g. *C. glabrata* and *C. parapsilosis* or *C. tropicalis* (Pfaller and Diekema, 2007; Yapar, 2014; Playford *et al.*, 2010). Additionally, there are

regional differences in species distribution. While in North America, *C. glabrata* is the second most common cause of invasive candidiasis, *C. parapsilosis* is the second most common cause in Latin America (Yapar, 2014). Mice experiments from 2002 compared the virulence of the most common pathogenic *Candida* spp. (Arendrup *et al.*, 2002). *C. albicans* and *C. tropicalis* were identified as the most virulent *Candida* species followed by *C. glabrata*, *C. lusitaniae* and *C. kefyr*. In these experiments, *C. parapsilosis*, *C. krusei* and *C. guilliermondii* were the least virulent of the species tested (Arendrup *et al.*, 2002).

1.2.1. The polymorphism of *C. albicans* and virulence

During its long coevolution with the human host, *C. albicans* gained the ability to quickly adapt to changing environments and stresses. This great repertoire of adaptation skills includes its ability to readily switch between yeast, pseudohyphal and hyphal growth form depending on the external conditions. *C. albicans*' unicellular budding yeast cells have a round to oval shape with a diameter between 5-10 μm (Erwig and Gow, 2016). After budding, mother and daughter cell readily separate from each other. True hyphae build long, tube-like, highly polarized filaments with parallel sides (Sudbery, 2011). Pseudohyphae are chains of elongated cells that adhere to each other. They can be differentiated from true hyphae, since they are wider and have constrictions at septation sites (Sudbery, 2011). While true hyphae are said to be the invasive form of the fungus, for a long time yeast cells were thought to be the commensal and noninvasive form (Jacobsen *et al.*, 2012; Berman and Sudbery, 2002). However, during invasive infections not only hyphae but also yeast cells can be found (Odds, 1988). The ability to reversibly switch between yeast and hyphal growth form is believed to be the major virulence trait of *C. albicans*. During infection, yeast cells are deemed to support dissemination via the bloodstream (Berman and Sudbery, 2002) whereas hyphae are reckoned to play a crucial role in tissue invasion (Saville *et al.*, 2003; Jacobsen *et al.*, 2012). This idea is backed by studies which showed that yeast-locked (Lo *et al.*, 1997; Zheng *et al.*, 2004) or hyphae-locked mutants (Braun *et al.*, 2000) were avirulent. A mutant lacking *TUP1*, a known repressor of hyphal growth, only grows as filaments and is avirulent in mouse models for systemic infections (Braun *et al.*, 2000; Cleary *et al.*, 2016). It was already shown that the yeast-locked *cph1* Δ /*efg1* Δ mutant is avirulent in a mouse tail vein model and unable to escape from macrophages by forming hyphae (Lo *et al.*, 1997), which is a known mechanism of *C. albicans* to evade immune cells (Lorenz *et al.*, 2004). However, this mutant lacks two major transcription factors which are known activators of hyphal growth and influence not only morphology but also cell wall composition, adhesion and other virulence associated traits of the fungus. Another research focusing on the virulence of non-filamentous mutants was conducted by Zheng *et al.* (2004). They focused on the gene *HGC1* which encodes for a G1 cyclin-related protein and whose expression is induced in *C. albicans* hyphae. Deletion of *HGC1* led to a mutant unable to form hyphae under standard laboratory conditions and within mice kidneys. In the *hgc1* Δ mutant, the expression of other hypha-specific genes, such as *HWP1*, *HYR1* and *ECE1* was not impaired, making the *hgc1* Δ mutant a better candidate to research the necessity of dimorphism for virulence than the *cph1* Δ /*efg1* Δ mutant. Since the *hgc1* Δ mutant showed reduced virulence compared to a revertant in a mouse tail vein model, it supports the idea that morphological plasticity and virulence are connected in *C. albicans*.

1.2.1.1. Regulation of hyphal development in *C. albicans*

Hyphal formation of *C. albicans* is induced by environmental conditions which resemble adverse growth conditions in the human host. Among others, the presence of serum (Taschdjian *et al.*, 1960), elevated temperatures, neutral pH (Buffo *et al.*, 1984), 5% carbon dioxide (CO₂, similar to bloodstream conditions) (Mardon *et al.*, 1969; Klengel *et al.*, 2005; Bahn and Mühlischlegel, 2006), N-acetylglucosamine (GlcNAc) (Simonetti *et al.*, 1974) and the growth in an embedded matrix (Sudbery, 2011) stimulate hyphal growth. Additionally, synthetic growth medium such as Lee's medium (Lee *et al.*, 1975), Spider medium (Liu *et al.*, 1994) or mammalian tissue culture media like M199 or RPMI 1640 can be used in the laboratory to induce hyphae formation (Sudbery, 2011). One of the strongest inducers of hyphal formation is the combination of 37°C and serum, which is therefore readily used in diagnostics to discriminate *C. albicans* from other yeasts (Sudbery, 2011).

Three main signal transduction pathways have been described to induce yeast-to-hyphae transition: the mitogen-activated protein kinase (MAPK) signaling pathway, the cyclic adenosine monophosphate-dependent protein kinase A (cAMP-PKA) pathway and the pH-dependent pathway (Fig. 1).

Important transcription factors which positively influence hyphal formation and the expression of hypha-specific genes in these pathways are Efg1, Cph1, Flo8, and Rim101 (Ernst, 2000; Liu, 2001).

Through serum or low nitrogen availability, the transmembrane ammonium permease Mep2 activates both cAMP as well as MAPK signaling (Biswas and Morschhäuser, 2005). Ras1, a guanine nucleotide binding protein, acts downstream of Mep2 and is an activator of both pathways though changing from inactive GDP-bound to the active GTP-bound state (Leberer *et al.*, 2001). Furthermore, the cAMP pathway is induced indirectly via Ras1 physically interacting with Cyr1 or directly via Cyr1 (Fang and Wang, 2006; Rocha *et al.*, 2001). Cyr1 is the sole adenylyl cyclase in *C. albicans* and thus the only source of cAMP in the fungus, which it synthesises from adenosine triphosphate (ATP) (Rocha *et al.*, 2001). CO₂ and peptidoglycans in serum can directly stimulate Cyr1, which induces the cAMP production (Wang *et al.*, 2010). Intracellular levels of cAMP positively regulate yeast-to-hyphae transition (Harcus *et al.*, 2004). The phosphodiesterases Pde1 and Pde2 convert cAMP to AMP which makes them negative regulators of filamentation (Jung and Stateva, 2003). Intracellular cAMP activates the PKA complex. It consists of the two catalytic subunits Tpk1 and Tpk2 and the regulatory subunit Bcy1, which functions as an essential negative regulator of PKA complex (Bockmühl *et al.*, 2001). The PKA complex directly phosphorylates the enhanced filamentous growth protein 1 (Efg1) at T206 (Bockmühl and Ernst, 2001). Efg1 is regarded as the master regulator of hyphae formation. Alternatively, Efg1 can also be directly activated in the presence of GlcNAc by Ngt1 (Alvarez and Konopka, 2007). It is a sequence-specific deoxyribonucleic acid (DNA) binding protein and binds to the E-box (5'-CANNTG-3'), which is present in the promoters of several hypha-specific genes, such as *ALS3*, *ECE1*, *HWP1*, *HYE1* and *RBT4* (Leng *et al.*, 2001). It is activated via the cAMP pathway in response to serum, elevated CO₂ levels, neutral pH, GlcNAc and growth on solid media. Deletion of *EFG1* leads to filamentation defects under various conditions (Lo *et al.*, 1997; Stoldt *et al.*, 1997; Braun and Johnson, 2000).

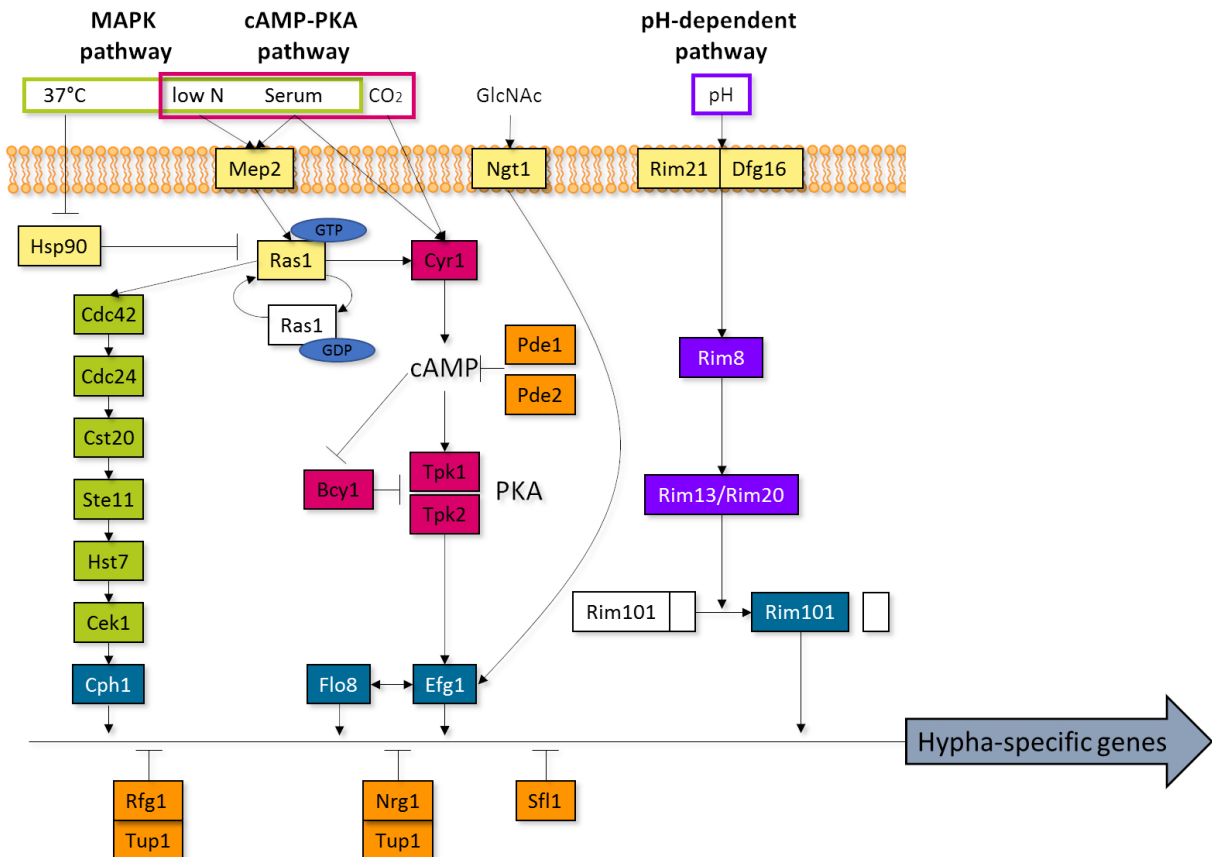


Fig. 1: Schematic display of the regulation of hyphal development via MAPK, cAMP-PKA and pH-dependent pathway in *C. albicans*.

Different environmental cues induce the MAPK (green), cAMP-PKA (pink) and pH-dependent (purple) pathways via signal transduction factors (yellow). This leads to the activation of the transcription factors Cph1, Flo8, Efg1 and Rim101 (blue) which induce the transcription of hypha-specific genes and hyphae formation. Transcriptional repressors (orange) prevent the expression of hypha-specific genes in yeast cells.

Modified from: Basso *et al.* (2019); Shapiro *et al.* (2011); Sudbery (2011); Liu (2001)

Another transcription factor which is supposed to act downstream of PKA is Flo8. It is required for filamentous growth under many conditions, interacts with Efg1 and controls a subset of Efg1-regulates genes (Du *et al.*, 2012; Cao *et al.*, 2006).

Despite the already mentioned low levels of ammonium and serum, also temperatures of 37°C and higher induce the MAPK pathway through blocking of Hsp90 (Shapiro *et al.*, 2009). As already mentioned, Ras1 also works upstream of the MAPK signaling cascade. Downstream of Ras1 lies the Rho-type guanosine triphosphatase Cdc42 and its guanine exchange factor Cdc24 (Bassilana *et al.*, 2003; Ushinsky *et al.*, 2002). Together they activate the MAPK cascade in which kinase Cst20 (p21-activated kinase (PAK)) phosphorylates Ste11 (MAPK kinase kinase (MAPKKK)) (Alonso Monge *et al.*, 2006). Ste11 in turn phosphorylates Hst7 (MAPK kinase (MAPKK)), which phosphorylates Cek1 (MAPK) (Alonso Monge *et al.*, 2006). Cek1 then activates the transcription factor Cph1, which induces the expression of hypha-specific genes (Liu *et al.*, 1994). Since Efg1 and Cph1 are the main transcription factors regulating the expression of hypha-specific genes in the cAMP and MAPK pathway, the *cph1*Δ/*efg1*Δ mutant in yeast-

locked.

C. albicans also forms hyphae under alkaline conditions. This is facilitated via the pH pathway, which is defined by the transcription factor Rim101 and corresponding upstream activators. The membrane proteins Rim21 and Dfg16 sense environmental pH (Barwell *et al.*, 2005). In alkaline condition, they activate Rim8 (Gomez-Raja and Davis, 2012). Subsequently, the C-terminal inhibitory domain of Rim101 is cleaved off by the protease complex Rim13/Rim20 (Xu and Mitchell, 2001). This activates Rim101, which in turn positively regulates the expression of hypha-specific genes (Bensen *et al.*, 2004).

Under yeast growth conditions the expression of hypha-specific genes is inhibited. The general corepressor Tup1 targets the promoters of hypha-specific genes via DNA-binding proteins such as Nrg1 and the Rox1p-like regulator of filamentous growth (Rfg1), thereby negatively regulating hyphal formation (Kadosh and Johnson, 2005). The deletion of any of these regulators (Tup1, Nrg1 or Rfg1) induces the growth as long pseudohyphae and the derepression of hypha-specific genes (Braun and Johnson, 1997; Kadosh and Johnson, 2005; Braun *et al.*, 2001; Murad *et al.*, 2001a). Constitutive overexpression of *NRG1* using a tet-promotor locked *C. albicans* in its yeast state (Saville *et al.*, 2006). Under these conditions the mutant remained in yeast state during the infection of mice and was avirulent (Saville *et al.*, 2006). Another transcription factor acting downstream of PKA is the negative regulator of hyphal growth Sfl1 (Bauer and Wendland, 2007). Furthermore, several transcription factors have already been described to play a role in hyphal formation and the expression of hypha-specific genes, which do not directly fit into the pathway system. Here, they will be described briefly.

The expression of the transcription factor *UME6* is induced upon different hypha-inducing conditions and was shown to be important for hyphal extension *in vitro* and during infection in mice (Banerjee *et al.*, 2008). Furthermore, a *ume6* Δ mutant exhibited reduced virulence in a systemic mouse model (Banerjee *et al.*, 2008). Constitutive high-level and ectopic *UME6* expression led to the induction of several filament-specific genes (*ECE1*, *HYR1*, *HWP1*, *HGC1*, *RBT1*) and a complete switch to hyphal morphology under non-inducing conditions (Zeidler *et al.*, 2008; Carlisle *et al.*, 2009). Furthermore, the virulence of this mutant was increased in a mouse model (Carlisle *et al.*, 2009). However, inoculated cells were in yeast form and only in the mouse constitutive *UME6* expression was induced. This means yeast cells had some time to disperse in the body before unanimously turning into hyphae (Carlisle *et al.*, 2009).

Ndt80 was shown to regulate cell separation, germ tube formation, hyphal growth and virulence (Yang *et al.*, 2012; Sellam *et al.*, 2010). Consequently, the *ndt80* Δ mutant was incapable of forming biofilms in a venous catheter model of infection (Nobile *et al.*, 2012) and avirulent in mouse models (Sellam *et al.*, 2010; Yang *et al.*, 2012). Furthermore, Ndt80 regulates the expression of the multidrug transporter gene *CDR1* and therefore has an influence on drug resistance of *C. albicans* (Chen *et al.*, 2004). Deletion of *NDT80* also negatively influenced the expression of the hypha-specific genes *ALS3*, *ECE1*, *HWP1* and *RBT4* (Sellam *et al.*, 2010).

The forkhead transcription factor Fkh2 was shown to be needed for wild-type like expression of core filamentation response (CFR, see Section 1.2.1.2) genes *ECE1* and *HWP1* after serum-induction (Bensen *et al.*, 2002). Knock-out of *FKH2* lead to pseudohyphal formation under yeast and hyphal growth conditions (Bensen *et al.*, 2002). Additionally, the *fkh2* Δ mutant was unable

to induce damage to human epithelial and endothelial cells *in vitro* (Bensen *et al.*, 2002).

Askew *et al.* (2011) intensively studied the adhesion and hyphal regulator 1 (Ahr1). They identified the zinc-cluster transcription factor as a cofactor of Mcm1. Furthermore, they showed that Ahr1 binds to promoters of genes encoding for adhesins (*ALS2*, *ALS4*, *HWP1*) and hyphal regulators (*EFG1* and *TEC1*) and recruits Mcm1 to these binding sites. Subsequently the Ahr1-Mcm1-complex activated the expression of these genes. Lack of *AHR1* resulted in significantly reduced adhesion on polystyrene, biofilm density and attenuated virulence in a systemic mouse model (Askew *et al.*, 2011).

Tec1, a member of the TEA/ATTS family of transcription factors, is significantly upregulated during serum-induction at 37°C (Schweizer *et al.*, 2003). Deletion of *TEC1* disabled formation of germ tubes and true hyphae through serum-induction and led to pseudohyphae formation *in vitro* (Schweizer *et al.*, 2003). Further on, Schweizer *et al.* (2003) showed that a *tec1* Δ mutant was unable to evade monocytes, which the authors connected its inability to express secreted aspartyl proteinases 4-6 (*SAP4-6*, for more information on Saps see Section 1.2.2.3). Mutants lacking *TEC1* were attenuated in a systemic mouse model but were able to form hyphae *in vivo* (Schweizer *et al.*, 2003).

Next to transcriptional regulators also other factors were already identified to have an influence on hyphal morphology. In a microevolution experiment the yeast-locked *cph1* Δ /*efg1* Δ mutant was passaged 42 times through macrophages until it regained its ability to filament and escape macrophages (Wartenberg *et al.*, 2014). Furthermore, CFR genes like *ECE1*, *ALS3* and *HWP1* as well as *EED1*, a gene encoding a regulator of hyphal extension (Zakikhany *et al.*, 2007; Martin *et al.*, 2011), were again upregulated in the evolved *cph1* Δ /*efg1* Δ mutant after serum-induction. Wartenberg *et al.* (2014) identified a heterozygous, single nucleotide polymorphism (SNP) in *SSN3* as the causative mutation for these effects. Ssn3 is a cyclin-dependent kinase, which phosphorylates important regulators such as Ume6 (Lu *et al.*, 2019).

1.2.1.2. Core filamentation response genes of *C. albicans*

As already mentioned, several different environmental cues can lead to hyphal formation and the expression of hypha-specific genes of *C. albicans*. Transcriptome analyses and network modeling showed that using three different of these well-defined stimuli (pH shift, addition of human serum and N-acetylglucosamine) only eight genes were upregulated under all conditions (Martin *et al.*, 2013). This core filamentation response (CFR) network comprises of the genes *ALS3*, *DCK1*, *ECE1*, *HGT2*, *IHD1*, *HWP1*, *RBT1* and orf19.2457. Most of the CFR genes encode proteins associated with the cell wall or the cell membrane (Martin *et al.*, 2013). Promoters of hypha-specific genes are unusually long compared to other genes (Argimón *et al.*, 2007). Argimón *et al.* (2007) calculated that the 5' intergenic regions of seven hypha-specific genes (*ALS3*, *ECE1*, *HGC1*, *HWP1*, *HYR1*, *RBT1* and *RBT4*) have an average size of 4.5 kilo base pairs (bp), while estimated average lengths of intergenic regions of divergently transcribed genes is 1,088 bp (Holton *et al.*, 2001). This is, with exception for *DCK1*, also true for the CFR genes (Martin *et al.*, 2013). It has already been speculated that the length of promoters of hypha-specific genes correlates to a highly complex regulation of these genes. Corresponding to this, the intergenic regions of these genes usually contain several possible binding sites of known transcription factors (Argimón *et al.*, 2007; Leng *et al.*, 2001).

1.2.2. Filament-associated virulence factors of *C. albicans*

Polymorphism is an important virulence determinant of *C. albicans*. Additionally, the transition from yeast to hyphal growth form is prerequisite for the expression of several genes encoding for virulence factors. Furthermore, the polymorphism of *C. albicans* plays a crucial role in biofilm formation which supports virulence. The next sections will shine a light on very important virulence factors that were already identified in the human fungal pathogen, several of them are filament-associated.

1.2.2.1. Adhesion and biofilm formation

Candida spp. are able to form biofilms on medical devices such as catheters, dentures, joint prosthetics and pacemakers (Kojic and Darouiche, 2004). Fungi residing in these biofilms are intrinsically resistant to antimicrobials, which leads to considerable problems, especially in the clinical setting (Kojic and Darouiche, 2004; Ahlquist Cleveland *et al.*, 2015). Nobile and Johnson (2015) describe the formation of biofilms in four stages. First, yeast cells adhere to a surface. This surface can be hard (e. g. medical device) or soft (e. g. mucosal layer). Secondly, cell proliferation is initiated and a primal cell layer is built. Next, the biofilm matures. This includes the formation of hyphae and a simultaneous construction of an extracellular matrix, which operates as a physical barrier to drug seepage. The last step is the dispersal of yeast cells from the biofilm. These yeast cells can then conquer new sites in the human host. Depending on the case of *Candida* infections and on whether or not the infection is device-related, a removal of the device additional to concomitant antifungal therapy can be beneficial for the recovery (Kojic and Darouiche, 2004). The main adhesins studied in *C. albicans* belong to the agglutinin-like sequence (Als) family, the hyphal cell wall protein (Hwp) family and the IPF family F/hyphally upregulated protein (Hyr) family and possess a glycosylphosphatidylinositol (GPI) anchor (de Groot *et al.*, 2013). The transcription factor Bcr1 has been identified as a major regulator of adherence. It activates the expression of adhesin and cell surface protein genes (such as *ALS1*, *HWPI* and *ALS3*) and thus regulates the ability of *C. albicans* to form biofilms (Nobile and Mitchell, 2005; Nobile *et al.*, 2006). Bcr1 is dependent on Tec1 which plays an important role in hyphal formation (Nobile and Mitchell, 2005). This shows that hyphal formation is connected to the expression of cell surface genes which provide adhesive traits to the hyphae. This further supports robust formation of biofilms.

1.2.2.2. Agglutinin-like sequence 3 - Als3

Als3 is a member of the ALS gene family (for review see Hoyer *et al.* (2008)), a CFR gene (cf. Sec. 1.2.1.2, Martin *et al.* (2013)) and an important virulence factor of *C. albicans*. The Als family includes eight genes (*ALS1-7* and *ALS9*) encoding for large cell-surface glycoproteins. Each one consists of three domains. The N-terminal domain contains a substrate-binding region which mediates binding to different materials. The central part is made of a number of 36-amino acid tandem repeats which varies in size between different alleles and family members (Oh *et al.*, 2005; Hoyer *et al.*, 2008). The third domain, the C-terminal domain, is rich in serine and threonine. Additionally, it contains a GPI anchorage sequence, which suggests that all Als proteins are cell wall associated (Hoyer *et al.*, 2008). Due to the structure it was suggested that

all Als proteins mediate binding to different substrates. This would confer the adaptation of *C. albicans* to different host niches (Hoyer *et al.*, 2008). However, only for some members of the Als family adhesive functions were demonstrated (*ALS1*, *ALS2*, *ALS3*), while the contribution to adhesion of others remains elusive (Hoyer *et al.*, 2008). This study will focus on the CFR gene Als3 (Martin *et al.*, 2013), which was first described as a hypha-specific gene in 1998 (Hoyer *et al.*, 1998).

Als3 was shown to be crucial for the adherence to endothelial cells, epithelial cells and the reconstituted human epithelium but not to fibronectin-coated plates (Phan *et al.*, 2007; Zhao *et al.*, 2004). Furthermore, it is important for biofilm formation. Nobile *et al.* (2006) showed that the ability of the *als3* Δ mutant to form biofilms after 2.5 h incubation in spider medium at 150 rpm and 37°C was dramatically reduced. Only a biofilm of 20 μ m depth, consisting of mainly yeast and only few hyphal cells could be formed by the *als3* Δ mutant. Under the same conditions, a corresponding wild type was able to form a biofilm of 200 μ m depth, that comprised of mainly hyphae (Nobile *et al.*, 2006). This is especially interesting since deletion of *ALS3* does not inhibit hyphal formation under normally hypha-inducing conditions. Nevertheless, the mutant was still able to form biofilms in the rat venous catheters model after 24 h incubation (Nobile *et al.*, 2006). The same study also found that *ALS3* expression is mediated by Bcr1 which is believed to act downstream of Tec1.

Furthermore, Als3 is a important invasin. Phan *et al.* (2007) found that *als3* Δ hyphae were 90% less endocytosed by endothelial and epithelial cells compared to wild type hyphae. Additionally, they found that *C. albicans* needs Als3 to bind to different host cell surface proteins. They identified N-cadherin on endothelial cells and E-cadherin on oral epithelial cells as targets of Als3. Comparative structural analyses revealed that the N-terminus of Als3 strongly resembles the N-termini of N- and E-cadherins. Due to this, the binding mechanism of Als3 to cadherins is similar to that of cadherins binding to cadherins. This binding of Als3 to host cell cadherins is necessary for the induction of endocytosis (Phan *et al.*, 2007).

Additionally, Als3 is required for iron acquisition from host cell ferritin (Almeida *et al.*, 2008). Almeida *et al.* (2008) showed that while the *als3* Δ mutant only grew poorly on agar plates with ferritin as sole carbon source, heterologous expression of *ALS3* in *S. cerevisiae* allowed the yeast to bind ferritin, which it normally is not able to do. The same study also found that deletion of *ALS3* resulted in a mutant unable to damage epithelial cells in vitro. This was also shown with epithelial and endothelial cells in an earlier study (Phan *et al.*, 2007). Additionally, it was demonstrated that invading wild type hyphae were surrounded by ferritin, which was not the case for the *als3* Δ mutant (Almeida *et al.*, 2008). Summing up, Als3 is an important adhesin and invasin which is crucial for iron acquisition from host cell ferritin.

1.2.2.3. Secreted aspartyl proteinases - Saps

Other known virulence determinants of *C. albicans* are the secreted aspartyl proteinases, short Saps. Other pathogenic *Candida* species have also been shown to produce Saps, such as *C. dubliniensis* (Gilfillan *et al.*, 1998), *C. tropicalis* (Zaugg *et al.*, 2001; Monod *et al.*, 1994) and *C. parapsilosis* (De Viragh *et al.*, 1993; Monod *et al.*, 1994). In *C. albicans* the Sap family is encoded by 10 described *SAP* genes (reviewed by Naglik *et al.* (2003)). It is important to note that Saps are differentially expressed in the different morphologies of the fungus. In yeast cells

SAP1-3 are upregulated (Hube *et al.*, 1997). It was shown that deletion of one of these *SAP* genes (*SAP1*, *SAP2* and *SAP3*) led to attenuated virulence (Hube *et al.*, 1997).

Hypha-associated Saps are encoded by *SAP4*, *SAP5* and *SAP6* and their expression is regulated by Tec1 and Efg1 (Schweizer *et al.*, 2003; Hube *et al.*, 1994; Felk *et al.*, 2002). These hydrolytic enzymes were described to be important for the liberation of nutrients from host cells and to play a role in the destruction and active penetration of tissue (Felk *et al.*, 2002) and the evasion of immune cells (Borg-von Zepelin *et al.*, 1998). *C. albicans* hyphae require Sap4-6 for full virulence and tissue penetration *in vivo* (Sanglard *et al.*, 1997; Felk *et al.*, 2002), but not for survival after contact with neutrophils in blood (Fradin *et al.*, 2005). Also, a correlation between Sap production and adherence to host cells and subsequent virulence has already been described (Abu-Elteen *et al.*, 2001).

1.2.2.4. Superoxide dismutases - Sods

C. albicans and other pathogens encounter reactive oxygen species (ROS) in a variety of situations. During contact with the host immune system, the fungi can be confronted with ROS in immune cells. Phagocytes produce superoxide radicals in the phagosome that can react with cellular components and result in the disruption of cell membranes and ultimately death of the pathogenic entity (Baldrige and Gerard, 1932; Bedard and Krause, 2007). This mechanism is called oxidative burst. Apart from these external sources, the fungus can also be exposed to internal sources of superoxide radicals, for example in the mitochondrial respiratory chain (Boveris, 1978; Casteilla *et al.*, 2002).

As protection mechanism, *C. albicans*, as well as other *Candida* spp., are able to express several superoxide dismutases (SODs), which neutralize superoxide anions. In *C. albicans* six Sods have already been identified. *SOD1* encodes a cytosolic copper- and zinc-containing superoxide dismutase. Deletion of *SOD1* leads to increased susceptibility to macrophages and a reduced virulence in a mouse model (Hwang *et al.*, 2002). This suggests that Sod1 is important for coping with external oxidative stress and thus has an influence on the virulence of *C. albicans* (Hwang *et al.*, 2002). The gene *SOD3* encodes for a cytoplasmic manganese-containing Sod, probably involved in the protection against ROS during stationary phase of growth (Lamarre *et al.*, 2001). Sod5 has an GPI-anchor and is located on the cell surface, which suggests that it plays a role in detoxifying external ROS (Fradin *et al.*, 2005). Expression of *SOD5* was shown to be induced during hyphae formation (Martchenko *et al.*, 2004; Fradin *et al.*, 2005), osmotic and oxidative stress (Martchenko *et al.*, 2004) and in yeast cells when exposed to neutrophils (Fradin *et al.*, 2005). Sod5 plays a critical role for the survival of *C. albicans* in blood, especially in terms of surviving contact with neutrophils (Fradin *et al.*, 2005) but not with macrophages (Martchenko *et al.*, 2004). Deletion of *SOD5* has a detrimental effect on the virulence in systemic mouse models (Martchenko *et al.*, 2004; Fradin *et al.*, 2005). Summing up, *C. albicans* can express different superoxide dismutases which help the fungus to deal with oxidative stress from internal and external sources. Furthermore, some Sods were shown to play an important protective role for the fungus during infection and thus have an influence on overall virulence.

1.2.2.5. Candidalysin

Candidalysin was discovered by Moyes *et al.* (2016) as the first cytolytic peptide toxin in a human

fungal pathogen. Since then, it was shown to be a major virulence factor of *C. albicans*. It is encoded by *ECE1* (extent of cell elongation 1), a CFR gene (Martin *et al.*, 2013) which belongs to the most upregulated genes in *C. albicans* hyphae (Birse *et al.*, 1993). However, *ECE1* expression is not necessary for hyphal formation (Birse *et al.*, 1993). After translation, the 271 amino-acid polypeptide Ece1 is being cleaved by Kex2 (golgi-located protease) after lysine-arginine (KR) motifs (Bader *et al.*, 2008; Moyes *et al.*, 2016). This results in a total of eight peptides (Ece1-I to Ece1-VIII), which are secreted by *C. albicans* hyphae (Bader *et al.*, 2008; Moyes *et al.*, 2016). For Ece1-III (Candidalysin, encoded by bases 62-93) a subsequent second cleavage of the terminal R by Kex1 was proven (Moyes *et al.*, 2016). The two consecutive processing steps by Kex2 and Kex1 are required to yield mature Candidalysin from the precursor Ece1 protein and critical for the virulence of *C. albicans* (Richardson *et al.*, 2018a). From all Ece1 peptides secreted by *C. albicans*, only Candidalysin induces phosphorylation of MAPK phosphatase 1 (MKP1), c-Fos, cytokines and damage in oral epithelial cells (Moyes *et al.*, 2016). Thereby, low Candidalysin concentrations from 1.5 to 70 μM resulted in c-Fos DNA binding, while higher concentrations over 70 μM were necessary to induce cell damage (Moyes *et al.*, 2016). Candidalysin has lytic as well as immunostimulatory activities. Due to its amphipathic nature with a hydrophobic N-terminus with an alpha-helical structure and a hydrophilic C-terminus, it is able to intercalate into cell membranes (Moyes *et al.*, 2016). Even though an *ece1* Δ mutant was able to form normal hyphae, adhered to and invaded human epithelial cells in a wild type-like fashion, it was not able to induce epithelial danger responses (Moyes *et al.*, 2016). An *ece1* Δ +*ECE1* $\Delta_{184-279}$ mutant, reconstituted with an *ECE1* gene which lacks the coding region for Candidalysin, resulted in a mutant similar to the *ece1* Δ mutant. It formed invasive hyphae but did not trigger epithelial immune activation, damage or mucosal activation in a murine oropharyngeal candidiasis and a zebrafish swimbladder model for mucosal infections (Moyes *et al.*, 2016). Moyes *et al.* (2016) concluded with a model of mucosal infections of *C. albicans*, which goes as follows. While hyphae are invading epithelial cells they are forming membrane-bound invasion pockets into which they secrete Candidalysin. There, the peptide accumulates. During the early phase of infection, low concentrations of Candidalysin induce epithelial immunity without lysing the cell. While the infection progresses, the Candidalysin level increases and the peptide intercalates into the membrane. This leads to pore formation, subsequent permeabilization of the membrane and calcium influx. Thus, Candidalysin directly damages epithelial membranes and induces innate recognition (Moyes *et al.*, 2016).

Since the first description of Candidalysin, various research has been conducted to shine a light on this critical virulence factor (for a detailed review on Candidalysin see Naglik *et al.* (2019)). Several findings will be summarized here.

A screen of fungal genome assemblies found that not only *C. albicans* but also *C. tropicalis* and *C. dubliniensis* secrete Candidalysin. Interestingly, the Candidalysins of *C. tropicalis* and *C. dubliniensis* showed increased potency on TR146 epithelial cells compared to *C. albicans*' Candidalysin (Richardson *et al.*, 2019). This is interesting, since an earlier mentioned study found that *C. albicans* was the most virulent of several pathogenic *Candida* spp. tested (Arendrup *et al.*, 2002). This emphasizes that next to Candidalysin secretion also the other, earlier mentioned as well as so far undiscovered factors are important for the virulence of different *Candida* species.

Richardson *et al.* 2018 investigated the role of Candidalysin in vulvovaginal candidiasis (VVC) and found that Candidalysin is also required for vaginal immunopathogenesis *in vivo*. First, they applied Candidalysin to A431 vaginal epithelial cells and noticed dose-dependent proinflammatory cytokine response, damage and activation of c-Fos and MAPK signaling. This reaction was similar to the normal response after fungal infection (Richardson *et al.*, 2018b). Further on, they used a mouse model for VVC, where different *C. albicans* mutants were intravaginally applied to mice. While *ece1* Δ +*ECE1* mutant showed wild type like neutrophil recruitment, damage and proinflammatory cytokine expression, this was significantly decreased in the *ece1* Δ and the *ece1* Δ +*ECE1* $\Delta_{184-279}$ mutants, which lacked the part coding for Candidalysin, despite all mutants forming hyphae in vaginal mucosa and there being no differences in colonization noted after three or seven days of infection (Richardson *et al.*, 2018b).

During oropharyngeal candidiasis Candidalysin drives IL-1 α/β production, which in turn activates innate IL-17⁺TCR $\alpha\beta$ ⁺ cells. This induces the expression of IL-17, a proinflammatory cytokine, which is necessary for innate and adaptive immunity against *C. albicans* (Verma *et al.*, 2017). This protective response was shown to work only, once *C. albicans* hyphae start to invade tissue and release Candidalysin and not during commensal growth of the fungus (Verma *et al.*, 2017).

Once commensal *C. albicans* switch to a pathogenic state, they are recognized by the immune system and taken up by macrophages. In the phagosome of the macrophages, the fungus forms hyphae, putting mechanical force on the membranes and ultimately killing the host cell. The fungus can then grow out and escape the immune cell (Vylkova and Lorenz, 2014; McKenzie *et al.*, 2010). During pyroptosis, inflammasome-mediated proinflammatory cytokine IL-1 β is secreted through pores in cellular membranes which leads to swelling, membrane rupture and ultimately cell death (Wellington *et al.*, 2014; Uwamahoro *et al.*, 2014). A combination of pyroptosis and hyphal formation are known mechanisms by which macrophage cell death is achieved after uptake of *C. albicans* cells. Kasper *et al.* (2018) took a closer look at the effect of Candidalysin on macrophages and dendritic cells. They found that Candidalysin activates the NLRP3 inflammasome via potassium influx, which leads to caspase-1-dependent maturation and IL-1 β secretion of human macrophages (Kasper *et al.*, 2018). This suggests that there is a third mechanism of *C. albicans*-mediated cell death of mononuclear phagocytes through Candidalysin, apart from pyroptosis and hyphal formation (Kasper *et al.*, 2018).

Swidergall *et al.* (2019) showed that Candidalysin is critical for MAPK signaling (induction of c-Fos and phospho-c-Jun, phospho-MEK1/2 and phospho-ERK1/2) and lactate dehydrogenase (LDH) release in endothelial cells. Furthermore, they revealed that Candidalysin is required for neutrophil recruitment and virulence during systemic infections in mice and zebrafish (Swidergall *et al.*, 2019).

Ho *et al.* (2019) demonstrated that Candidalysin indirectly induces the phosphorylation and thus activation of the epithelial growth factor receptor *in vitro* and *in vivo* in a murine model of oropharyngeal candidiasis. In case this receptor was inhibited, induction of c-Fos, phosphorylation of MPK1 and various cytokines by *C. albicans* and Candidalysin was repressed (Ho *et al.*, 2019). Impairment of the epithelial growth factor receptor with inhibitors led to fish death in 70% of the cases in a zebrafish swimbladder model for mucosal *C. albicans* infections. Control fish

treated with dimethyl sulfoxide completely survived the infection with *C. albicans*. Additionally, the authors noted a significant reduction in neutrophil recruitment to infection sites, when the epithelial growth factor receptor was inhibited (Ho *et al.*, 2019).

Recently, Candidalysin was shown to foster alcohol-related liver diseases (Chu *et al.*, 2019).

1.3. Aim of this study

Candidalysin is necessary for the induction of host cell damage and therefore plays a critical part in mucosal and systemic infections of *Candida albicans*. *ECE1*, the gene encoding Candidalysin, is usually the most abundant transcript in hyphae but barely detectable in yeast cells. Defects in hyphal morphology are usually accompanied by a reduced *ECE1* expression. However, the regulatory network which induces the expression of *ECE1* in *C. albicans* hyphae is so far not fully understood. In this work, the activation of *ECE1* transcription in hyphae was investigated.

The specific aims of this works were:

- Identification of important transcriptional activators of *ECE1* and possible interaction partners in *C. albicans* hyphae
- Investigation of possible regulatory overlaps between *ECE1* and other core filamentation response genes such as *ALS3*
- Determine if known activators of hyphae-specific genes are required for the expression of *ECE1* and other core filamentation response genes
- Evaluation of activator binding on chromatin and identification of possible targets

2. Material and Methods

2.1. Strains

Tab. 1: *C. albicans* strains used in this study

Strain name	Genotype	Source	Strain no. (parental strain no.)
<i>ahr1</i> Δ	<i>ahr1</i> Δ :: <i>FRT</i> <i>ahr1</i> Δ :: <i>FRT</i>	B. Böttcher	271 (1)
<i>ahr1</i> Δ + p <i>ADH1-AHR1</i> -GAD	<i>ADH1/adh1</i> :: <i>AHR1-GAD-SAT1</i>	This study	517 (271)
<i>ahr1</i> Δ + p <i>ADH1-MCM1</i>	<i>ADH1/adh1</i> :: <i>MCM1-SAT1</i>	E. Garbe	352 (271)
<i>ahr1</i> Δ + p <i>ADH1-SSN3_m</i>	<i>ADH1/adh1</i> :: <i>SSN3_m-SAT1</i>	This study	460 (271)
<i>ahr1</i> Δ X	<i>leu2</i> Δ / <i>leu2</i> Δ <i>his1</i> Δ / <i>his1</i> Δ , <i>arg4</i> Δ / <i>arg4</i> Δ , <i>URA3/ura3</i> Δ :: <i>imm434</i> , <i>IRO1/iro1</i> Δ :: <i>imm434</i> , <i>ahr1</i> :: <i>LEU2/ahr1</i> :: <i>HIS1</i>	Homann <i>et al.</i> (2009)	95 (SN152)
<i>ahr1</i> Δ + p <i>ECE1</i> -GFP	<i>ECE1/ece1</i> :: <i>GFP-ARG4</i>	R. Martin	128 (95)
<i>ahr1</i> Δ + p <i>ECE1</i> -GFP + p <i>ADH1-MCM1</i>	<i>ADH1/adh1</i> :: <i>MCM1-SAT1</i>	This study	414 (128)
<i>ahr1</i> Δ p <i>ADH1-SSN3_m</i>	<i>ADH1/adh1</i> :: <i>SSN3_m-SAT1</i>	R. Martin	218 (128)
<i>bcr1</i> Δ X2	<i>leu2</i> Δ / <i>leu2</i> Δ <i>his1</i> Δ / <i>his1</i> Δ , <i>arg4</i> Δ / <i>arg4</i> Δ , <i>URA3/ura3</i> Δ :: <i>imm434</i> , <i>IRO1/iro1</i> Δ :: <i>imm434</i> , <i>bcr1</i> :: <i>LEU2/bcr1</i> :: <i>HIS1</i>	Homann <i>et al.</i> (2009)	141 (SN152)
<i>bcr1</i> Δ + p <i>ECE1</i> -GFP	<i>ECE1/ece1</i> :: <i>GFP-ARG4</i>	R. Martin	147 (141)
<i>brg1</i> Δ X1	<i>leu2</i> Δ / <i>leu2</i> Δ <i>his1</i> Δ / <i>his1</i> Δ , <i>arg4</i> Δ / <i>arg4</i> Δ , <i>URA3/ura3</i> Δ :: <i>imm434</i> , <i>IRO1/iro1</i> Δ :: <i>imm434</i> , <i>brg1</i> :: <i>LEU2/brg1</i> :: <i>HIS1</i>	Homann <i>et al.</i> (2009)	143 (SN152)
<i>brg1</i> Δ + p <i>ECE1</i> -GFP	<i>ECE1/ece1</i> :: <i>GFP-ARG4</i>	R. Martin	148 (143)
<i>cph1</i> Δ / <i>efg1</i> Δ	<i>cph1</i> :: <i>FRT/cph1</i> :: <i>FRT</i> , <i>efg1</i> :: <i>FRT/efg1</i> :: <i>FRT</i>	Wartenberg <i>et al.</i> (2014)	104 (1)
<i>cph1</i> Δ / <i>efg1</i> Δ + p <i>ADH1-AHR1</i> -GAD	<i>ADH1/adh1</i> :: <i>AHR1-GAD-SAT1</i>	R. Martin	157 (104)
<i>cph1</i> Δ / <i>efg1</i> Δ + p <i>ADH1-SSN3_m</i>	<i>ADH1/adh1</i> :: <i>SSN3_m-SAT1</i>	Wartenberg <i>et al.</i> (2014)	109 (104)
<i>cph1</i> Δ / <i>efg1</i> Δ + p <i>ADH1-MCM1</i>	<i>ADH1/adh1</i> :: <i>MCM1-SAT1</i>	This study	462 (104)

Strain name	Genotype	Source	Strain no. (parental strain no.)
<i>cph1</i> Δ	<i>cph1::hisG/cph1::hisG</i> , <i>ura3::imm434/ura3::imm434</i>	Liu <i>et al.</i> (1994)	349 (CAI4)
<i>cph1</i> Δ + p <i>ECE1</i> -GFP	<i>ECE1/ece1::GFP-SAT1</i>	E. Garbe	201 (349)
<i>cph1</i> Δ / <i>efg1</i> Δ + p <i>ADH1</i> - <i>SSN3_m</i>	<i>ADH1/adh1::SSN3_m-SAT1</i>	Wartenberg <i>et al.</i> (2014)	109 (104)
<i>cph1</i> Δ / <i>efg1</i> Δ	<i>cph1::hisG /cph1::hisG</i> , <i>efg1::hisG /efg1::hisG-URA3-hisG</i>	Lo <i>et al.</i> (1997)	5 (CAI4)
<i>cph1</i> Δ / <i>efg1</i> Δ + p <i>ECE1</i> -GFP	<i>ECE1/ece1::GFP-SAT1</i>	A. Haeder	78 (5)
<i>efg1</i> Δ	<i>efg1::hisG/efg1::hisG-URA3-hisG</i>	Lo <i>et al.</i> (1997)	4 (CAI4)
<i>efg1</i> Δ + p <i>ECE1</i> -GFP	<i>ECE1/ece1::GFP-SAT1</i>	A. Haeder	81 (4)
<i>fkh2</i> Δ	Δ <i>ura3::imm434</i> / Δ <i>ura3::imm434</i> , <i>his1::hisG/his1::hisG</i> , <i>arg4::hisG/arg4::hisG</i> , <i>frt-frt::fkh2/fkh2::ARG4</i>	Greig <i>et al.</i> (2015)	206 (BWP17)
<i>fkh2</i> Δ + p <i>ECE1</i> -GFP	<i>ECE1/ece1::GFP-SAT1</i>	E. Garbe	207 (206)
<i>fkh2</i> Δ	<i>leu2</i> Δ / <i>leu2</i> Δ <i>his1</i> Δ / <i>his1</i> Δ , <i>URA3/ura3</i> Δ :: <i>imm434</i> , <i>IRO1/iro1</i> Δ :: <i>imm434</i> , <i>fkh2::CdHIS1/fkh2::CmLEU2</i>	R. Martin	196 (SN87)
<i>fkh2</i> Δ + p <i>ECE1</i> -GFP	<i>ECE1/ece::GFP-SAT1</i>	E. Garbe	224 (196)
Homann wild type	<i>leu2</i> Δ / <i>leu2</i> Δ + <i>LEU2</i> , <i>his1</i> Δ / <i>his1</i> Δ + <i>HIS1</i> , <i>arg4</i> Δ / <i>arg4</i> Δ , <i>URA3/ura3</i> Δ :: <i>imm434</i> , <i>IRO1/iro1</i> Δ :: <i>imm434</i>	Homann <i>et al.</i> (2009)	94 (SN152)
Homann wild type + p <i>ECE1</i> -GFP	<i>ECE1/ece1::GFP-ARG4</i>	R. Martin	127 (94)
Homann wild type + p <i>ECE1</i> -GFP + p <i>ADH1</i> - <i>AHR1</i> -GAD	<i>ADH1/adh1::AHR1-GAD-SAT1</i>	R. Martin	154 (127)
Homann wild type + p <i>ECE1</i> -GFP + p <i>ADH1</i> - <i>MCM1</i>	<i>ADH1/adh1::MCM1-SAT1</i>	This study	413 (127)
Homann wild type + p <i>ECE1</i> -GFP + p <i>ADH1</i> - <i>SSN3_m</i>	<i>ADH1/adh1::SSN3_m-SAT1</i>	This study	364 (127)
<i>ndt80</i> Δ	<i>leu2</i> Δ / <i>leu2</i> Δ <i>his1</i> Δ / <i>his1</i> Δ , <i>arg4</i> Δ / <i>arg4</i> Δ , <i>URA3/ura3</i> Δ :: <i>imm434</i> , <i>IRO1/iro1</i> Δ :: <i>imm434</i> , <i>ndt80::LEU2/ndt80::His1</i>	Noble <i>et al.</i> (2010)	261 (SN152)

2. Material and Methods

Strain name	Genotype	Source	Strain no. (parental strain no.)
<i>ndt80</i> ΔM4A	<i>ndt80::FRT/ndt80::FRT</i>	Sasse <i>et al.</i> (2011)	374 (SC5314)
<i>ndt80</i> Δ + p <i>ECE1</i> -GFP	<i>ECE1/ece1::GFP-SAT1</i>	This study	504 (374)
SC5314	<i>C. albicans</i> Wildtyp (clinical isolate)	Gillum <i>et al.</i> (1984)	1
SC5314 + p <i>ADH1-AHR1</i> -GAD	<i>ADH1/adh1::AHR1-GAD-SAT1</i>	R. Martin	177 (1)
SC5314 + p <i>ADH1-AHR1</i> -GAD, w/o HA ₃ -Tag	<i>ADH1/adh1::AHR1-GAD-SAT1</i> w/o HA ₃ -Tag	R. Martin	427 (1)
SC5314 + p <i>ADH1-MCM1</i>	<i>ADH1/adh1::MCM1-SAT1</i>	E. Garbe	350 (1)
SC5314 + p <i>ADH1-SSN3_m</i>	<i>ADH1/adh1::SSN3_m-SAT1</i>	Wartenberg <i>et al.</i> (2014)	106 (1)
<i>ssn3</i> Δ M2	<i>arg4</i> Δ/ <i>arg4</i> Δ <i>orf19.794::CdHIS1</i> / <i>orf19.794::CmLEU2</i>	Noble <i>et al.</i> (2010)	251 (M1747)
<i>ssn3</i> Δ + p <i>ECE1</i> -GFP	<i>ECE1/ece1::GFP-ARG4</i>	This study	522 (251)
<i>ssn3</i> Δ + p <i>ADH1-AHR1</i> -GAD	<i>ADH1/adh1::AHR1-GAD-SAT1</i>	This study	279 (251)
<i>ssn3</i> Δ + p <i>ECE1</i> -GFP + p <i>ADH1-AHR1</i> -GAD	<i>ADH1/adh1::AHR1-GAD-SAT1</i>	This study	552 (278)
<i>tec1</i> Δ X2	<i>leu2</i> Δ/ <i>leu2</i> Δ, <i>his1</i> Δ/ <i>his1</i> Δ, <i>arg4</i> Δ/ <i>arg4</i> Δ, <i>URA3/ura3Δ::imm434</i> , <i>IRO1/iro1Δ::imm434</i> , <i>tec1::LEU2/tec1::HIS1</i>	Homann <i>et al.</i> (2009)	145 (SN152)
<i>tec1</i> Δ + p <i>ECE1</i> -GFP	<i>ECE1/ece1::GFP-ARG4</i>	R. Martin	150 (145)
<i>tup1</i> Δ + CIp10	<i>tup1::hisG/ tup1::hisG, CIp10</i>	Martin <i>et al.</i> (2011)	14 (CAI4)
<i>tup1</i> Δ + p <i>ADH1-AHR1</i> -GAD	<i>ADH1/adh1::AHR1-GAD-SAT1</i>	This study	438 (14)
<i>tup1</i> Δ + p <i>ADH1-MCM1</i>	<i>ADH1/adh1::MCM1-SAT1</i>	This study	439 (14)
<i>tup1</i> Δ + p <i>ADH1-SSN3_m</i>	<i>ADH1/adh1::SSN3_m-SAT1</i>	This study	461 (14)
<i>tup1</i> Δ	<i>leu2</i> Δ/ <i>leu2</i> Δ <i>his1</i> Δ/ <i>his1</i> Δ, <i>arg4</i> Δ/ <i>arg4</i> Δ, <i>URA3/ura3Δ::imm434</i> , <i>IRO1/iro1Δ::imm434</i> , <i>tup1::LEU2/tup1::HIS1</i>	Homann <i>et al.</i> (2009)	116 (SN152)
<i>tup1</i> Δ + p <i>ECE1</i> -GFP	<i>ECE1/ece1::GFP-ARG4</i>	R. Martin	132 (116)

Strain name	Genotype	Source	Strain no. (parental strain no.)
<i>tup1</i> Δ + p <i>ECE1</i> -GFP + p <i>ADH1-AHR1</i> -GAD	<i>ADH1/adh1::AHR1-GAD-ARG4</i>	This study	268 (132)
<i>tup1</i> Δ + p <i>ECE1</i> -GFP + p <i>ADH1-SSN3_m</i>	<i>ADH1/adh1::SSN3_m-SAT1</i>	This study	267 (132)
<i>ume6</i> Δ	<i>ume6::CdHIS1/ume6::CmLEU2, URA3/ura3, IRO1/iro1</i>	Zeidler <i>et al.</i> (2008)	12 (SN87)
<i>ume6</i> Δ +p <i>ECE1</i> -GFP	<i>ECE1/ece1::GFP-SAT1</i>	R. Martin	214 (12)

2.2. Plasmids

Tab. 2: *E. coli* strains and Plasmids used in this study

Plasmid (restriction sites for transformation)	Description	Source
pSK-p <i>ECE1</i> -GFP- <i>ARG4</i> (<i>AscI</i> / <i>PflMI</i>)	<i>GFP</i> , <i>CaACT1</i> terminator, <i>CaARG4</i> gene, homology regions for integration into <i>CaECE1</i> locus	R. Martin
pSK-p <i>ECE1</i> -GFP- <i>SAT1</i> (<i>AscII</i> / <i>SacI</i>)	<i>GFP</i> , <i>CaACT1</i> terminator, <i>CaSAT1</i> gene, homology regions for integration into <i>CaECE1</i> locus	(Moyes <i>et al.</i> , 2016)
p <i>AHR1</i> -GAD- <i>SAT1</i> (<i>SacI</i> / <i>ApaI</i>)	<i>AHR1</i> ORF without stop codon, fused with GAL4 activator domain and HA ₃ -tag, <i>CaSAT1</i> gene, homology regions for integration into <i>CaADH1</i> locus	(Schillig and Morschhäuser, 2013)
p <i>AHR1</i> -GAD- <i>SAT1</i> w/o HA ₃ -Tag (<i>SacI</i> / <i>ApaI</i>)	<i>AHR1</i> ORF without stop codon, fused with GAL4 activator domain and HA ₃ -tag, <i>CaSAT1</i> gene, homology regions for integration into <i>CaADH1</i> locus	This study
p <i>ADH1</i> - <i>MCM1</i> - <i>SAT1</i> (<i>AscII</i> / <i>SacI</i>)	<i>MCM1</i> , <i>CaACT1</i> terminator, <i>CaSAT1</i> gene, homology regions for integration into <i>CaADH1</i> locus	E. Garbe
pSK- <i>ADH1</i> prom- <i>SSN3_m</i> - <i>SAT1</i> (<i>AscII</i> / <i>SacI</i>)	mutated <i>SSN3</i> , <i>CaACT1</i> terminator, <i>CaSAT1</i> gene, homology regions for integration into <i>CaADH1</i> locus	R. Martin

2.3. Primers

Tab. 3: Primers used for RT-qPCR analyses

Name	Sequence (5'→3')
ACT1-R1	TCAGACCAGCTGATTTAGGTTTG
ACT1-R2	GTGAACAATGGATGGACCAG
ECE1-R2	AGCATTTTCAATACCGACAG
HWP1-R1	ATCAGCTCCTGCCACTGAAC
HWP1-R2	TGAGTGGAAGTATTCTAATGTAGTTG
R1-CaALS3	ATGGTCCTTATGAATCACCATCTA
R2-CaALS3	TAGCAGTTGTAGTTGTAGATGGAG
R1-CaDCK1	TCGATGAAACTGTCCACATCA
R2-CaDCK1	TGATGCTCTACCTGATCTAGTG
R1-CaHGT2	TGCTAATTGGATTTTGAATTTTCGCTA
R2-CaHGT2	TGATGTTCAACTTCCATCTTTCTTG
R1-CaIHD1	ATGGAACCAGCAGCAGATC
R2-CaIHD1	AGTAGCAGCAAACCACCAG
R1-CaRBT1	CTACTCCAGTTGCACCAGTTG
R2-CaRBT1	CAAGACCAATAATAGCAGCACC
R1-Ca19.2457	AGACTCGCCAGAATTGGCTCA
R2-Ca19.2457	TGCCATGGGGATCAGATTCAG
SFL2_F2	GAATTC AACCAACTATCGTA
SFL2_R2	GATTGAGATGATGAAATCAG
UME6-R1	TCTACTTCTAATCCAATGGTG
UME6-R2	TATCATTACTTGATTTTTTCCGAG
NDT80_F2	TACTTTGATAGGGGAAACTA
NDT80_R2	TAAAGTATCTAGCAGTTGTG
TCC1_F2	AATGAATCCTCCACAAATG
TCC1_R2	GATGAATATTGCAGGTTTTG
EFG1-R1	ACTAGTCCGGTAAATACCAAG
EFG1-R2	TGTTGCTTTTGTTCGTGCTGTG
R1-AHR1	AGGGAAGAGTTACTGATACTG
R2-AHR1	CAAATTGTTGGCAGCTTCTGGA
R1-BRG1	GGTTATTCCACGCTAAATTGGTAAAG
R2-BRG1	ATGTGGCGATTCCCTCCTTGTTG
R1-BCR1	ACTTTACCCCCAGTATCAAGCA
R2-BCR1	ATCCAGTTTATTCACTACAACCATAG
EED1-R1	TAGTGGTAATACCCAACGTG
EED1-R2	CTGATATTTGAAATTTTGGAAGCTTTTC
HGC1-R1	AGTCAGCTTCCTGCACC
HGC1-R2	GATGAAGCAATACTAACTGCTGA
TEC1-R1	ACTTGCAACCACACCAAATGTG
TEC1-R2	TTCGTGATATTTCCATATCCGGTATTC

Tab. 4: Primers used for plasmid generation

Name	Sequence (5'→3')
5'XhoI-AHR1	CCATtctcgagATGGCAAAGAAGAAACTAAATTCAACAATAAAG*
3'AflII-GAD	ATGGcttaagCTCTTTTTTTGGGTTTGGTGGGG*

* lower case letters indicate restriction sites, homology regions to the target gene are written in italics

Tab. 5: Primers used for verification of *C. albicans* transformants

Name	Sequence (5'→3')
G1-ADH1	TATTCGGGAAGCTGGTAGCG
pTET-CaAHR1-veri	TACTGGATTTGGCTCTAGATTGGGA
GFP veri rev	TGATCTGGGTATCTCGCAAAGCAT
G4-AGO1-2	CTGGGCCAATTTCTGAGGCAGCA
CaACT1term veri rev	GAATACAAAACCAGATTTCCAGATTTCCAG
19.794fwd (<i>SSN3</i> ORF)	AACCAATTCCATGTCCTACCA
Mcm1-veri_rev	AGTGACCAAAGGTTGTAATTTAGG
I1-SAT1	CGGTGATCCCTGAGCAGGTGGCG
G2-ADH1	CCTAGTTGCCCTCCTTATGA
MCM1 intern	GACAGGTACTCAAGTGTTATTATTAGTTG

2.4. Strain maintenance and growth conditions

Routinely, *C. albicans* strains were taken from cryo stocks and incubated for one to three days on yeast extract peptone dextrose agar plates (YPD, 20 g/l peptone, 10 g/l yeast extract, 20 g/l glucose, 20 g/l agar-agar, pH 5) at 30°C. Subsequently, these plates were stored at 4°C for two to three months. For transformations, *C. albicans* strains were picked from YPD plates and used to inoculate 10 ml YPD (20 g/l peptone, 10 g/l yeast extract, 20 g/l glucose, pH 5). The cells were incubated over night at 37°C, 180 rpm and at ambient CO₂. For ribonucleic acid (RNA) extractions, Als3 staining and microscopy, if not noted otherwise, two subsequent over night cultures in synthetically defined glucose medium (SDG, 6.7 g/l yeast nitrogen broth (YNB) without amino acids (Sigma, Taufkirchen), 20 g/l glucose, ph 5.0-5.5) at 37°C and 180 rpm were diluted 1:100 in SDG, SDG + 10% human serum (Sigma-Aldrich, Taufkirchen) or synthetically defined N-acetylglucosamine medium (SDN, 6.7 g/l YNB without amino acids, 20 g/l N-acetylglucosamine). For medium switch, YPD over night cultures at 37°C were diluted 1:100 in Lee's (Lee *et al.*, 1975), Spider (Liu *et al.*, 1994), or Roswell Park Memorial Institute medium-1640 (RPMI, Merck, Darmstadt). Over night cultures in M199 (Sigma, Taufkirchen, 9.5 g/l, ph 4, 37°C, 180 rpm, ambient CO₂) were used to inoculate M199 (pH 4 or pH 8, 1:100). Incubation for four to six hours at 37°C and ambient CO₂ followed under shaking (180 rpm, RNA extraction, GFP fluorescence microscopy) or non-shaking (Als3 staining) conditions.

2.5. Plasmid creation

For the creation of the p*AHR1*-GAD w/o HA₃-tag plasmid, the already published p*AHR1*-GAD plasmid was utilized (Schillig and Morschhäuser, 2013). With the primers 5'*Xho*I-*AHR1* and 3'*Afl*II-GAD the *AHR1* ORF fused to the Gal4 activator domain was amplified from the p*AHR1*-GAD plasmid and restriction sites were introduced. The resulting DNA band of approximately 2226 bp was excised from an agarose gel and cleaned up by gel extraction (QIAquick Gel Extraction Kit, Qiagen, Hilden) according to the manufacturer's instructions. Next, the DNA fragment was digested using the restriction enzymes *Xho*I and *Afl*II (both New England Biolabs (NEB), Frankfurt a. M.) and again cleaned up via gel extraction. Next, the cleaned up *AHR1*-GAD insert was ligated into the linearized vector (p*AHR1*-GAD backbone digested with *Xho*I and *Afl*II, cleaned via gel extraction) using T4 DNA ligase and T4 DNA ligase buffer (with 10 mM ATP, NEB, Frankfurt a. M.) at 16°C for 18 h.

2.6. *E. coli* transformation and plasmid extraction

For an *E. coli* transformation one vial of NEB Express competent *E. coli* (NEB, Frankfurt a. M.) was thawed on ice for 30 min. To 27 µl of competent cells, 1.5 µl of ligated plasmid or digested plasmid (negative control) was added. After another 30 min of incubation on ice, cells were heat shocked for 20 s at 42°C and put on ice for 5 minutes. Subsequently, 500 µl super optimal broth with catabolite repression outgrowth medium (NEB, Frankfurt a. M., preheated to 30°C) was added to the cells and the mixture was incubated for 1 h at 37°C and 1200 rpm. For each transformation approach 100 µl were plated on lysogeny broth selection plates (LB, Carl Roth, Karlsruhe, 25 g/l + 20 g/l Agar) containing ampicillin (amp, 100 µg/m, Carl Roth, Karlsruhe) and incubated over night at 37°C.

For initial screens, plasmids of colonies were extracted using a mini prep protocol. For this, 1 ml of *E. coli* over night culture in LB-amp was harvested and resuspended in ice-cold 250 µl P1 buffer (50 mM glucose, 1 M Tris, 10 mM EDTA, 5 µl/l RNase A (10 mg/l)). 250 µl P2 buffer (200 mM NaOH, 1 % (v/v) SDS) was added. The mixture was incubated for 5 min at room temperature (RT) with occasional inversion. Next, 250 µl P3 buffer (2.55 M potassium acetate, pH 4.8) was added and the reaction was mixed by inverting the tubes several times. The suspension was centrifuged for 20 min at 16,000 x g and the supernatant was added to 750 µl ice-cold isopropanol in order to precipitate the DNA. The mixture was inverted carefully and centrifuged for 25 min at 16,000 x g. The supernatant was removed and the pellet was washed once with 100 µl 70% ethanol. The pellet was air-dried and redissolved in 50 µl H₂O. For large scale harvest of plasmids the QIAgen plasmid midi kit (Qiagen, Hilden) was used according to manufacturer's instructions. DNA pellets were resuspended in H₂O instead of Tris-EDTA (TE) buffer.

2.7. *C. albicans* transformation

Transformations of *C. albicans* were performed using the the lithium acetate protocol (Walther and Wendland, 2003). A YPD over night culture of *C. albicans* was used to inoculate 50 ml YPD in a dilution of 1:100 or 1:50, depending on the density of the over night culture. After 4 h

growth at 37°C shaking, the cells were harvested by centrifugation for 5 to 10 min at 4000 rpm. The pellet was washed once with 50 ml distilled water and again centrifuged as described above. In the meantime, sheared salmon sperm DNA (10 mg/ml, Thermo Fisher Scientific, Dreieich) was heated up to 95°C for 15 minutes to part double strand DNA into single strand DNA and put on ice. The cell pellet was taken up in 1 ml distilled water and transferred into a sterile microcentrifuge tube. After centrifugation for 1 min at 13,000 x g, the pellet was resuspended in 0.75 to 1.5 ml freshly prepared lithium acetate solution (100 mM LiAc in 1 x TE), depending on pellet size. For each transformation approach and negative control, 10 µl of salmon sperm DNA was added to 100 µl cell solution, vortexed shortly and incubated for 2 to 3 min. Subsequently, 20 µl of the transformation cassette (plasmids digested as indicated in Tab. 2) and cleaned up by gel extraction (QIAquick Gel Extraction Kit) or nothing (negative control) and 600 µl of freshly prepared polyethylene glycol/lithium acetate solution (100 mM LiAc, 1 x TE, 40% PEG3640 (w/v, Sigma Aldrich, Taufkirchen)) was added to the cell solutions. The mixture was vortexed rigorously and incubated for 15 to 18 h at 30°C. Afterwards, the cells were heat shocked for 15 min at 44°C and 1000 rpm. After 1 min on ice, the cells were harvested by centrifugation for 1 min at 13,000 x g and washed in 1 ml YPD. Centrifugation was repeated and the pellet was resuspended in 10 ml YPD and incubated at 37°C shaking for 4 h. Finally, cells were harvested, resuspended in 200 µl YPD and plated on selection plates. If *SAT1* was used as selection marker, YPD plates supplemented with 200 µg/ml nourseothricin (NTC, HKI, Jena) were used. If *ARG4* was used as selection marker, cells were plated on SDG plates (6.7 g/l YNB without amino acids, DIFCO, 20 g/l glucose, pH 5.0-5.5, 20 g/l agar-agar). Transformations were incubated for 2 to 3 days. Growing colonies were verified with colony polymerase chain reaction (PCR) and corresponding primers displayed in Tab. 5.

2.8. Ribonucleic acid extraction

RNA extraction was performed using the phenol chloroform method, as already described (Martin *et al.*, 2013). In short, cells were grown under indicated conditions and harvested by centrifugation. The cell pellet was resuspended in 440 µl AE buffer (50 mM sodium acetate, 10 mM EDTA (pH 7), 1% SDS) and transferred to a new screw cap tube. After 30 s of thorough vortexing, 440 µl Phenol-Chloroform-Isoamylalcohol (acidic pH, Thermo Fisher Scientific, Dreieich) was added and vortexing was repeated as described above. The solution was incubated for 5 min at 65°C and then incubated at -20°C for at least 30 min. Subsequently, the mixture was thawed for 5 min at 65°C and centrifuged for 2 min at full speed. The upper phase was transferred into a new screw cap tube and one tenth volume of 3 M sodium acetate (pH 5.3) and one volume of isopropanol were added. The mixture was carefully inverted and again frozen for at least 30 min at -20°C. RNA was pelleted for 10 min at 12000 x g (RT), and washed twice with 70% ethanol. Eventually, the RNA pellet was resuspended in 20 to 50 µl RNase-free water (depending on pellet size). The RNA concentration was analyzed using the Agilent 2100 Bioanalyzer or the Nanodrop. RNA was stored at -80°C.

2.9. Reverse transcriptase quantitative polymerase chain reaction

The expression levels of certain genes under specific conditions in different *C. albicans* strains was assessed with reverse transcriptase quantitative polymerase chain reaction (RT-qPCR) analysis in biological triplicates. RT-qPCR was performed using the Brilliant III Ultra-Fast SYBR Green RT-qPCR Master Mix (Agilent Technologies, Waldbronn) according to the manufacturer's instructions. Reaction mixes for every well were prepared following this scheme:

1 µl 100 ng/µl RNA
 0.2 µl dithiothreitol (RT)
 5.8 µl H₂O
 1 µl primer 1
 1 µl primer 2
 1 µl RT/RNase Block (kept on ice)
 10 µl SYBR Green 2x Master Mix (RT)

RT-qPCR was performed in the Agilent MX3000P (Agilent Technologies, Waldbronn) using the following protocol:

10 min	50°C		reverse transcriptase reaction
<hr/>			
3 min	95°C		
<hr/>			
30s	95°		
30s	60°C*	40 cycles	q PCR
1 min	95°C		
<hr/>			
30s	55°C**		dissociation curve
30s	95°C		

*measurement at the end of each cycle

**measurement after every $\Delta 0.5^\circ\text{C}$

The relative expression levels were calculated using the $\Delta\Delta\text{Ct}$ method (Pfaffl, 2001). In short, Ct-values for the house-keeping gene *ACT1* of each RNA sample were subtracted from the Ct-values of genes of interest of the same RNA sample to generate the ΔCt -value. Next, the Ct-value of control RNA (wild type SC5314, 6 h in YPD at 37°C) was subtracted from the ΔCt -value to create the $\Delta\Delta\text{Ct}$ -value. Finally, the relative expression was calculated by taking 2 to the negative power of the $\Delta\Delta\text{Ct}$ -value.

2.10. Als3 staining

500 μ l of SDG resp. SDG with 10% human serum (H6914, Sigma-Aldrich, Taufkirchen) was inoculated with 1×10^6 cells/ml or 1×10^5 cells/ml of *C. albicans*. Cells were incubated for 5 to 6 h in petri dishes with glass bottom (μ Dish, MoBiTec, Göttingen) at 37°C (no shaking). Cells were then washed once with 1 x PBS. Subsequently, the cells were incubated for 1 h at RT with a rabbit polyclonal antiserum raised against the recombinant N-terminal region of Als3 (Phan *et al.* (2007), 0.7 mg/ml, 1:166 diluted in phosphate buffered saline (PBS)). After one washing step with PBS, incubation with a goat-anti-rabbit-488-immunoglobulin G (IgG, 1:250 diluted in PBS, Jackson Immuno Research; Suffolk, England) followed for 1 h at RT. Cells were washed once with 1 x PBS, fixed for 5 min at RT using 200 μ l Histofix (containing 4% formaldehyde, Carl Roth, Karlsruhe) and then washed again three times. Finally, cells were stained with enough calcofluor white (1 g/l calcofluor white, Remel BactiDrop, Thermo Fisher Scientific, Frankfurt a. M.) volume to cover the whole dish surface for up to 10 min at RT. After one last washing step with 1 x PBS, cells were ready for microscopy and stored at 4°C.

2.11. Microscopy

If not stated otherwise, the Axio-Observer Z1 (Carl Zeiss, Jena) was used for differential interference contrast (DIC) and fluorescence microscopy in the green fluorescing protein (GFP) channel. Standard excitation time of 1700 ms for GFP detection was used.

Micrographs of the invasion assay were taken with the same microscope in DIC, GFP and 4',6-diamidino-2-phenylindole (DAPI) channels. For Als3-staining microscopy, the Laser scanning microscope (LSM) 780 (Carl Zeiss, Jena) was used with the Zen black 2.3 SP1 software and following settings:

Plan-Apochromat 20x/0.8M27
Scan Mode: Frame
Frame size: x=1024; y=1024 (Optimal)
Avergeing:
Number: 4
Bit Depth: 16 bit
Mode: Line
Direction: —>
Method: Mean

Track 1
A488 Laser (Range:495-630 nm)
Gain: 790
Digital Offset: 0
Digital Gain: 1.0

Track 2
405 Laser (DAPI, Range: 410-473nm, for Calcofluor white detection)

Gain: 358

Digital Offset: 0

Digital Gain: 1.0

TPMT

Gain: variable

Digital Offset: 0

Digital Gain: 1.0

Z-stacks were taken of hyphal and pseudohyphal cells. For image processing the Zen blue software was used. Z-stacks were merged using the method Sharpen → Extended Depth of Focus → Method → Maximum Projection (only A488 and DAPI display). In the merged Z-stacks or the images of yeast cells, which were taken only on one focal plane, the histogram settings were changed from white 65.535 to 30.000 for a brighter signal.

2.12. Measurement of secreted Candidalysin

The Candidalysin secreted into the culture supernatant was processed and measured by S. Mogavero of the group Microbial Pathogenicity Mechanisms (MPM) and T. Krüger from the group Molecular and Applied Microbiology (MAM) at the Hans-Knöll-Institute (HKI). For this, indicated strains were grown for 18 h in either yeast (YNB medium with 2% sucrose, pH 4) or hyphae (YNB medium with 2% sucrose, 75 mM 2-hydroxy-3-morpholinopropanesulfonic acid (MOPSO) buffer, pH 7.2, 5 mM GlcNAc) inducing medium at 37°C and 180 rpm, starting at an OD₆₀₀ of 0.05. Subsequently, supernatants were collected, processed and further analyzed by liquid chromatography-mass spectrometer/mass spectrometer system (Ultimate 3000 nano RSLC system coupled to a QExactive Plus mass spectrometer) as previously described (Moyes *et al.*, 2016).

2.13. Lactate dehydrogenase (LDH) assay

LDH assays were carried out at the laboratories of the MPM department at the HKI with the help of Rita Müller and Stefanie Allert. 2×10^4 TR146 buccal epithelial carcinoma cells in 200 µl Dulbecco's Modified Eagle Medium (DMEM)/F12 (Gibco; Thermo Fisher Scientific, Frankfurt a. M.) + 10% heatinactivated fetal bovine serum (FBS) were seeded into the wells of 96-well plates and incubated for 1 to 2 days at 37°C 5% CO₂, until a confluent monolayer could be observed under the microscope. Over night cultures (YPD, 30°C, 180 rpm) of sought out *C. albicans* strains were used for infection. They were washed twice with PBS and counted in a Neubauer counting chamber. A stock solution of 4×10^5 cells per ml DMEM/F12 was generated. The medium was removed from the prepared TR146 cells in the 96-well plates and 100 µl fresh DMEM/F12 (without FBS) was added (200 µl for low and high control). 100 µl of the *C. albicans* stock solutions were added to the wells in triplicates, so that 4×10^4 cells were added per well. Incubation at 37°C and 5% CO₂ followed. After 24 h, 10 µl 5% Triton-x 100 was added to the high control wells and the plate was again incubated for 10 min at 37°C and 5% CO₂. The plate was then centrifuged at $250 \times g$ for 5 min. Subsequently, 10 µl of each supernatant was added to 90 µl of PBS in new wells. Lactatedehydrogenase (Roche, Mannheim) from rabbit muscle was used to

generate a standard curve. Supernatant from uninfected TR146 cells served as a 'low control'. Supernatant from Triton-x 100 treated cells was used as 'high control'. The release of LDH was measured using the Cytotoxicity Detection Kit (LDH) (Roche, Mannheim), according to the manufacturer's instructions. In short, 100 μ l of freshly prepared LDH-Kit solution was added to each well. The mixture was incubated 10 to 15 min in the dark at RT. The reaction was stopped by the addition of 50 μ l 1 M hydrochloric acid (HCL). The absorption at the wavelengths of 490 nm (LDH assay) and 660 nm (background) was measured using a plate reader. The absorbance at 660 nm was subtracted from the absorbance at 490 nm. The calculated value was used for further analyses. The measured value for the low control was subtracted from all values. To evaluate the % cytotoxicity, this value was then divided by the value of the high control and multiplied by 100.

2.14. Invasion assay

The invasion assay was carried out with the help of Rita Müller and Stefanie Allert at the laboratories of the MPM department at the HKI in Jena. 1×10^5 TR146 cells in 250 μ l DMEM/F12 + 10% heatinactivated FBS were seeded into each well of a 24-well plate with coverslip and incubated for 1-2 days at 37°C 5% CO₂, until a confluent monolayer was built up. Over night cultures (YPD, 30°C, 180 rpm) of sought out *C. albicans* strains were used for infection. They were washed twice with PBS, counted in a Neubauer counting chamber and stock solutions of 4×10^5 cells/ml in DMEM/F12 were created. The medium of the TR146 cells in the 24-well plate was removed and replaced with 250 μ l of the stock solutions, so that each well was infected with 1×10^5 cells. Subsequently the plates were incubated for 4 h at 37°C and 5% CO₂. Next, the cells were carefully washed twice with PBS for 1 min each to remove non-adherent cells. Fixation with 400 μ l Histofix per well followed at 4°C over night. Then, the cells were washed twice in PBS for one minute each. For outside staining, cells were incubated with 200 μ l/well Concanavalin A solution (5 mg/ml stock 1:500 in PBS) for 1 h at 30°C in the dark. Two washing steps with PBS for one minute each followed. Subsequently, cells were permeabilized by adding 300 μ l 0.5% triton-x per well for 5 min at RT. Washing with PBS was repeated three times. For inside staining, 400 μ l 0.01-0.035 mg/ml calcofluor white in Tris-HCl (0.1 M, pH 9.0) were added per well and incubation for 20 min at RT in the dark followed. Cells were washed three times for 10 min in 1 ml bidistilled water at 30°C. Coverslides were removed from the wells and invertedly mounted on a microscope slide with about 5 μ l mounting medium. Slides were stored at 4°C prior to microscopic analysis with the Axio-Observer.Z1 (Carl Zeiss, Jena).

2.15. Chromatin Immuno Precipitation DNA Sequencing (ChIP-Seq)

A protocol for formaldehyde fixation was provided by the company Active Motif, which performed the Chromatin Immuno Precipitation DNA Sequencing (ChIP-Seq) analysis. For this, strains of interest (SC5314+AHR1-GAD and SC5314+AHR1-GAD w/o HA-tag as negative control, ref. no. 177 and 427) were grown in double over night cultures in two times 20 ml SDG medium at 37°C shaking. On the third day, two times 250 ml prewarmed SDG medium was inoculated with 7.5 ml double over night culture each and incubated shaking at 37°C (1:33.3). After six hours of incubation, falcon tubes filled with 3.12 ml 16% formaldehyde (methanol-free, Thermo

Fisher Scientific, Frankfurt a. M.) were filled up to 50 ml with the SDG cultures. The tubes were inverted several times during a total incubation time of 15 min at RT. The fixation procedure was stopped with the addition of 2.5 ml 2.5 M glycine solution. The reaction was inverted several times during a subsequent incubation of 5 min at RT. Cells were centrifuged at 4,000 x g for 10 minutes at 4°C and the supernatant was removed. From now on, cells were kept on ice. Pellets were resuspended in 10 ml chilled PBS-Igepal (PBS, final conc. of 0.5% Igepal) and pellets from the same strains were pooled. The cells were again centrifuged as described above and the pellets were resuspended in 10 ml chilled PBS-Igepal and 100 µl phenylmethylsulfonyl fluoride (100 mM in ethanol, final conc. 1 mM). Cells were centrifuged again and pellets were snap-frozen in liquid nitrogen and stored at -80°C. Formaldehyde fixed pellets were sent for further ChIP-Seq analysis to Active Motif. The mutant without the HA₃-tag was important for the antibody validation. ChIP-Seq reads were analyzed by Active Motif including peak calling and peak filtering resulting in 325 peaks. The peak data was further analysed by Daniela Albrecht-Eckardt from BioControl Jena GmbH. Using the chromosomal position of the peaks, neighboring genes on both forward and backward strands were identified in the genome. A sequence of 500 nucleotides centering at the maximum of each peak region was extracted. These 325 sequences were used as input for the online motif analysis tool Meme-ChIP (v. 5.1.0, Machanick and Bailey (2011)). Default parameters with background Markov model generated from the supplied sequences were chosen and searched for motifs with a length of 8 to 20 base pairs (bp). The identified motif was confirmed by the motif finder utility of MochiView (v. 1.46, Homann and Johnson (2010)). The Integrated Genome Browser (IGB) was used to visualize peaks in front of genes of interest.

3. Results

3.1. Ahr1 is a regulator of *ECE1* expression

3.1.1. Identification of possible activators of *ECE1* expression

One of the most strongly upregulated genes in the *C. albicans* hyphae is *ECE1*. To identify transcription factors which play a role in the activation of *ECE1* expression, the 5' intergenic region of *ECE1* was examined. It is made up of 3197 base pairs and contains several possible binding sites of known activators of hyphal growth. An *in silico* analysis showed that Bcr1, Cph1 and Tec1 possess one, Fkh2 two, Ahr1, Brg1, Mcm1 and Ume6 three, Ndt80 six and Efg1 15 possible binding sites in the 5' intergenic region, as displayed schematically in Fig. 2. For a detailed list of the exact motifs and locations see Tab. VII (Sec. VII).

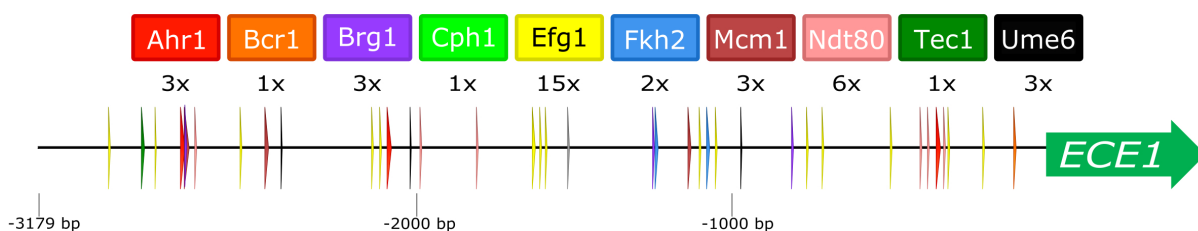


Fig. 2: Schematic display of putative transcription factor binding sites in the 5' intergenic region of *ECE1*.

The transcription factors Ahr1, Bcr1, Brg1, Cph1, Efg1, Fkh2, Mcm1, Ndt80, Tec1 and Ume6 possess possible binding sites upstream of the *ECE1* open reading frame (ORF).

3.1.2. Screen of activator mutants reveals that Ahr1 is necessary for high-level *ECE1* expression in hyphal morphology

Deletion mutants of the transcription factors mentioned in Sec. 3.1.1 were tested for their influence on *ECE1* expression under hypha-inducing conditions (strain no.: 127, 128, 147, 148, 201, 81, 78, 207, 504, 150 and 129, see Tab. 1). No deletion mutant of *MCM1* was available, since the gene is essential (Rottmann *et al.*, 2003). A *cph1*Δ/*efg1*Δ mutant was included into the screen, since both transcription factors possess possible binding sites in the *ECE1* 5' intergenic region. Furthermore, the double mutant is known for being locked in the yeast growth state. For the screen, the *GFP* gene was transformed into the *ECE1* locus of these mutants to visualize *ECE1* expression (GFP reporter system). Figure 3A shows micrographs of the GFP reporter strains taken 4 h after hyphal induction in SDG with 10% human serum at 37°C. The *cph1*Δ and *fkh2*Δ mutants displayed normal hyphal formation and a wild type-like GFP signal. The *bcr1*Δ mutant showed a mixture of green fluorescing hyphae and not or only faintly fluorescing pseudohyphal cells (Fig. 3A). This suggests, that binding of Cph1, Fkh2 and Bcr1 to their possible binding sites in the 5' intergenic region, was not necessary for *ECE1* expression under the tested conditions. The *ume6*Δ mutant only displayed pseudohyphal growth. Nevertheless, as indicated in Fig. 3A, a GFP signal could be observed from these pseudohyphae. 53% (n=366) of *brg1*Δ cells showed no, and 47% (n=326) a faint or strong GFP signal. The morphologies of *brg1*Δ cells after hyphal induction varied between yeast cells, short filaments and pseudohyphae. Interestingly, 50%

3. Results

(n=488) of the *efg1* Δ yeast cells showed a GFP signal, while the *cph1* Δ /*efg1* Δ yeasts did not exhibit any GFP signal. The *ndt80* Δ and the *tec1* Δ mutants did not form hyphae and displayed no or only a faint GFP signal, as depicted in Fig. 3A. An abnormal growth of these mutants could be due to a variety of dysregulated transcription mechanisms. Since a direct regulator of *ECE1* expression in the hyphal morphology was wanted, these mutants were disregarded for further analyses. From the screened mutants, only the *ahr1* Δ mutant was able to form phenotypically normal hyphae while showing no or only a faint GFP signal (Fig. 3A). Due to this, Ahr1 was an interesting candidate for a possible direct regulation of the *ECE1* transcription.

In order to verify these results concerning *ECE1* expression, RNA of wild type and deletion mutants (strain no. 94, 95, 141, 143, 261, 349, 4, 104, 196, 261, 145 and 12, see Tab. 1) was extracted after 4 h growth in SDG with 10% human serum (Fig. 3B). In accordance to the GFP reporter assay, relative expression of *ECE1* in the *cph1* Δ and the *fkh2* Δ mutants was similar to that of wild type hyphae, as depicted in Fig. 3B.

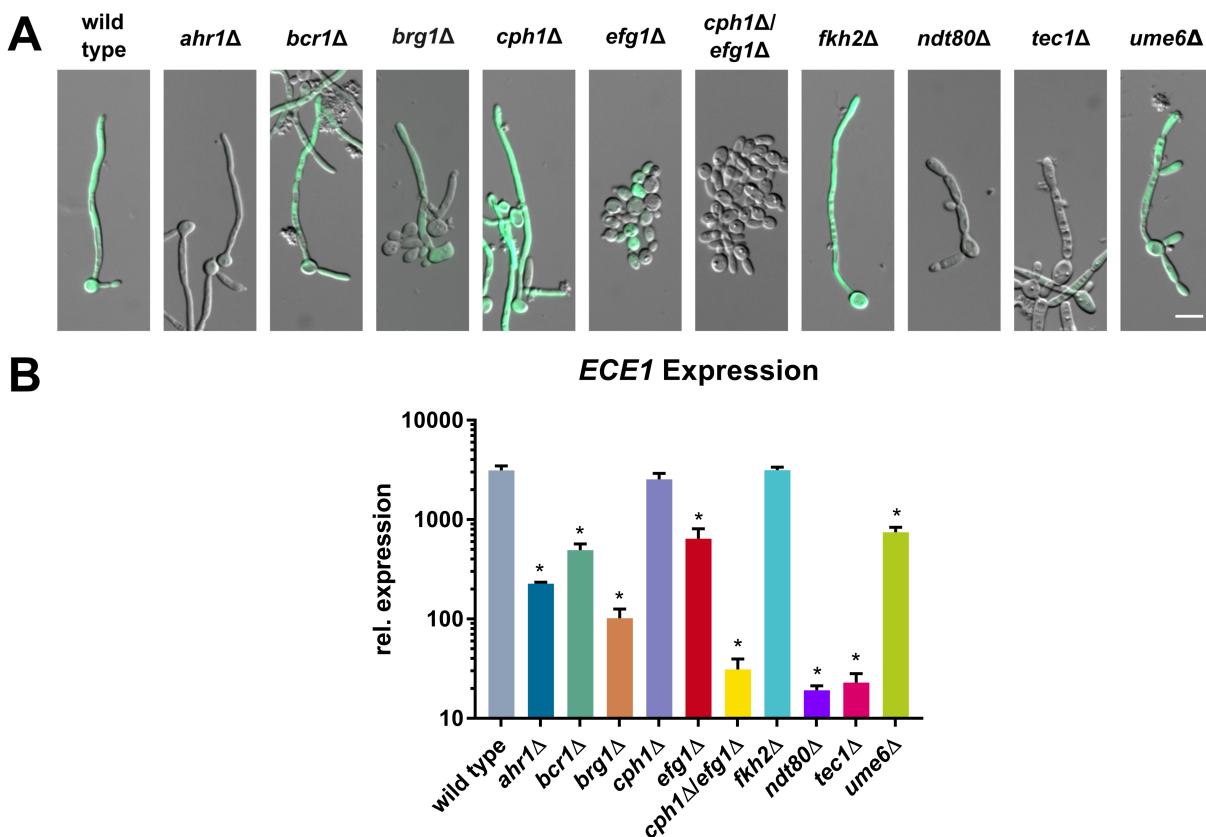


Fig. 3: The transcription factor Ahr1 is important for *ECE1* expression in *Candida albicans* hyphae.

A Wild type and regulatory mutants with the GFP reporter system, where the *GFP* gene was integrated into the *ECE1* locus, were grown for 4 h in SDG with 10% human serum at 37°C prior to microscopy. DIC and GFP channel were merged. Bar=10 μ m.

B Total RNA of wild type and regulatory mutants was isolated after 4 h growth in SDG with 10% human serum in biological triplicates. 100 ng/ μ l of this RNA was used for RT-qPCR to determine the relative gene expression of *ECE1*. Data was normalized to a control RNA (wild type, 6 h YPD, 37°C) and the housekeeping gene *ACT1*. Asterisks mark significant differences of mutants compared to the wild type (* $p \leq 0.05$, two tailed, unpaired student's t-test).

All other mutants showed a significant reduction in *ECE1* expression, with the *bcr1* Δ , the *efg1* Δ and the *ume6* Δ mutants having higher and the *brg1* Δ , the *cph1* Δ /*efg1* Δ , the *tec1* Δ and the *ndt80* Δ mutants having lower *ECE1* expressions than the *ahr1* Δ hyphae (Fig. 3B). These results supported the findings of the GFP reporter assay.

3.2. Ahr1 is important for Candidalysin secretion

As shown above, *ECE1* expression was significantly downregulated in an *ahr1* Δ mutant compared to wild type under hyphal growth conditions. The question arose whether this downregulation was associated with a decrease in Candidalysin secretion. Following an already established protocol (Moyes *et al.*, 2016), S. Mogavero and T. Krüger (both: Hans-Knöll-Institute, Jena), measured the amount of secreted Candidalysin by the wild type and the *ahr1* Δ mutant (strain no. 1 and 95, Tab. 1) after 18 h growth in hyphae-inducing medium (YNBS, pH 7.2, 37°C) using LC-MS/MS. Results depicted in Fig. 4A show that the amount of detected peptides that matched to Candidalysin (PSM=peptide spectrum matches) was with 68 PSM indeed lower in the *ahr1* Δ mutant compared to 345 PSM in the wild type. A detailed listing of measured peptides can be see in Tab. 7 (Sec. VII).

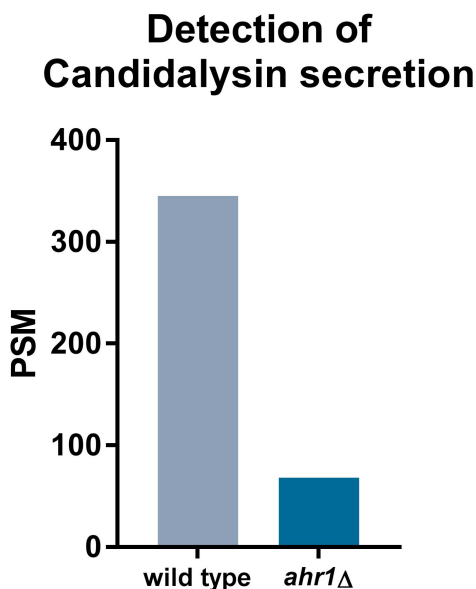


Fig. 4: **Ahr1 is important for Candidalysin secretion of *C. albicans*.**

Wild type and the *ahr1* Δ mutant were incubated for 18 h under hyphal growth conditions (YNBS, pH 7.2, 37°C). Candidalysin was extracted from supernatant and measured by LC-MS/MS. PSM= peptide spectrum matches.

3.3. Hyperactive Ahr1 induces high-level *ECE1* expression

3.3.1. Hyperactive Ahr1 induces *ECE1* expression in wild type and independent of Cph1 and Efg1 under yeast growth conditions

For further elucidating the role of Ahr1 in terms of *ECE1* expression, we transformed a hyperactive Ahr1 into the *ADH1* locus of different *C. albicans* strains. Schillig and Morschhäuser found that by C-terminal fusion of a zinc cluster transcription factor to a heterologous Gal4 activator domain (GAD), an artificial activation of the transcription factor could be achieved (Schillig and Morschhäuser, 2013). Integration of such an *AHR1*-GAD allele into a *C. albicans* strain with the *ECE1*-promotor driven GFP (strain no. 127 and 154, Tab. 1) was able to induce a GFP signal in cells, already under yeast growth conditions, as can be seen in Fig. 5A. Additionally, it increased clustering of cells and resulted in a more elongated morphology or even pseudohyphae formation (Fig. 5A). This correlated to a significant increase in relative *ECE1* expression after 4 h growth under yeast growth conditions (strain no. 1 and 177, Tab. 1), as shown in Fig. 5B. This *ECE1*

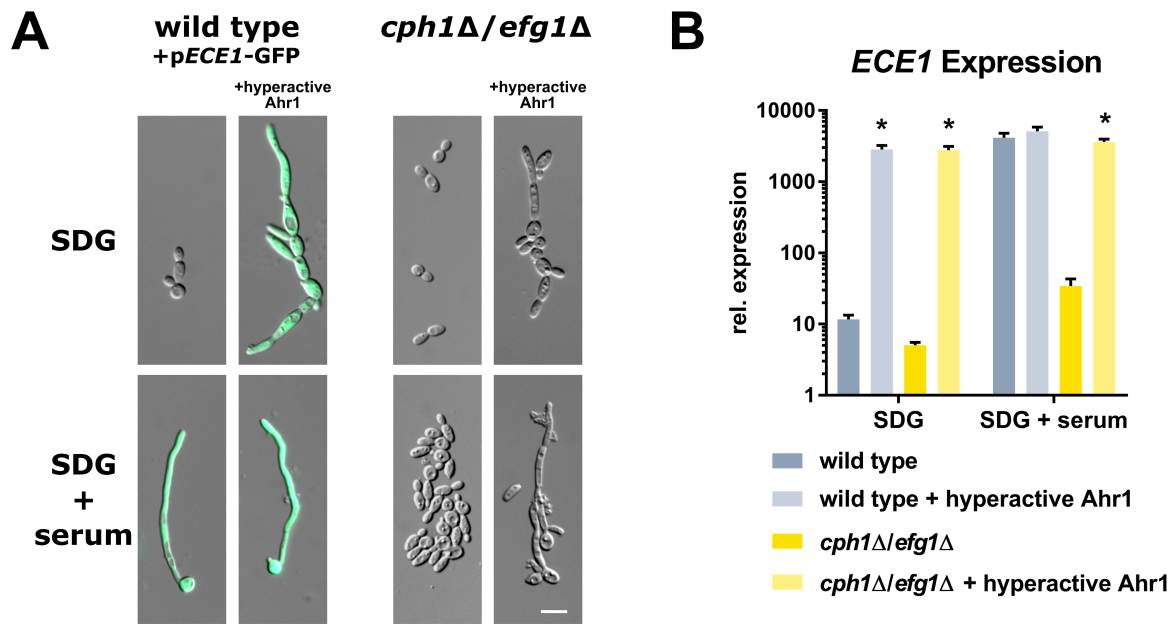


Fig. 5: **Hyperactive Ahr1 induces *ECE1* expression under yeast growth conditions and independent of Cph1 and Efg1.**

A A hyperactive Ahr1 was transformed into the *ADH1* locus of the *C. albicans* wild type (including *ECE1* promotor-driven GFP system, p*ECE1*-GFP) and the *cph1*Δ/*efg1*Δ mutant. Cells were grown for 4 h in SDG with or without 10% human serum at 37°C prior to microscopy. DIC and GFP channels were merged. Bar=10 μm.

B Total RNA of the wild type and the *cph1*Δ/*efg1*Δ mutants with or without hyperactive Ahr1 was isolated after 4 h growth in SDG with or without 10% human serum in biological triplicates. 100 ng/μl of this RNA was used for RT-qPCR to determine the relative gene expression of *ECE1*. Data was normalized to a control RNA (wild type, 6 h YPD, 37°C) and the housekeeping gene *ACT1*. Asterisks mark significant differences of hyperactive Ahr1 mutants compared to the respective parental strain (*p ≤ 0.05, two tailed, unpaired student's t-test).

expression was comparable to that of wild type hyphae.

Cph1 and Efg1 are known activators of hyphal growth and the *cph1* Δ /*efg1* Δ double mutant is nonfilamentous under most hyphae-inducing conditions. *ECE1* expression in this mutant was significantly decreased compared to the wild type under hyphal growth conditions (Fig. 3B). Integration of a hyperactive Ahr1 into the *cph1* Δ /*efg1* Δ mutant resulted in clustering and elongation of some cells in yeast growth medium and pseudohyphae formation of some cells after serum-induction (strain no. 104 and 157, Tab. 1, Fig. 5A). Due to a lack of available selection markers for further transformation of the double mutant, it was not possible to additionally examine the *ECE1* GFP reporter system in these strains. RT-qPCR results, revealed that a hyperactive Ahr1 was able to induce *ECE1* expression in the *cph1* Δ /*efg1* Δ mutant under yeast and hyphal growth conditions up to the level of wild type hyphae (strain no. 104 and 157, Tab. 1, Fig. 5B). This observation indicated, that the mechanism by which a hyperactive Ahr1 induced *ECE1* expression was independent from Cph1 and Efg1 and environmental stimuli like human serum.

3.3.2. Hyperactive Ahr1 increases Candidalysin secretion

Due to the significantly increased *ECE1* expression in the wild type and the *cph1* Δ /*efg1* Δ mutant with hyperactive Ahr1, it was further tested if this increased transcription correlated with an increased Candidalysin secretion. The wild type and the *cph1* Δ /*efg1* Δ mutants with and without hyperactive Ahr1 were grown for 18 hours under yeast (YNBS, pH 4, 37°C) or hyphal (YNBS, pH 7.2, 37°C) growth conditions (strain no. 1, 177, 104 and 157, Tab. 1). Candidalysin measurement followed as described above. Surprisingly, elevated *ECE1* expression under yeast growth conditions of the wild type and the *cph1* Δ /*efg1* Δ mutant due to a hyperactive Ahr1, did not result in an increase in Candidalysin secretion as depicted in Fig. 6. Small amounts of secreted Candidalysin were detected in the *cph1* Δ /*efg1* Δ mutants with or without hyperactive Ahr1 under yeast growth conditions. A possible explanation for this is the contamination of the LC column (see also tab. 7, section VII). Since the Ece1-III peptide is very sticky, washing steps in between measuring different samples potentially did not suffice to completely remove the peptide. Subsequently, ECE1-III peptides sticking to the LC column could have led to false positives.

Under hyphal growth conditions, a hyperactive Ahr1 was able to elevate the amount of detected Candidalysin (Fig. 6). Interestingly, due to a hyperactive Ahr1 secreted Candidalysin levels in the wild type background rose from 345 to 612 PSM under hyphal growth conditions (Fig. 6), even though *ECE1* expression was not significantly increased after 4 h serum induction (cf. Fig. 5B). In the *cph1* Δ /*efg1* Δ mutant Candidalysin secretion increased from 0 to 352 PSM due to the hyperactive Ahr1 (Fig. 6), which correlates to *ECE1* expression data (cf. Fig. 5B).

More detailed information about the results of the peptide measurement can be found in Tab. 7 (Sec. VII). Summing up, even though a hyperactive Ahr1 was able to significant increase *ECE1* expression in the wild type and the *cph1* Δ /*efg1* Δ mutant, an increase in Candidalysin secretion was only detectable under hyphal growth conditions. This indicates that proper hyphae formation is crucial for correct processing of Ece1 and Candidalysin secretion.

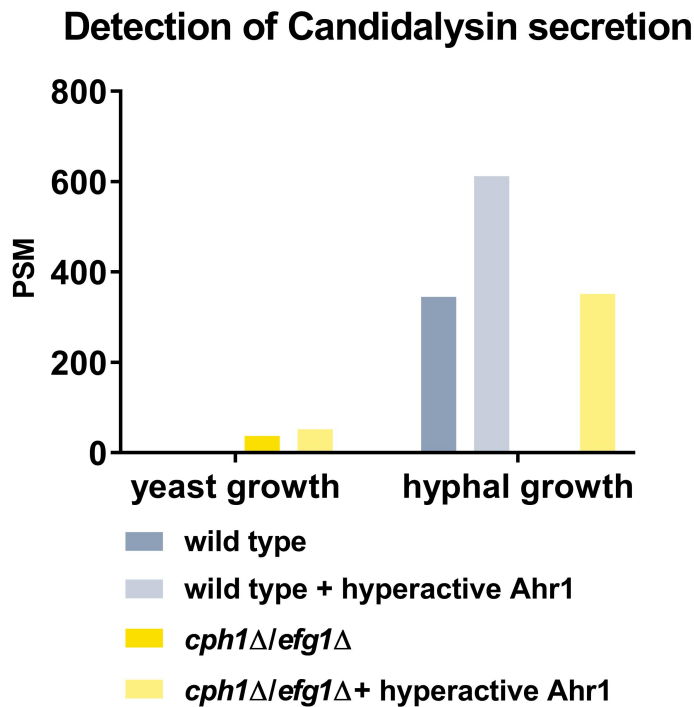


Fig. 6: **Hyperactive Ahr1 increases Candidalysin secretion under hyphal-growth conditions in *C. albicans*.**

Wild type and the *cph1*Δ/*efg1*Δ mutants with or without hyperactive Ahr1 were incubated for 18 h under yeast (YNBS, pH 4, 37°C) or hyphal (YNBS, pH 7.2, 37°C) growth conditions. Candidalysin was extracted from supernatant and measured by LC-MS/MS. PSM= peptide spectrum matches.

3.3.3. Hyperactive Ahr1 only leads to slight increase of cytotoxicity of the *ahr1*Δ and the *cph1*Δ/*efg1*Δ mutants

Candidalysin is a toxin and, upon secretion from *C. albicans* hyphae, directly damages epithelial membranes (Moyes *et al.*, 2016). The secretion of Candidalysin could be increased in the wild type and the *cph1*Δ/*efg1*Δ mutant with hyperactive Ahr1 (Fig. 6). Accordingly, the ability to induce damage should be increased due to a hyperactive Ahr1. To investigate this, LDH release assays were performed with the help of Stefanie Allert and Rita Müller (both: HKI, Jena). Therefore, the wild type and the *ahr1*Δ and the *cph1*Δ/*efg1*Δ mutants with and without hyperactive Ahr1 were coincubated with TR146 buccal epithelial carcinoma cells for 24 h (strain no. 1, 177, 104, 157, 271 and 517, Tab. 1). Subsequently, the release of LDH was measured. Cytotoxicity of each strain was calculated in relation to uninfected, triton-x killed TR146 cells. The result is displayed in Fig. 7. In accordance to the *ECE1* transcription (cf. Fig. 3 and 5) and Candidalysin secretion data (cf. Fig. 6 and 4), the cytotoxicity of the *ahr1*Δ and the *cph1*Δ/*efg1*Δ mutants was significantly lower compared to the wild type. This correlates to already published data (Allert *et al.*, 2018; Lo *et al.*, 1997). In the wild type background, no additional damage was induced due to a hyperactive Ahr1. This could be due to fact that a certain (wild type) level of Candidalysin was sufficient to induce damage to host cells. A hyperactive Ahr1 was able to

increase the cytotoxicity of the *ahr1* Δ mutant from 16.6% to 36.4% and in the *cph1* Δ /*efg1* Δ mutant from 3.0% to 23.4%. However, these increases were not significant.

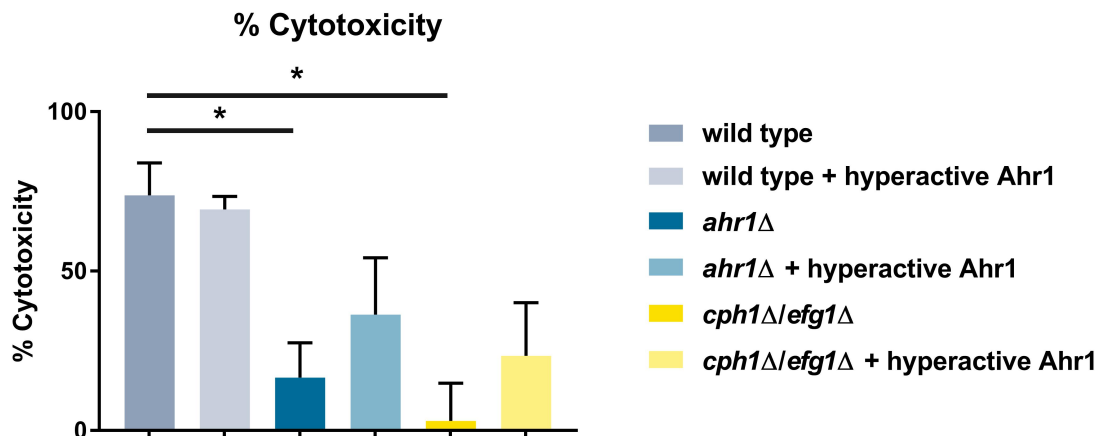


Fig. 7: Cytotoxicity of the wild type and the *ahr1* Δ and the *cph1* Δ /*efg1* Δ mutants with and without hyperactive Ahr1.

TR146 cells were coincubated with wild type and the *ahr1* Δ and the *cph1* Δ /*efg1* Δ mutants with and without hyperactive Ahr1 for 24 h. Cell damage was quantified by LDH release assay. Cytotoxicity of each strain was calculated in relation to uninfected cells killed with triton-x. The assay was performed in triplicates and values of three independent experiments were combined. Asterisks mark significant differences (* $p \leq 0.05$, two tailed, unpaired student's t-test).

3.3.4. Mutants lacking *AHR1* or *CPH1* and *EFG1* can still invade epithelial cells

Due to a low cytotoxicity of the *ahr1* Δ and the *cph1* Δ /*efg1* Δ mutants, which could not be significantly increased via a hyperactive Ahr1, the ability of the mutants to invade TR146 was analyzed. Therefore, TR146 cells were infected with wild type, *ahr1* Δ and *cph1* Δ /*efg1* Δ cells with and without the hyperactive Ahr1 (strain no. 1, 177, 104, 157, 271 and 517, Tab. 1). After 4 h growth at 37°C and 5% CO₂, non-adherent fungal cells were washed away. Extracellular *C. albicans* cells were stained with concanavalin A conjugated to fluorescein (Fig. 8, red). Subsequently, cells were permeabilized and whole fungal cells were stained using calcofluor white (Fig. 8, blue). Fluorescence microscopy revealed that not only wild type but also the *ahr1* Δ and the *cph1* Δ /*efg1* Δ mutants were able to invade TR146 cells (Fig. 8, arrows mark points of invasion). Since the fungal cells were alive and not fixed for the invasion assay, it can not be excluded that the fungi were endocytosed by the epithelial cells. Interestingly, the *cph1* Δ /*efg1* Δ mutant formed elongated cells after incubation on TR146 cells. Unsurprisingly, a hyperactive Ahr1 did not influence the ability to invade TR146 cells (Fig. 8) but did lead to further elongation of *cph1* Δ /*efg1* Δ cells under these conditions. While 37% of counted wild type cells were invasive (total n=421), 44% of the *cph1* Δ /*efg1* Δ cells (total n=200) and 50% of the *ahr1* Δ (total n=562) cells were invading epithelial cells. This was unexpected and contradictory to prior experiments (cf. Fig. 7). However, at least for the wild type and the *cph1* Δ /*efg1* Δ mutant, it can be explained with a general decreased ability of the deletion mutant to adhere to epithelial cells. On

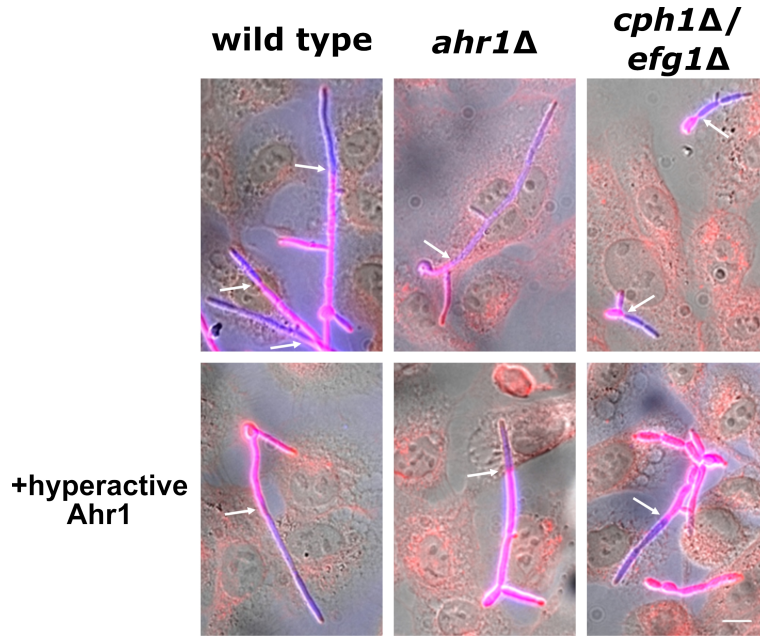


Fig. 8: **Invasion capacities are not inhibited in the *ahr1*Δ and the *cph1*Δ/*efg1*Δ mutants.**

C. albicans wild type and the *cph1*Δ/*efg1*Δ and the *ahr1*Δ mutants with or without hyperactive Ahr1 were coincubated with TR146 cells at 37°C and 5% CO₂. After 4 h, extracellular *C. albicans* cells were stained with concanavalin A conjugated to fluorescein (red). Subsequently cells were permeabilized and whole *C. albicans* cells were stained with calcofluor white (blue). An overlay of the DIC, the GFP (red) and the DAPI (blue) channel is displayed. Arrows indicate points of invasion of *C. albicans* cells into TR146 cells. Bar=10 μm.

average 359 wild type but only 32 *cph1*Δ/*efg1*Δ cells were counted per mm² coverslip (cells on 4 mm² coverslip were counted per strain). Probably, those adherent *cph1*Δ/*efg1*Δ cells only adhered because they were invading or endocytosed by the epithelial cells. Due to this, further quantification of invasive cells with hyperactive Ahr1 was not performed.

3.3.5. Hyperactive Ahr1 induces *ECE1* expression independent of Ume6, Tec1, Ndt80 and Brg1

A screen of activator mutants (see section 3.1.2) revealed that not only in the *cph1*Δ/*efg1*Δ and the *ahr1*Δ but also in the *ume6*Δ, the *tec1*Δ, the *ndt80*Δ and the *brg1*Δ mutants *ECE1* expression was significantly downregulated compared to the wild type. Additionally, morphology under hyphae-inducing conditions varied from that of the wild type. Thus, it was investigated whether the ability of the hyperactive Ahr1 to induce *ECE1* expression was dependent on one of these transcription factors. Further on, microscopy should reveal if the hyperactive Ahr1 changed the morphology of these mutants in a similar fashion as in the wild type and the *cph1*Δ/*efg1*Δ mutant. A hyperactive Ahr1 did not have an influence on the morphology of the *ume6*Δ and the *tec1*Δ mutants after 4 h incubation in SDG (strain no. 12, 214, 145 and 150, Tab. 1, Fig. 9A). For the *ndt80*Δ and the *brg1*Δ mutants, a hyperactive Ahr1 led to the elongation and increased the clustering of yeast cells, as shown in Fig. 9A and C (strain no. 374, 504 and 143, 148, Tab. 1).

An *ECE1* promoter driven GFP reporter system was transformed into the *brg1* Δ mutant with and without hyperactive Ahr1. Already under yeast growth conditions a bright GFP fluorescence was visible in the mutant with hyperactive Ahr1 (Fig. 9C). After 4 h of hyphal induction with 10% human serum, the *ume6* Δ mutant was able to form short filaments (Fig. 9A). It is already known that this mutant is unable to extend hyphal formation (Carlisle and Kadosh, 2010).

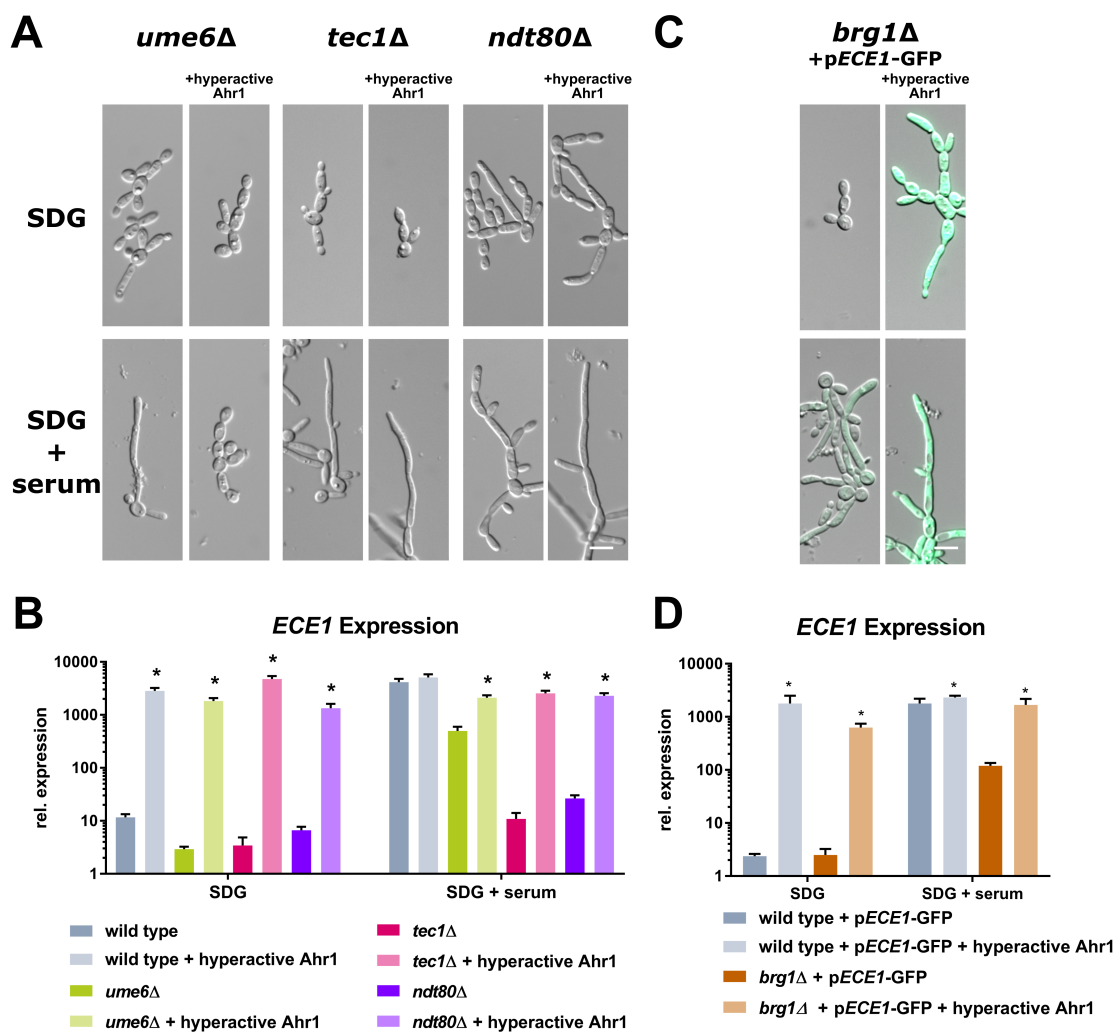


Fig. 9: Hyperactive Ahr1 induces *ECE1* expression independent of Ume6, Tec1, Ndt80 and Brg1.

Micrographs of the *ume6* Δ , the *tec1* Δ , the *ndt80* Δ (A) and the *brg1* Δ mutants (with GFP reporter system, C) with or without hyperactive Ahr1. Strains were grown for 4 h in SDG with or without 10% human serum prior to microscopy. Bar=10 μ m.

Total RNA of the wild type and the *ume6* Δ , the *tec1* Δ , the *ndt80* Δ mutants (B) and the wild type and the *brg1* Δ mutants (with GFP reporter system, D) with or without hyperactive Ahr1 was isolated after 4 h growth in SDG with or without 10% human serum in biological triplicates. 100 ng/ μ l of this RNA was used for RT-qPCR to determine the relative expression of *ECE1*. Data was normalized to a control RNA (wild type, 6 h YPD, 37°C) and the housekeeping gene *ACT1*. Asterisks mark significant differences of hyperactive Ahr1 mutants compared to the respective parental strain (* $p \leq 0.05$, two tailed, unpaired student's t-test).

In contrast to this, the *ume6* Δ mutant with hyperactive Ahr1 only grew as yeast after 4 h serum induction, as depicted in Fig. 9A. The mutant lacking *TEC1* with or without hyperactive Ahr1 was only able to form pseudohyphae under hyphal growth conditions. After serum induction, the *ndt80* Δ mutant formed short elongated cells, which regularly branched off. This correlated to already published data (Sellam *et al.*, 2009). A hyperactive Ahr1 in the *ndt80* Δ background led to increased elongation of cells but only pseudohyphae and no true hyphae formation. While only a faint GFP signal was visible in some *brg1* Δ filaments, the *brg1* Δ mutant with hyperactive Ahr1 showed a bright GFP fluorescence under hyphal growth conditions (Fig. 9C).

As shown in Figures 9B and D, RT-qPCR analyses revealed that a hyperactive Ahr1 was able to significantly increase *ECE1* expression in all of these mutants up to or close to wild type level expression under hyphae-inducing but also non-inducing conditions (strain no. 266, 145, 374, 380, 12, 215, 262 and 148, Tab. 1). For the *brg1* Δ mutants with and without hyperactive Ahr1, strains with the GFP reporter system were analysed. Since the GFP gene was transformed into the *ECE1* locus in these mutants, a wild type which also possessed the GFP reporter system was used as control. The analyses indicate that the mechanism by which the hyperactive Ahr1 induces *ECE1* expression is independent of the transcription factors Ume6, Tec1, Ndt80 and Brg1.

3.3.6. Hyperactive Ahr1 has no effect on *ECE1* expression in the *tup1* Δ mutant

It was shown that a hyperactive Ahr1 is able to induce *ECE1* expression in wild type *C. albicans* cells even without the usual hyphal induction by human serum (cf. Fig. 5). This significant increase in expression was independent from several transcription factors with possible binding sites in the 5' intergenic region of *ECE1* (cf. Fig. 5 and 9). It has already been postulated that Tup1 may play a regulating role in *C. albicans* hyphae (Garbe, 2016). The question arose whether a hyperactive Ahr1 was able to induce *ECE1* expression in the absence of Tup1. Therefore, the hyperactive Ahr1 was transformed into a *tup1* Δ mutant with the *ECE1*-promotor-driven GFP reporter system.

Fig. 10A illustrates that after 4 h growth in yeast and hyphal growth medium, a hyperactive Ahr1 had no beneficial effect on the GFP signal in the absence of Tup1 (strain no. 94, 127, 116 and 132, Tab. 1). The same phenomenon was observed in RT-qPCR analysis displayed in Fig. 10B (strain no. 1, 177, 14 and 438, Tab. 1). Even though *ECE1* expression of the *tup1* Δ mutant was higher than in the wild type under yeast growth conditions, *ECE1* expression could neither be elevated due to incubation with human serum nor due to a hyperactive Ahr1 (Fig. 10B). This suggests that the function of a hyperactive Ahr1 is dependent on Tup1, a known repressor of hyphal growth, for high level expression of *ECE1*. Corresponding to the low *ECE1* expression of the *tup1* Δ mutant, Candidalysin secretion of this mutant was much lower than in the wild type after 4 h serum-induction, as depicted in Fig. 10C.

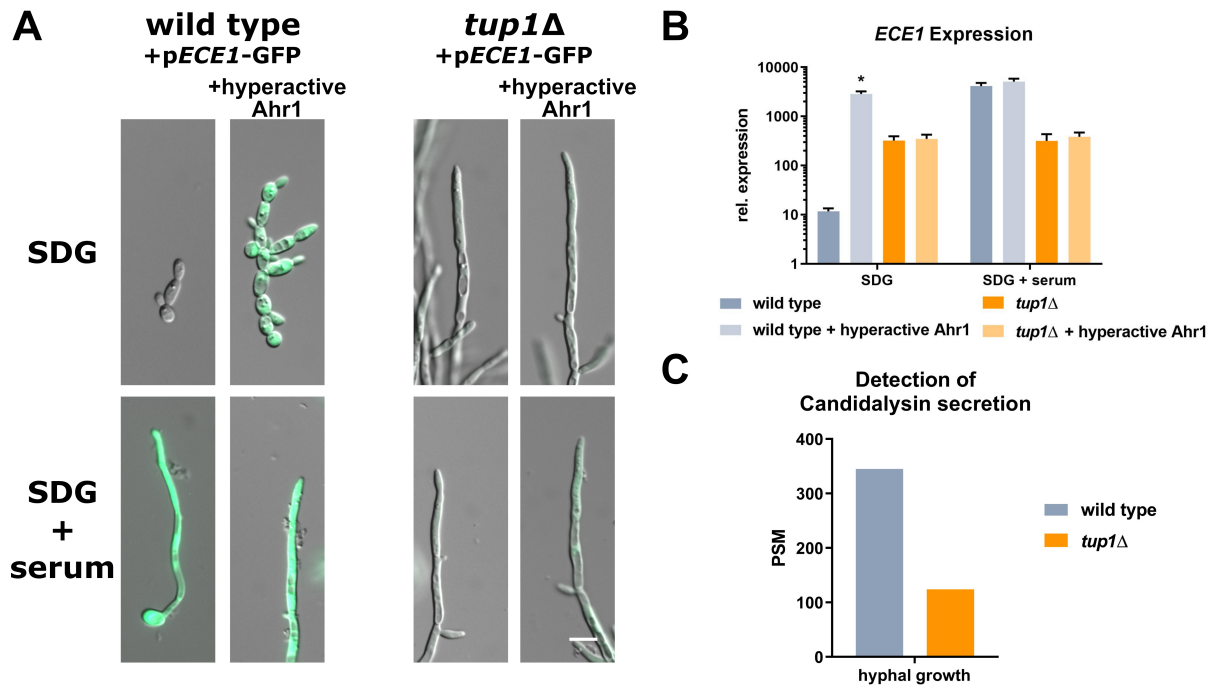


Fig. 10: **Hyperactive Ahr1 depends on Tup1 for induction of high-level *ECE1* expression.**

A Wildtype and *tup1Δ* with *ECE1*-promotor-driven GFP and with or without hyperactive Ahr1 were incubated for 4 h in SDG with or without 10% human serum prior to microscopy. Images from the DIC and the GFP channel were merged. Bar=10 μ m.

B Total RNA of the wild type and the *tup1Δ* mutants with or without hyperactive Ahr1 was isolated after 4 h growth in SDG with or without 10% human serum in biological triplicates. 100 ng/ μ l of this RNA was used for RT-qPCR to determine the relative gene expression of *ECE1*. Data was normalized to a control RNA (wild type, 6 h YPD, 37°C) and the housekeeping gene *ACT1*. Asterisks mark significant differences of hyperactive Ahr1 mutants compared to the respective parental strain (* $p \leq 0.05$, two tailed, unpaired student's t-test).

C Wild type and the *tup1Δ* mutant were incubated for 18 h under hyphal growth conditions (YNBS pH 7.2, 37°C). Candidalysin was extracted from supernatants and measured by LC-MS. PSM= peptide spectrum matches.

3.4. Ahr1 activates expression of core filamentation response genes

3.4.1. Ahr1 is important for the expression of other core filamentation response genes in hyphae

Upon hyphal formation of *C. albicans* a certain set of core filamentation response (CFR) genes is upregulated (Martin *et al.*, 2013). Knowing that Ahr1 plays an important role in the regulation of *ECE1*, it was determined if this transcription factor also played a role in the expression of other CFR genes.

RT-qPCR analyses of RNA extracted after 4 h growth at 37°C in SDG with 10% humans serum suggest that Ahr1 was also important for high-level expression of *ALS3*, *DCK1*, *HGT2*, *HWP1*, *IHD1* and orf19.2457 (strain no. 1 and 271, Tab. 1, Fig. 11). Interestingly, *RBT1* expression was

significantly increased in the *ahr1* Δ mutant compared to the wild type. Summing up, Ahr1 has an influence on the expression of several CFR genes under hyphae-inducing conditions.

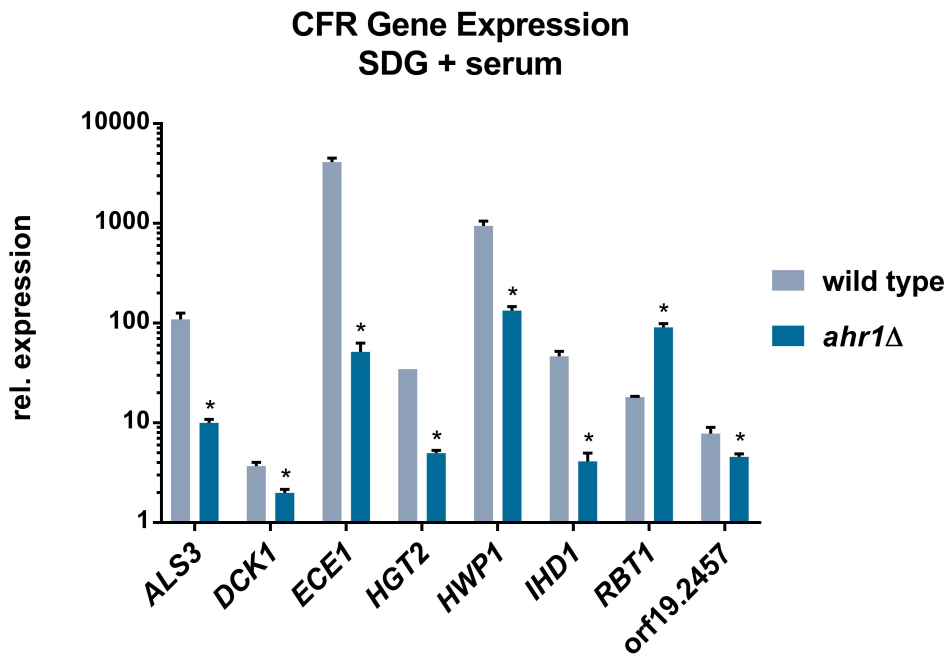


Fig. 11: **Ahr1 is important for the expression of core filamentation response genes in *C. albicans* hyphae.**

Total RNA of the wild type and the *ahr1* Δ mutant was isolated after 4 h growth in SDG with 10% human serum in biological triplicates. 100 ng/ μ l of this RNA was used for RT-qPCR to determine the relative gene expression of *ALS3*, *DCK1*, *ECE1*, *HGT2*, *HWP1*, *IHD1*, *RBT1* and orf19.2457. The data was normalized to a control RNA (wild type, 6 h YPD, 37°C) and the housekeeping gene *ACT1*. Asterisks mark significant differences between the wild type and the *ahr1* Δ mutant (* $p \leq 0.05$, two tailed, unpaired student's t-test).

3.4.2. Hyperactive Ahr1 is able to induce the expression of other core filamentation response genes independent of Cph1 and Efg1

As shown earlier, Ahr1 was important for the expression of other core filamentation response genes (Fig. 11) and a hyperactive Ahr1 was able to induce *ECE1* expression in the wild type background and the *cph1* Δ /*efg1* Δ mutant (Fig. 5). Due to this, it was investigated whether the hyperactive Ahr1 was also able to influence the expression of the other CFR genes. Indeed, a hyperactive Ahr1 was able to significantly induce *ALS3*, *HWP1* and *IHD1* expression in the wild type, independent of Cph1 and Efg1 and already under yeast growth conditions (strain no. 1, 177, 104 and 157, Tab. 1, Fig. 12). For *HGT2*, *RBT1*, *DCK1* and orf19.2457 this pattern could not be observed. A hyperactive Ahr1 was able to significantly induce *HGT2* expression in the wild type in yeast growth conditions. However, under hyphal growth conditions *HGT2* expression was significantly reduced in a wild type with hyperactive Ahr1. This was also true for *RBT1* and *DCK1* expression. Additionally, *RBT1* and *DCK1* expressions were significantly increased in the *cph1* Δ /*efg1* Δ double mutant with hyperactive Ahr1 under yeast growth condi-

tions. orf19.2457 expression was significantly increased in the wild type with hyperactive Ahr1 under yeast growth conditions. Apart from this, a hyperactive Ahr1 did not have an influence on orf19.2457 expression.

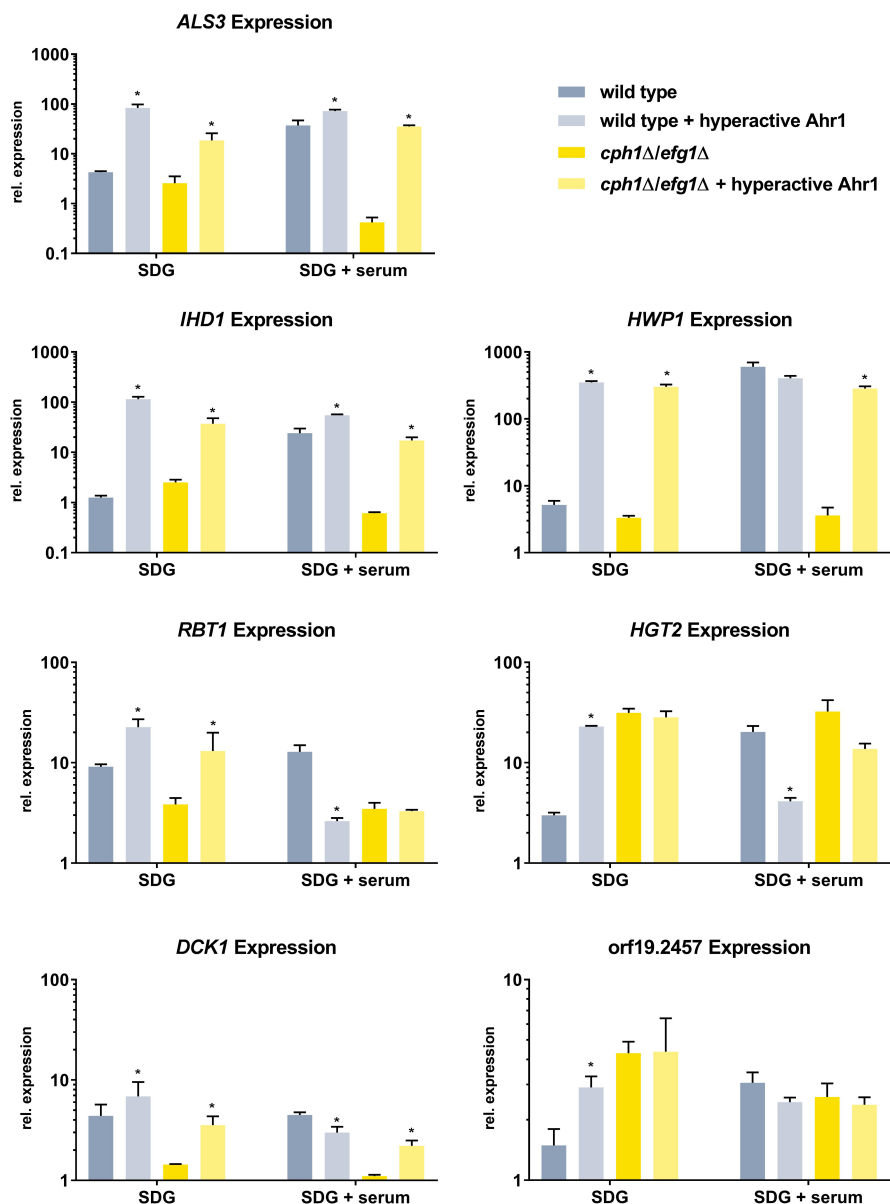


Fig. 12: **Hyperactive Ahr1 induces expression of *ALS3*, *HWP1* and *IHD1* independent from *Cph1*/*Efg1*.**

Total RNA of the wild type and the *cph1*Δ/*efg1*Δ mutants with and without hyperactive Ahr1 was isolated after 4 h growth in SDG with and without 10% human serum in biological triplicates. 100 ng/μl of this RNA was used for RT-qPCR to determine the relative gene expression of *ALS3*, *HWP1*, *IHD1*, *HGT2*, *RBT1*, *DCK1* and orf19.2457. Data was normalized to a control RNA (wild type, 6 h YPD, 37°C) and the house-keeping gene *ACT1*. Asterisks mark significant differences of hyperactive Ahr1 mutants compared to the respective parental strain (* $p \leq 0.05$, two tailed, unpaired student's t-test).

3.4.3. Hyperactive Ahr1 relies on Tup1 for the induction of high-level *ALS3* expression

A hyperactive Ahr1 was able to induce the expression of *ALS3* in a Cph1/Efg1- and stimulus-independent manner (cf. Fig. 12). To analyze whether this induction is dependent on *TUP1*, as it was shown earlier for *ECE1* expression (cf. Fig. 10), RNA was extracted from the wild type and the *tup1*Δ mutants with and without hyperactive Ahr1 (strain no. 1, 177, 14, 438, Tab. 1) after 4 h incubation in SDG with or without 10% human serum at 37°C. Interestingly, a hyperactive Ahr1 was not able to increase *ALS3* expression in *tup1*Δ, as illustrated in Fig. 13.

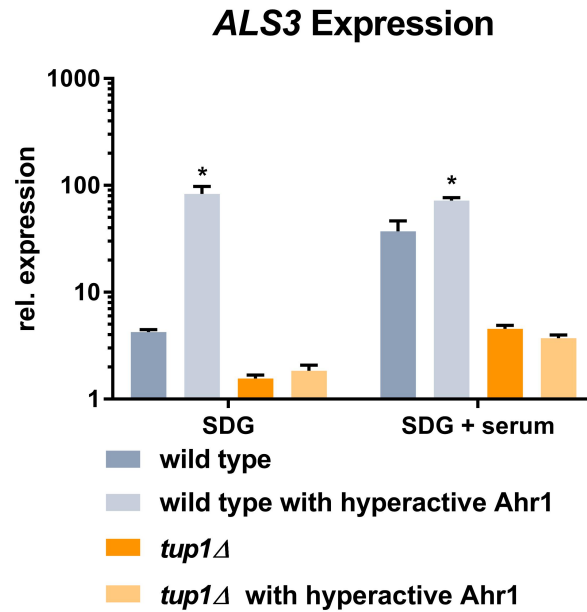


Fig. 13: **Hyperactive Ahr1 depends on Tup1 for induction of high-level *ALS3* expression.**

Total RNA of the wild type and the *tup1*Δ mutants with or without hyperactive Ahr1 was isolated after 4 h growth in SDG with or without 10% human serum in biological triplicates. 100 ng/μl of this RNA was used for RT-qPCR to determine the relative gene expression of *ALS3*. Data was normalized to a control RNA (wild type, 6 h YPD, 37°C) and the housekeeping gene *ACT1*. Asterisks mark significant differences of hyperactive Ahr1 mutants compared to the respective parental strain (* $p \leq 0.05$, two tailed, unpaired student's t-test).

3.4.4. Hyperactive Ahr1 induces Als3 localization on cell surface independent of Cph1 and Efg1

A hyperactive Ahr1 was able to significantly increase *ALS3* expression in the wild type and in the *cph1*Δ/*efg1*Δ double mutant (cf. Fig. 12). To analyze whether this increased *ALS3* expression correlated with an increase in Als3 localization on the cell walls, an Als3 antibody was employed to stain wild type and the *cph1*Δ/*efg1*Δ mutants with and without hyperactive Ahr1 after 6 h growth in yeast or hyphae-inducing medium (strain no. 1, 177, 104 and 157, Tab. 1). Additionally, cells were stained with calcofluor white to visualize the cell walls. Fig. 14 shows that Als3 could already be located on wild type filaments under yeast growth conditions if a hyperactive Ahr1 was present. In contrast to this, the wild type without hyperactive Ahr1 only formed yeast cells, which

did not show an Als3 signal under these conditions (Fig. 14). After serum-induction, the wild type hyphae showed an Als3 signal on the hyphal surfaces which increased towards the hyphal tip. A hyperactive Ahr1 induced clustering of wild type hyphae with the hyphae originating in the middle and elongating towards the outside. The Als3 signal of these cells also increased towards the hyphae tips and was overall a little more intense compared to the wild type without hyperactive Ahr1 (Fig. 14). In the *cph1* Δ /*efg1* Δ mutant with a hyperactive Ahr1, Als3 could

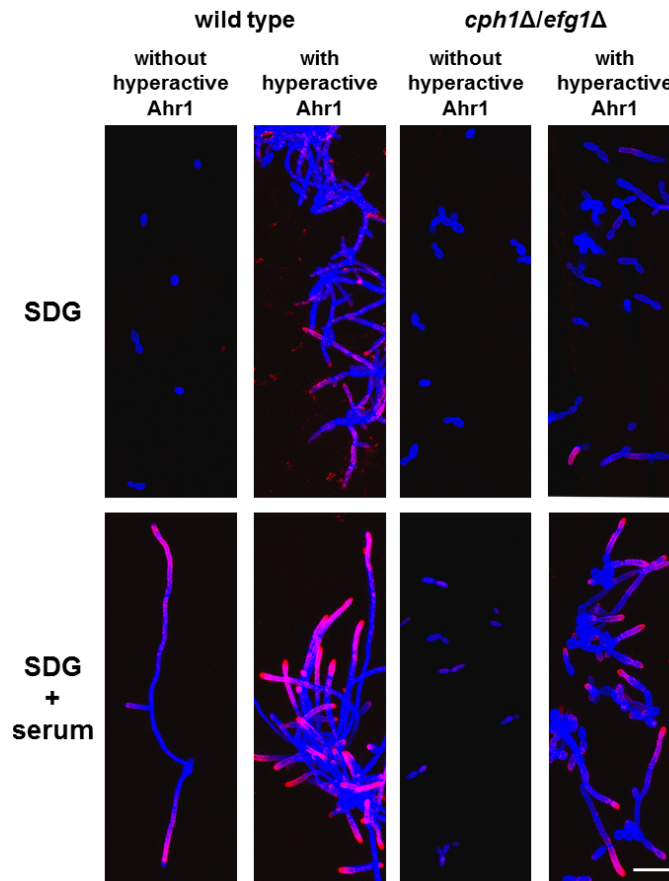


Fig. 14: **Hyperactive Ahr1 induces Als3 localization on cell surface independent of Cph1 and Efg1.**

The wild type and the *cph1* Δ /*efg1* Δ mutants with and without hyperactive Ahr1 were grown for 6 h in SDG with or without 10% human serum at 37°C on μ Dishes. Subsequently, cells were stained with serum raised against Als3 (secondary antibody: goat-anti-Rabbit-488-IgG (red)), fixed with Histofix and stained with calcofluor white (blue). An overlay of the DAPI and the A488 channel is depicted. Bar= 20 μ m.

be localized on some elongated cells and pseudohyphae already under yeast growth conditions (Fig. 14). After serum-induction this mutant formed pseudohyphae. They showed an Als3 signal that increased towards the tips. The respective *cph1* Δ /*efg1* Δ mutant without hyperactive Ahr1 was only able to form yeast cells under these conditions. Some of these cells showed a weak Als3 signal. This demonstrated that a hyperactive Ahr1 was not only able to increase *ALS3* expression independent of Cph1 and Efg1 but it also led to increased localization of the Als3 protein on the cell surface of elongated cells, pseudohyphae and true hyphae.

3.5. ChIP-Seq analyses of hyperactive Ahr1

3.5.1. Hyperactive Ahr1 binds upstream of *ECE1*, *ALS3* and other core filamentation response genes

The hyperactive Ahr1 had an influence on the expression of *ECE1*, *ALS3* and some other CFR genes (cf. Fig. 5 and 12). ChIP-seq experiments were performed to analyze a possible direct binding of the hyperactive Ahr1 upstream of CFR genes. Therefore the wild type with hyperactive Ahr1 with and without HA₃-tag (strain no. 177 and 427, Tab. 1) were grown for 6 h in SDG at 37°C prior to ChIP-Seq analyses. Fig. 15 depicts the ORFs of *ECE1* and *ALS3* (blue), the corresponding coordinates in the genome of the SC5314 wild type and the mapped ChIP-Seq reads (red). In the 5' upstream untranslated region of each gene multiple peaks, which represent binding sites, could be seen. This indicates that the hyperactive Ahr1 bound to multiple regions upstream of the genes.

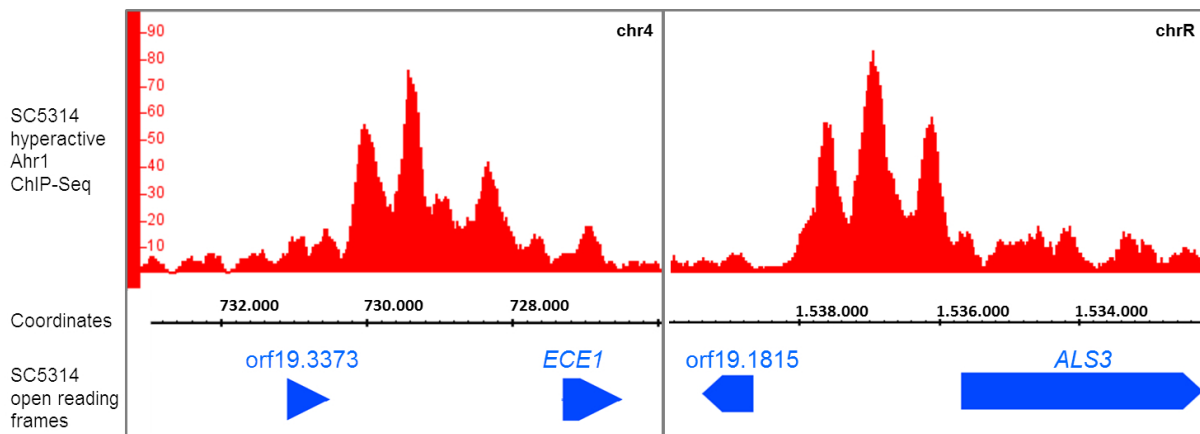


Fig. 15: **Hyperactive Ahr1 binds to 5' intergenic regions of *ECE1* and *ALS3*.**

ChIP-seq reads (red) mapped to the the genome of the SC5314 wild type. The ORFs of *ECE1* and *ALS3* are shown in blue. Images were created in the Integrated Genome Browser (IGB).

A similar pattern could be observed for the CFR genes *HWP1*, *IHD1* and *HGT2*. Fig. 16 shows that in each gene's 5' intergenic region the mapped reads resulted in multiple peaks. For *DCK1* and *RBT1*, one peak upstream of each ORF was identified (Fig. 16). However, these peaks were not as as large as the peaks for *ECE1*, *ALS3*, *HWP1*, *IHD1* and *HGT2* (Fig. 15 and 16). Upstream of orf19.2457 no peak could be identified, as depicted in Fig. 16.

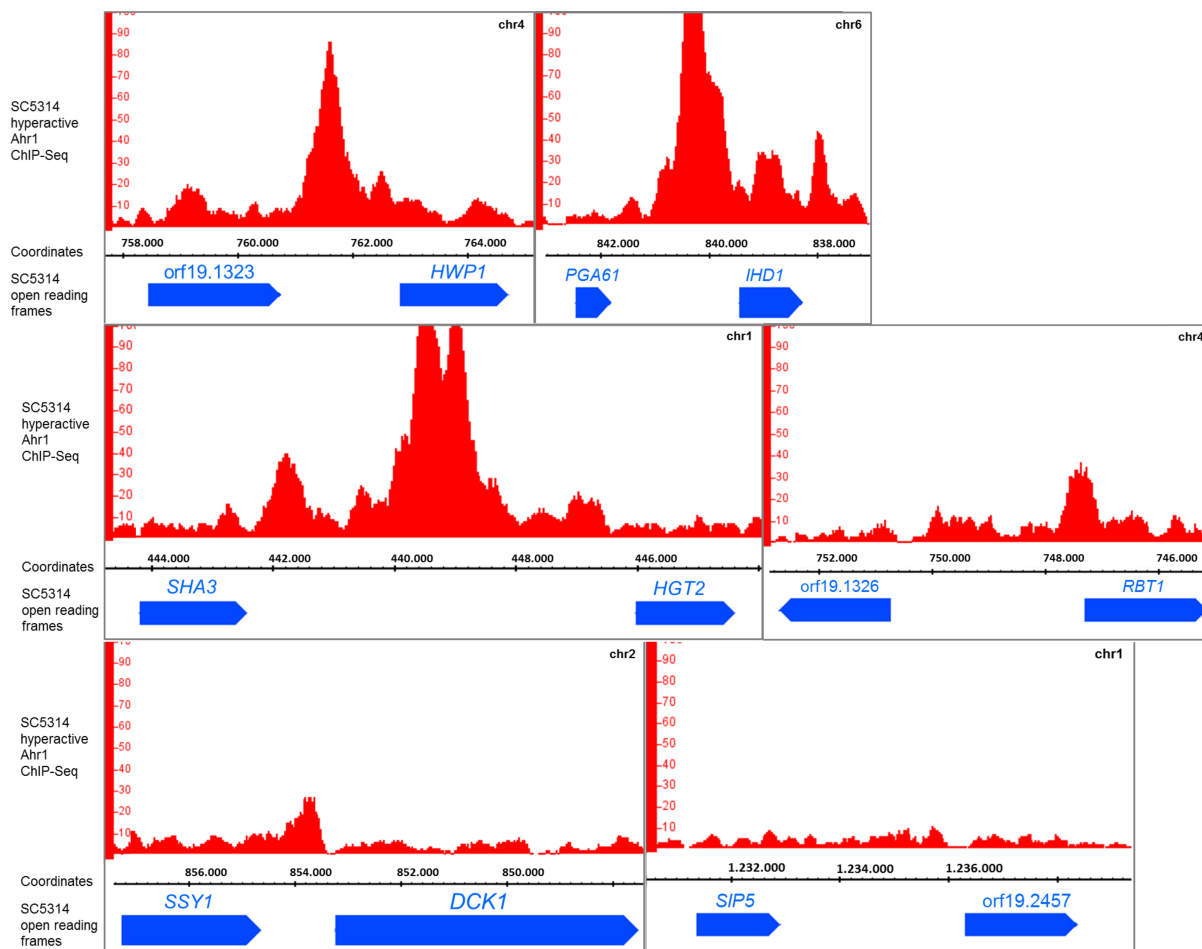


Fig. 16: Hyperactive Ahr1 binds to 5' intergenic regions of *HWP1*, *IHD1*, *HGT2*, *RBT1* and *DCK1* but not *orf19.2457*.

ChIP-seq reads (red) mapped to the the genome of the SC5314 wild type. The open reading frames of *HWP1*, *IHD1*, *HGT2*, *RBT1*, *DCK1* and *orf19.2457* are shown in blue. Images were created in IGB.

3.5.2. Hyperactive Ahr1 binds upstream of and activates the expression of hyphal regulators

The ChIP-Seq data was used to search for other interesting targets of the hyperactive Ahr1. The analyses revealed that the hyperactive Ahr1 bound to 5' intergenic regions of several known regulators of hyphal growth. Since binding does not always result in positive or negative regulation, RT-qPCR analyses were performed to complement the ChIP-Seq data. Therefore, RNA of the wild type and a mutant with hyperactive Ahr1 in the wild type background was extracted under non-inducing growth conditions (strain no. 1 and 177, Tab. 1). In Fig. 17 (left panel) you can see the binding profiles upstream of the ORFs of *AHR1*, *BCR1*, *BRG1* and *EED1*. While upstream of *AHR1*, *BRG1* and *EED1* several large peaks could be found, for *BCR1* only smaller peaks were identified. Fig. 17 (right panel) shows the relative expression of *AHR1*, *BCR1*, *BRG1* and *EED1*. In all cases, the expression was significantly upregulated in the mutant with hyperactive Ahr1. Since the *AHR1-GAD* was transformed into the *ADH1* locus, it was not clear if the binding of Ahr1 to its own promotor resulted in *AHR1* upregulation.

3. Results

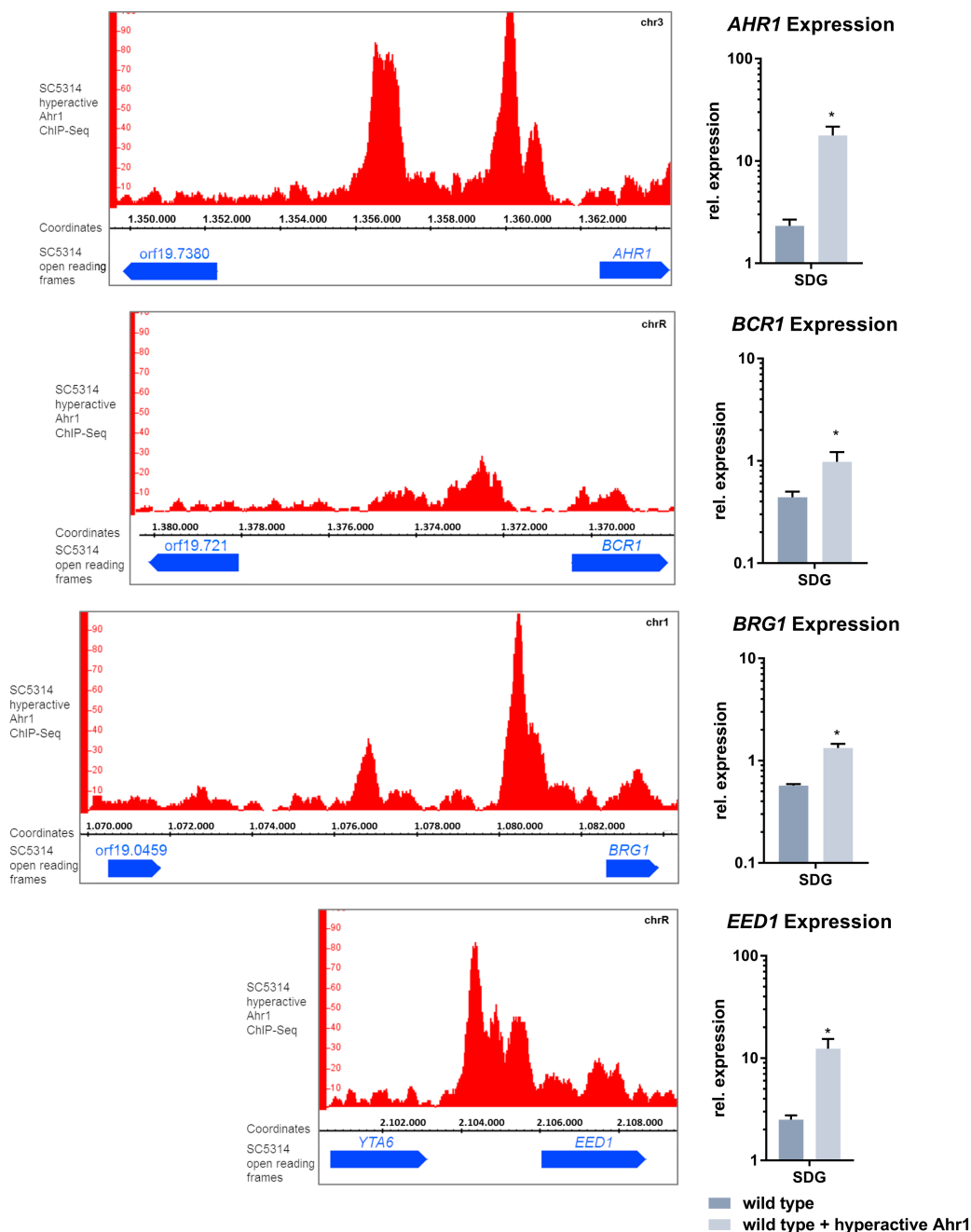


Fig. 17: **Hyperactive Ahr1 regulates *AHR1*, *BCR1*, *BRG1* and *EED1* expression**

Left panel: ChIP-seq reads (red) mapped to the the genome of the SC5314 wild type. The open reading frames of *AHR1*, *BCR1*, *BRG1* and *EED1* are shown in blue. Images were created in the IGB.

Right panel: Total RNA of wild type with and without hyperactive Ahr1 was isolated after 4 h growth in SDG at 37°C in biological triplicates. 100 ng/µl of this RNA was used for RT-qPCR to determine the relative gene expression of *AHR1*, *BCR1*, *BRG1* and *EED1*. Data was normalized to a control RNA (wild type, 6 h YPD, 37°C) and the housekeeping gene *ACT1*. Asterisks mark significant differences of hyperactive Ahr1 mutants compared to the wild type (* $p \leq 0.05$, two tailed, unpaired student's t-test).

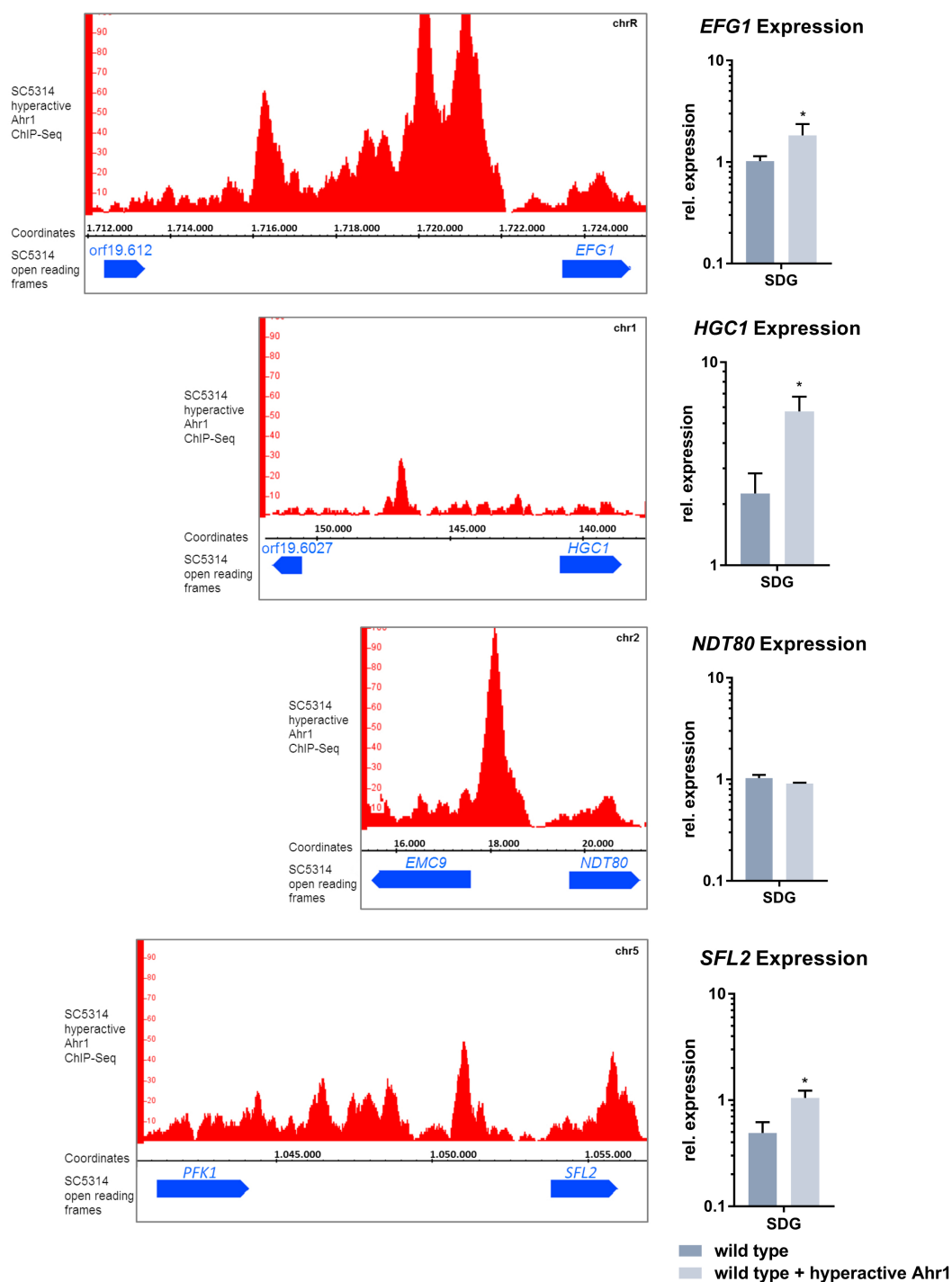


Fig. 18: Hyperactive Ahr1 regulates *EFG1*, *HGC1*, *SFL2* but not *NDT80* expression.

Left panel: ChIP-seq reads (red) mapped to the the genome of the SC5314 wild type. The open reading frames of *EFG1*, *HGC1*, *NDT80* and *SFL2* are shown in blue. Images were created in IGB.

Right panel: Total RNA of wild type with and without hyperactive Ahr1 was isolated after 4 h growth in SDG at 37°C in biological triplicates. 100 ng/μl of this RNA was used for RT-qPCR to determine the relative gene expression of *EFG1*, *HGC1*, *NDT80* and *SFL2*. Data was normalized to a control RNA (wild type, 6 h YPD, 37°C) and the housekeeping gene *ACT1*. Asterisks mark significant differences of hyperactive Ahr1 mutants compared to the wild type (* $p \leq 0.05$, two tailed, unpaired student's t-test).

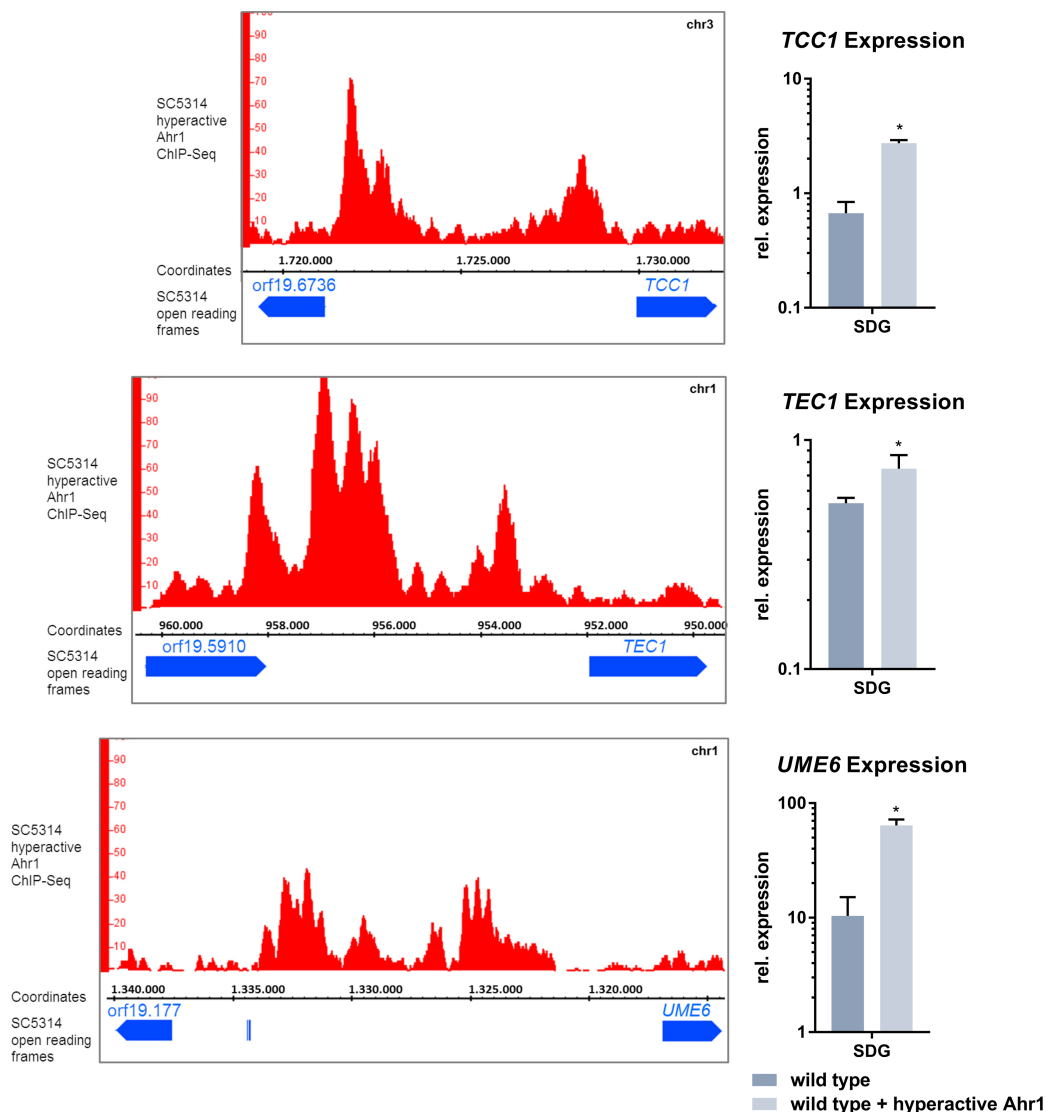


Fig. 19: **Hyperactive Ahr1 regulates *TCC1*, *TEC1* and *UME6* expression**

Left panel: ChIP-seq reads (red) mapped to the the genome of the SC5314 wild type. The open reading frames of *TCC1*, *TEC1* and *UME6* are shown in blue. Images were created in IGB.

Right panel: Total RNA of wild type with and without hyperactive Ahr1 was isolated after 4 h growth in SDG at 37°C in biological triplicates. 100 ng/μl of this RNA was used for RT-qPCR to determine the relative gene expression of *TCC1*, *TEC1* and *UME6*. Data was normalized to a control RNA (wild type, 6 h YPD, 37°C) and the housekeeping gene *ACT1*. Asterisks mark significant differences of hyperactive Ahr1 mutants compared to the wild type (* $p \leq 0.05$, two tailed, unpaired student's t-test).

Fig. 18 (left panel) depicts the ChIP-Seq binding profiles upstream of *EFG1*, *HGC1*, *NDT80* and *SFL2*. Again the binding profile of the hyperactive Ahr1 varied from region to region. For the upstream region of *EFG1* several large peaks were identified. For *HGC1* only one relatively small peak approx. 6,000 bp upstream the start codon was found. Approx. 2,000 bp upstream of the *NDT80* ORF, one large peak was spotted. In the nearly 10,000 bp long 5' intergenic region of *SFL2* several peaks were identified. For *EFG1*, *HGC1* and *SFL2*, expression in the mutant with the hyperactive Ahr1 was significantly upregulated in comparison to the wild type, as displayed

in Fig. 18 (right panel). It also shows that *NDT80* expression was not upregulated, even though the hyperactive Ahr1 bound upstream of the *NDT80* ORF. Since *NDT80* shares the intergenic region with another, so far uncharacterized gene (*EMC9*), it is also possible that the hyperactive Ahr1 regulated the expression of this gene and not *NDT80*. Furthermore, the hyperactive Ahr1 bound to several positions upstream of *TCC1*, *TEC1* and *UME6*, which is presented in Fig. 19 (left panel). The RT-qPCR data in Fig. 19 (right panel) shows that the binding resulted in a significant increase in *TCC1*, *TEC1* and *UME6* expression. Summarizing, the hyperactive Ahr1 bound to several 5' intergenic regions of known regulators of hyphal growth. For *AHR1*, *BCR1*, *BRG1*, *EED1*, *EFG1*, *HGC1*, *SFL2*, *TCC1*, *TEC1* and *UME6* this binding corresponded to an upregulated expression of each regulator. It is of note that several hyphal regulators have relatively large 5' intergenic regions encompassing up to 10,000 base pairs. RT-qPCR analyses showed that binding several thousand base pairs upstream of the start codon still had an influence on expression levels.

3.5.3. The hyperactive Ahr1 binds upstream of genes encoding for other cell wall proteins, hyphal regulators and virulence factors

Next to the already mentioned CFR genes and hyphal regulators, also other targets of the hyperactive Ahr1 could be identified through the ChIP-Seq data. Some interesting findings will be summarized here (detailed summary: Tab. 8 in Sec. VII).

The expression of several cell-wall proteins could potentially be influenced by a hyperactive Ahr1. Next to *ALS3*, also peaks upstream of the ORFs of *ALS1* and *ALS4* could be found. These members of the Als family also encode cell-surface adhesins in the *C. albicans* hyphae (Hoyer *et al.*, 2008). Similarly, peaks upstream of the gene encoding Hyr1, a GPI-anchored hyphal cell wall protein (Bailey *et al.*, 1996) and Eap1, a GPI-anchored cell wall adhesin (Li and Palecek, 2003) were identified.

The hyperactive Ahr1 could also play a role in stress response. It could be involved in the regulation of *CDR1* and *MDR1* expression, genes encoding a multidrug transporter and a multidrug efflux pump. Peaks in front of both ORFs were found. The hyperactive Ahr1 bound upstream of the *SOD5* ORF. The gene *SOD5* encodes superoxide dismutase 5, which is located on the hyphal cell surface. Sods play an important role in the reduction of oxidative stress imposed on the fungus by host immune cells (see Section 1.2.2.4).

Additionally, other important virulence factors could be influenced by the hyperactive Ahr1. Peaks were also identified in the 5' intergenic regions of genes encoding for the secreted aspartyl proteinases Sap4, Sap5 and Sap6. These hydrolases are associated with hyphal cell walls. They enable nutrient acquisition from host cells through tissue damage, thus enhancing virulence (cf. Sec. 1.2.2.3).

It is known that Ahr1 plays a critical role in white-opaque-switching of *C. albicans*. It has already been shown that Ahr1 directly binds upstream of and regulates the expression of the other regulators of the white-opaque switch *EFG1*, *WOR1*, *WOR2*, *WOR3* and *CZF1* (Hernday *et al.*, 2013). The ChIP-Seq experiments conducted in this study indicate that this binding pattern is also true for the hyperactive Ahr1.

Additionally, peaks upstream of *LMO1*, a gene encoding a protein involved in invasive filamen-

tous growth together with Dck1 and Rac1 (Hope *et al.*, 2010), were found. Next to the already mentioned regulation of the expression of the transcription factor Sfl2, which is required for filamentous growth, also Sfl1, a negative regulator of hyphal development (Cao *et al.*, 2006) could be a possible target of the hyperactive Ahr1. Several peaks lay upstream of the transcription factor's ORF. Another transcription factor, that could be influenced by the binding of the hyperactive Ahr1 to its 5' intergenic region is Flo8. It is required for hyphal formation as it regulates hyphal gene expression (Cao *et al.*, 2006).

Lastly, it should be mentioned that the hyperactive Ahr1 also bound upstream of genes encoding for Stp2 and Rim101. Stp2 is a transcription factor that is required for the alkalization of medium (Vylkova *et al.*, 2011). Rim101 drives hyphal formation under alkaline conditions (Bensen *et al.*, 2004).

A list of the genes mentioned in the last three sections and the corresponding properties of the read peaks (e. g. exact location, height) and identified motifs can be found in Tab. 8 in Sec. VII.

3.5.4. The binding motif of the hyperactive Ahr1

Using the ChIP-Seq data and the MEME-ChIP tool (Machanick and Bailey, 2011) one highly significant, centrally enriched binding motif of the hyperactive Ahr1 was identified. This motif, displayed in Fig. 20, correlates to an already published motif of Ahr1 (Hernday *et al.*, 2013). MochiView (Homann and Johnson, 2010) was used to visualize the motif in the genome with the corresponding ChIP reads.

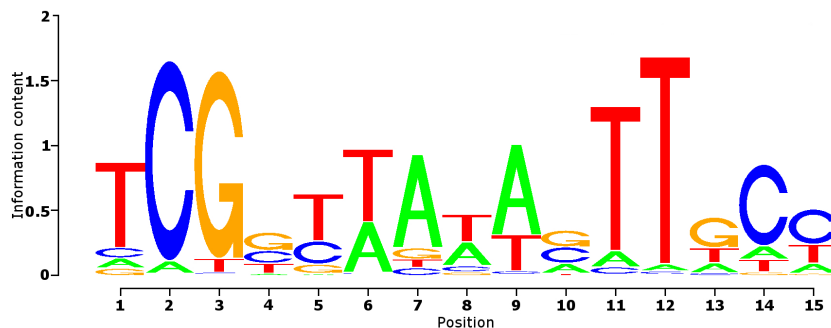


Fig. 20: **Binding site motif of hyperactive Ahr1 identified using MEME-ChIP.**

Distribution of adenine (A), cytosine (C), guanine (G) and thymine (T) bases in the binding motif. The higher the corresponding letter, the more likely this base is present on that position in the motif sequence.

Focussing on hypha-specific genes, it was found that several peaks contained one or more motifs. Oftentimes, the position of the motif coincided with local maxima (peak summit) in the peaks. An example for this can be seen in Fig. 21 which shows a screenshot of the *ECE1* ORF and its 5' upstream region. The identified peak, the peak summit and the identified motifs with motif scores are displayed here. The motif score (red) states how identical the identified binding motif (Fig. 20) is with the corresponding motif found in the genome (lowest score is 0, highest score is 6.58). A sought out list of CFR genes, hypha-specific transcription factors, virulence genes, other already mentioned genes (Sec. 3.5.3) and the corresponding motifs identified in their intergenic regions can be found in Sec. VII (Tab. 8).

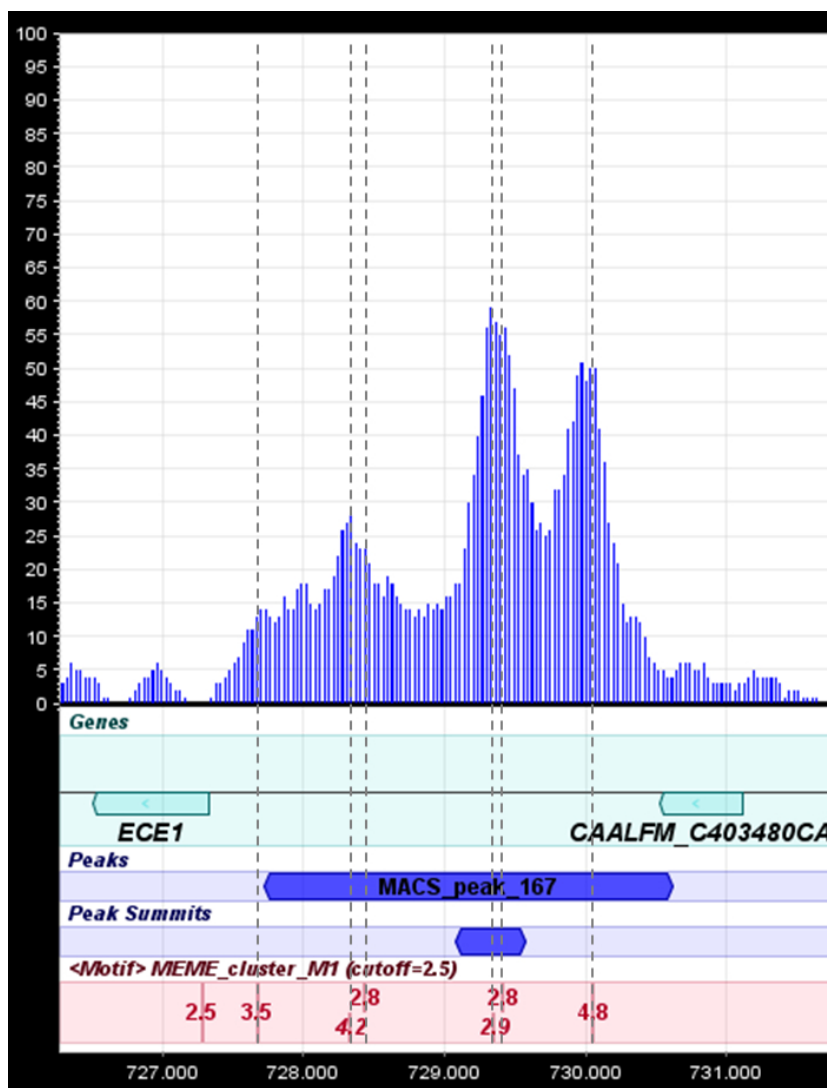


Fig. 21: Identified binding motifs coincide with local peak summits in 5' intergenic region of *ECE1*.

ECE1 ORF with corresponding ChIP-Seq reads, the identified peak with summit and identified binding motifs including motif score. The dashed lines indicate that identified motifs often coincide with local peak maxima. Image created with MochiView (v. 1.46, Homann and Johnson (2010)).

3.6. The role of Mcm1 in the expression of *ECE1* and other core filamentation response genes

3.6.1. *MCM1* overexpression induces expression of *ECE1* in a partly Ahr1-dependent manner

As established in this study, Ahr1 plays an important role in the in the high-level expression of *ECE1* and other core filamentation response genes. Further on, Askew *et al.* (2011) found that Ahr1 serves as a cofactor of Mcm1 by binding to the promoters of adhesion genes and recruiting Mcm1 to these binding sites. Subsequently, the Ahr1-Mcm1-complex was shown to activate the expression of these genes (e. g. *ALS1*, *ALS4*, *HWPI*, *EFG1*, *TEC1*, Askew *et al.* (2011)). Additionally, the transcription factor Mcm1 possesses three possible binding sites in the

5' intergenic region of *ECE1* (cf. sec. 3.1.1). Thus, the role of *Mcm1* in the expression of *ECE1* and other CFR genes was investigated. Since *MCM1* is an essential gene (Rottmann *et al.*, 2003), the influence of *MCM1* deletion on *ECE1* expression could not be investigated. Therefore, *MCM1* overexpression mutants in the wild type background and in the *ahr1* Δ mutant were generated by transforming the *MCM1* gene into the *ADH1* locus. Additionally, the *ECE1*-promotor-driven GFP reporter system was employed to visualize *ECE1* expression (strain no. 127, 413,128 and 414, Tab. 1). In the wild type *MCM1* overexpression induced cell elongation and a GFP signal in some cells, already under yeast growth conditions (Fig. 22A). In the *ahr1* Δ mutant there was neither a morphological change due to overexpression of *MCM1* nor a visible GFP signal under yeast growth conditions (Fig. 22A). After serum-induction *MCM1* overexpression induced a GFP signal in wild type hyphae, which was slightly more intense than in the corresponding parental strain (Fig. 22A). While no GFP signal was observable in the *ahr1* Δ hyphae, *MCM1* overexpression in the *ahr1* Δ mutant induced a faint GFP signal in hyphae (Fig. 22A). This data correlated with RT-qPCR data, displayed in Fig. 22B (strain no. 1, 350, 271, 352, Tab. 1).

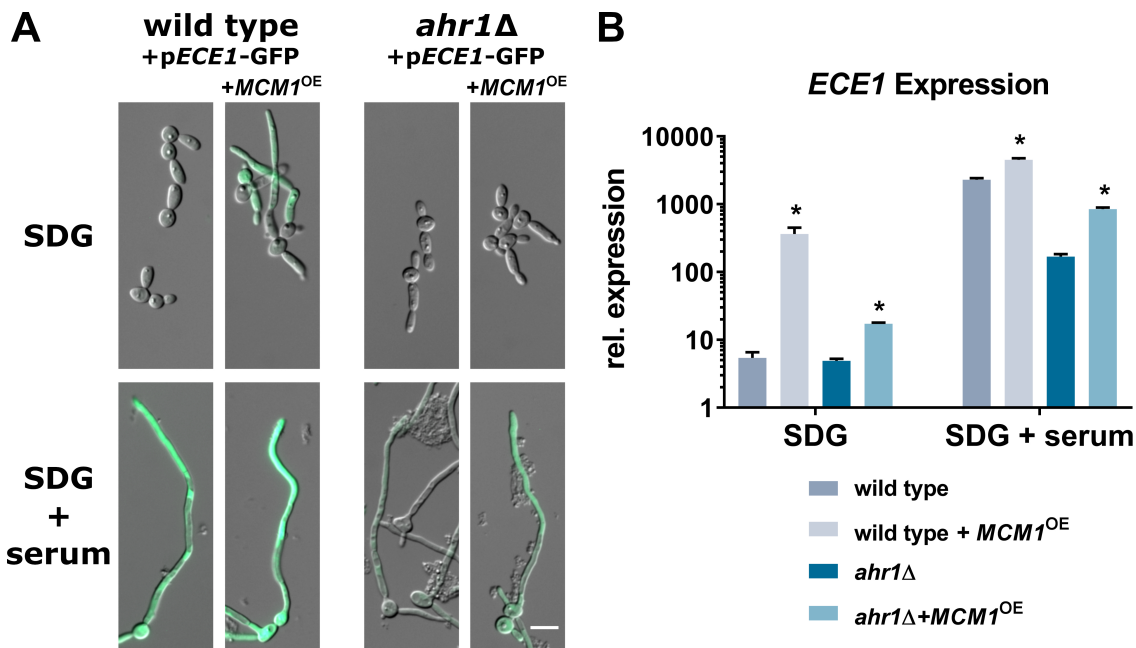


Fig. 22: *MCM1* overexpression (*MCM1*^{OE}) induces *ECE1* expression in partly Ahr1-dependent manner.

A *MCM1* overexpressing strains of the wild type and the *ahr1* Δ mutants with the *ECE1*-promotor driven GFP reporter system were grown for 4 h in SDG with or without 10% human serum prior to microscopy. DIC and GFP channel images were merged. Bar=10 μ m.

B Total RNA of the wild type and the *ahr1* Δ mutants with and without *MCM1* overexpression was isolated after 4 h growth in SDG with and without 10% human serum in biological triplicates. 100 ng/ μ l of this RNA was used for RT-qPCR to determine the relative gene expression of *ECE1*. Data was normalized to a control RNA (wild type, 6 h YPD, 37°C) and the housekeeping gene *ACT1*. Asterisks mark significant differences of hyperactive Ahr1 mutants compared to the respective parental strain (* $p \leq 0.05$, two tailed, unpaired student's t-test).

It showed a significant increase in *ECE1* expression in the wild type which overexpressed *MCM1* compared to the parental wild type strain. An increased expression of *ECE1* was also measured in the *ahr1* Δ mutant in which *MCM1* was overexpressed. However this increase was not as high as in the wild type. It appears that in order to induce high-level *ECE1* expression by *MCM1* overexpression, Ahr1 (a known cofactor of Mcm1 (Askew *et al.*, 2011)) needed to be present.

3.6.2. The induction of *ECE1* expression via *MCM1* overexpression relies on Tup1 and partly on Cph1 and Efg1

To further analyse the role of Mcm1 in *ECE1* regulation, the *MCM1*^{OE} construct was transformed into the *tup1* Δ and the *cph1* Δ /*efg1* Δ mutants. Fig. 23A shows micrographs of the strains taken after 4 h incubation in SDG with or without 10% human serum at 37°C (strain no. 1, 14, 104, 350, 439 and 462, Tab. 1). In the wild type background the overexpression of *MCM1* already led to the formation of short hyphae under non-inducing conditions. The *tup1* Δ mutant was hyperfilamentous, already under non-inducing conditions. Overexpression of *MCM1* did not change its morphology (Fig. 23A). After 4 h growth in SDG medium, the *cph1* Δ /*efg1* Δ mutants with or without *MCM1* overexpression did solely grow in yeast form.

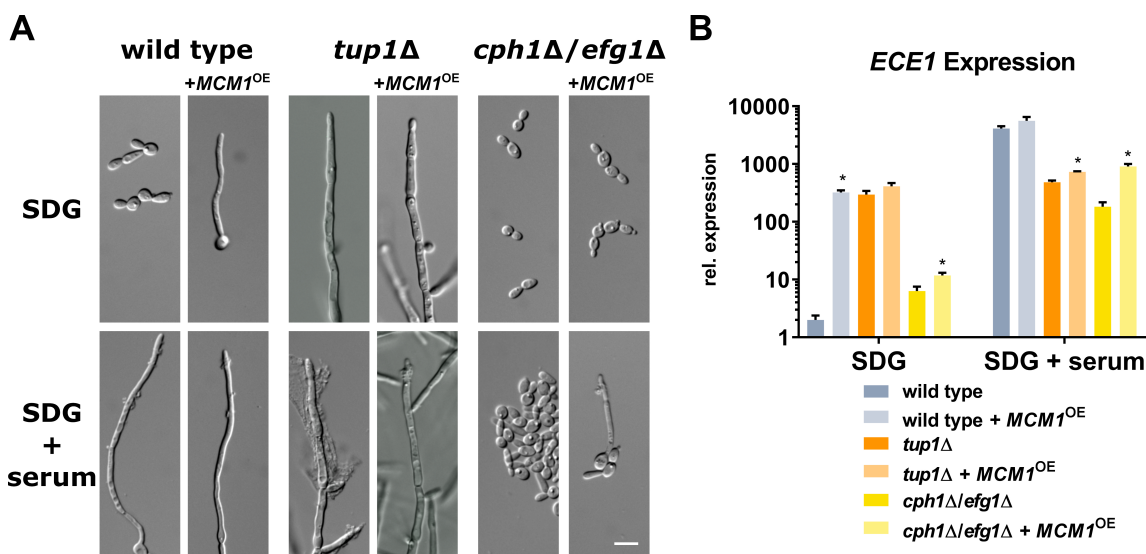


Fig. 23: Induction of *ECE1* expression via *MCM1* overexpression (*MCM1*^{OE}) partly relies on Tup1, Cph1 and Efg1.

A *MCM1* was transformed in the *ADH1* locus of the wild type and the *tup1* Δ and the *cph1* Δ /*efg1* Δ mutants. Cells were grown for 4 h in SDG with or without 10% human serum at 37°C prior to microscopy in the DIC channel. Bar=10 μ m

B Total RNA of the wild type and the *tup1* Δ and the *cph1* Δ /*efg1* Δ mutants with and without *MCM1* overexpression was isolated after 4 h growth in SDG with and without 10% human serum in biological triplicates. 100 ng/ μ l of this RNA was used for RT-qPCR to determine the relative gene expression of *ECE1*. Data was normalized to a control RNA (wild type, 6 h YPD, 37°C) and the housekeeping gene *ACT1*. Asterisks mark significant differences of hyperactive Ahr1 mutants compared to the respective parental strain (* $p \leq 0.05$, two tailed, unpaired student's t-test).

The addition of human serum led to the elongation of some *cph1* Δ /*efg1* Δ mutant cells with *MCM1* overexpression, while the parental strain stayed in yeast form (Fig. 23A). Fig. 23B depicts the relative *ECE1* expression in the above mentioned strains under non-inducing (SDG) and inducing (SDG + serum) conditions after 4 h growth at 37°C. While *MCM1* overexpression was able to significantly increase *ECE1* expression in the wild type and to a smaller amount in the *cph1* Δ /*efg1* Δ mutant, there was no measurable increase in the *tup1* Δ mutant under non-inducing conditions (Fig. 23B). Under hyphae-inducing conditions, *MCM1* overexpression was able to significantly increase *ECE1* expression in the *tup1* Δ and the *cph1* Δ /*efg1* Δ mutants. However, *ECE1* expression in these mutants could not reach the same level as in wild type hyphae, suggesting that induction of high-level *ECE1* expression via *MCM1* overexpression requires Tup1 or Cph1 and Efg1.

3.6.3. *MCM1* overexpression induces the expression of other CFR genes

The overexpression of *MCM1* led to an induction of *ECE1* expression, already under yeast growth conditions (cf. Fig. 22 and 23). This mechanism was partly dependent on Ahr1, a known co-factor of Mcm1 (cf. Fig. 22). Additionally, the lack of the transcription regulators Tup1 and Cph1 and Efg1 also had a negative influence on the induction of *ECE1* expression via *MCM1* overexpression (cf. Fig. 23). It was already shown that hyperactivation of Ahr1 induces not only the expression of *ECE1* but also the expression of other CFR genes, such as *ALS3*, *HWP1* and *IHD1* without necessary cues for hyphal formation and independent of Cph1 and Efg1 (cf. Fig. 12). Thus, it was tested whether the overexpression of *MCM1* also had an influence on the expression of other CFR genes in the wild type and the *ahr1* Δ , the *tup1* Δ and the *cph1* Δ /*efg1* Δ backgrounds (strain no. 1, 14, 104, 350, 439, 462, 271, 352, Tab. 1). The results of RT-qPCR analyses are displayed in Fig. 24.

MCM1 overexpression was able to significantly increase *ALS3*, *IHD1* and *HWP1* expression in the wild type background after 4 h growth in SDG medium, but not after serum-induction (Fig. 24). In the *ahr1* Δ background, *MCM1* overexpression did lead to no or only a slight increase in the expression of these genes without reaching the level of wild type hyphae (Fig. 24). In the *tup1* Δ mutant the expression of *IHD1* and *HWP1* was not increased due to an overexpression of *MCM1* under yeast growth conditions. Fig. 24 shows that *ALS3* expression was increased in the *tup1* Δ mutant with *MCM1* overexpression, but was not able to reach wild type hyphae level. After serum-induction, the expression of *ALS3*, *IHD1* and *HWP1* was either not or only slightly increased in the *tup1* Δ mutant with *MCM1* overexpression, without reaching wild type hyphae levels. In the *cph1* Δ /*efg1* Δ mutant *MCM1* overexpression did induce a slight increase in *IHD1* and no increase in *ALS3* and *HWP1* expression under the tested yeast growth conditions (Fig. 24). After serum-induction, *MCM1* overexpression induced a significant increase in *ALS3*, *IHD1* and *HWP1* expression in the *cph1* Δ /*efg1* Δ background, which did not reach the level of wild type hyphae. Fig. 24 shows that there was no clear pattern observable for *MCM1* overexpression induced expression of *DCK1* and orf19.2457. Interestingly, the expression of *HGT2* was much higher in the *tup1* Δ and the *cph1* Δ /*efg1* Δ mutants than in the wild type and the *ahr1* Δ mutant under yeast growth conditions. This is especially interesting since it is a CFR gene and while *tup1* Δ is a hyperfilamentous mutant (cf. Fig.23), the *cph1* Δ /*efg1* Δ mutant is locked in yeast

form (cf. Fig. 23). Strikingly, *HGT2* expression in the wild type and the *ahr1* Δ mutant was significantly downregulated due to *MCM1* overexpression under hyphal growth conditions (Fig. 24).

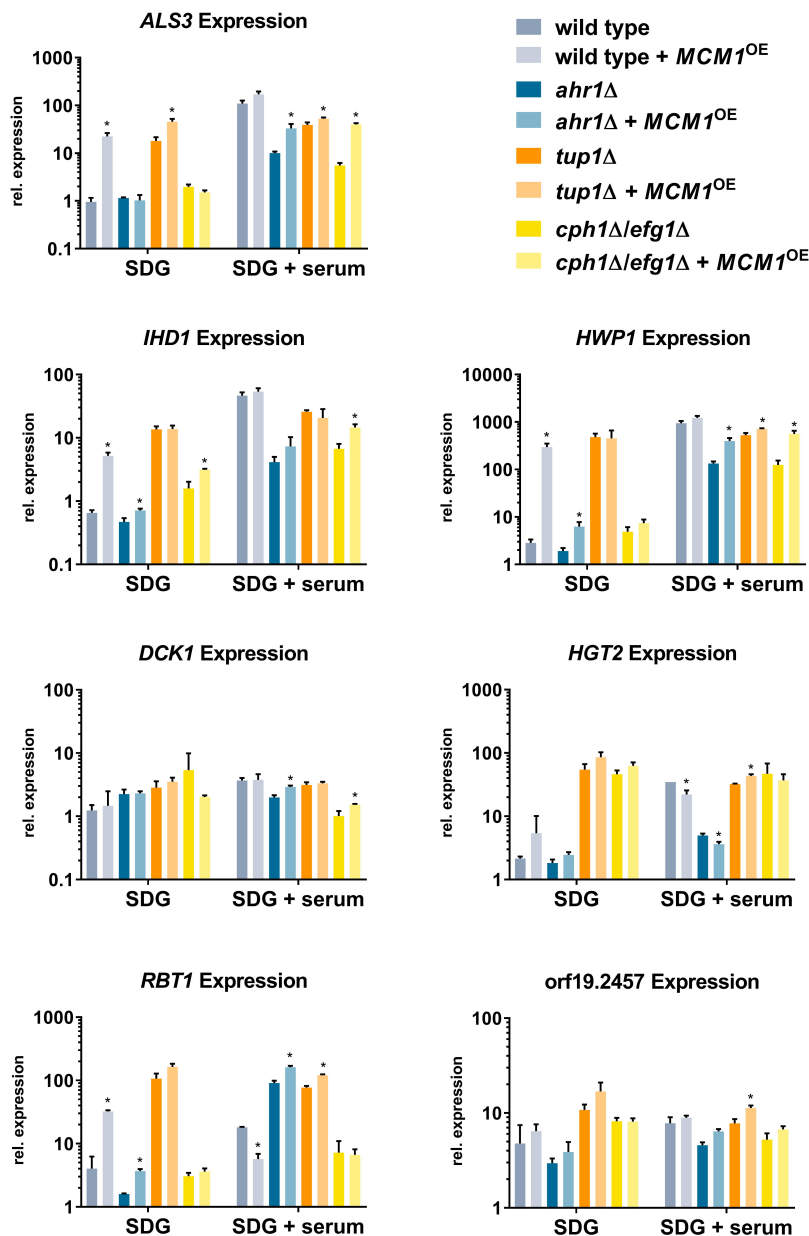


Fig. 24: *MCM1* overexpression induces the expression of some CFR genes but often-times depends on Ahr1, Tup1 or Cph1/Efg1.

Total RNA of the wild type and the *ahr1* Δ , the *tup1* Δ and the *cph1* Δ /*efg1* Δ mutants with and without *MCM1* overexpression was isolated after 4 h growth in SDG with and without 10% human serum in biological triplicates. 100 ng/ μ l of this RNA was used for RT-qPCR to determine the relative gene expression of *ALS3*, *HWP1*, *IHD1*, *HGT2*, *DCK1*, *RBT1* and orf19.2457. Data was normalized to a control RNA (wild type, 6 h YPD, 37°C) and the housekeeping gene *ACT1*. Asterisks mark significant differences of *MCM1* overexpression mutants compared to the respective parental strain (* $p \leq 0.05$, two tailed, unpaired student's t-test).

As shown earlier in Fig. 12 hyperactive Ahr1 led to increased *HGT2* expression in the wild type under yeast growth conditions, its expression was significantly downregulated after serum-induction. It appears that Mcm1 and its cofactor have a negative influence on the expression of *HGT2* under serum conditions. In the *tup1* Δ mutant on the other hand, *HGT2* expression was significantly increased due to *MCM1* overexpression under hyphal growth conditions, as shown in Fig. 24. Additionally, *HGT2* expression in the *tup1* Δ mutant was higher under yeast growth conditions than in hyphal growth conditions. *MCM1* overexpression had no influence on *RBT1* expression in the *cph1* Δ /*efg1* Δ mutant (Fig. 24). However, in the wild type and the *ahr1* Δ mutant it significantly increased *RBT1* expression under the tested yeast growth conditions. Under hyphal growth conditions, *MCM1* overexpression was also able to significantly increase *RBT1* expression in the *tup1* Δ mutant. Summing up, *MCM1* overexpression did not only have an effect on *ECE1* expression, but also on *ALS3*, *HWP1*, *IHD1* and *RBT1* expression. However, this effect appeared to be only intermediate or non-existent in the *ahr1* Δ , the *tup1* Δ and the *cph1* Δ /*efg1* Δ mutants.

3.6.4. *MCM1* overexpression induces Als3 localization on cell surface

As already described, *MCM1* overexpression increased *ALS3* expression in the wild type. This phenomenon was decreased in mutants lacking *AHR1*, *TUP1* and *CPH1/EFG1*. To examine if this correlated with Als3 localization on the surface, the strains were grown for 6 h under yeast and hyphal growth conditions (strain no. 1, 14, 104, 350, 439, 462, 271, 352, Tab. 1). Subsequently, Als3 staining was performed as described earlier. Fig. 25 illustrates these Als3-stained cells. Under yeast growth conditions, only *MCM1* overexpression in the wild type background led to a weak Als3 signal in some cells. Interestingly, *tup1* Δ with *MCM1* overexpression did not show

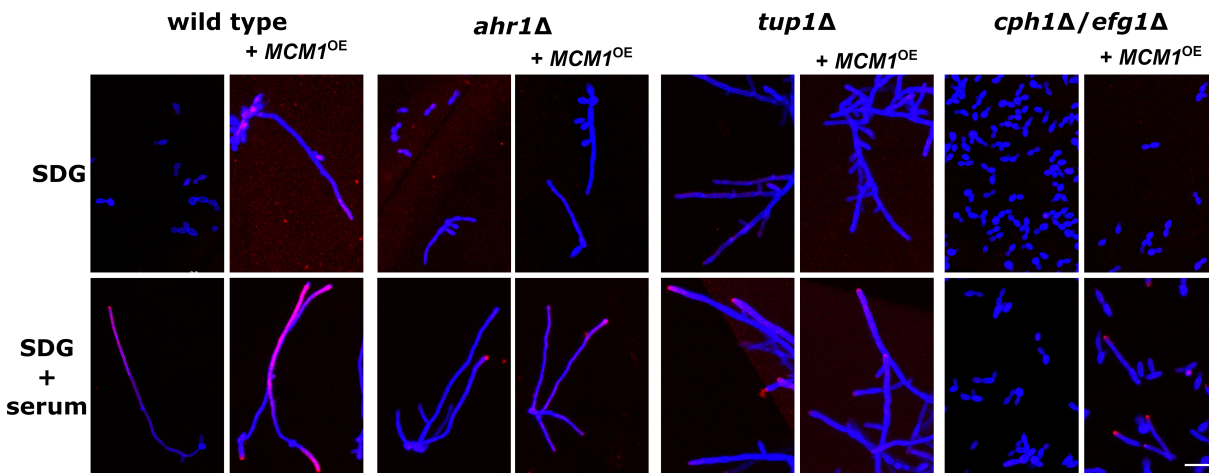


Fig. 25: *MCM1* overexpression induces Als3 localization on cell surface.

The wild type and the *ahr1* Δ , the *tup1* Δ and the *cph1* Δ /*efg1* Δ mutants with and without *MCM1* overexpression were grown for 6 h in SDG with or without 10% human serum at 37°C on μ Dishes. Subsequently, cells were stained with an anti Als3-antibody (secondary antibody: goat-anti-Rabbit-488-IgG (red)), fixed with Histofix and stained with calcofluor white (blue). An overlay of the DAPI and the A488 channel is depicted. Bar= 20 μ m.

any Als3 signal (Fig. 25), even though *ALS3* expression in this mutant was higher than in the wild type with *MCM1* overexpression (cf. Fig.24). After serum-induction, *MCM1* overexpression led to a brighter Als3 signal in the wild type background compared to the respective parental strain, as depicted in Fig. 25. The Als3 signal for the *ahr1* Δ mutants with or without *MCM1* overexpression only showed an Als3 signal on the very tip of some hyphal cells. Also in the *tup1* Δ mutant with and without *MCM1* overexpression, only the very tips of the cell filaments showed an Als3 signal (Fig. 25). As already shown before, the *cph1* Δ /*efg1* Δ mutant stayed in yeast form and did not show any Als3 signal (cf. Fig. 14). When *MCM1* was overexpressed, the *cph1* Δ /*efg1* Δ cells elongated and an Als3 signal was visible on the tips of some cells after serum induction.

3.7. The influence of a mutated *SSN3* allele on the expression of *ECE1*, *ALS3* and other CFR genes

3.7.1. Mutated *SSN3* allele induces *ECE1* expression

In this study, a hyperactive Ahr1 as well as the overexpression of *MCM1* were able to induce filamentation and expression of *ECE1* and *ALS3* in the normally yeast-locked *cph1* Δ /*efg1* Δ mutant (cf. Fig. 5 and 23). A similar phenomenon has been observed in a study from 2014. A single nucleotide polymorphism (SNP) in the *SSN3* gene of the yeast-locked *cph1* Δ /*efg1* Δ mutant was shown to rescue the double mutant's filamentation defect, along with inducing the expression of (among others) *ECE1* and *ALS3* (Wartenberg *et al.*, 2014). To investigate a possible link between the mutation in *SSN3* and the earlier identified roles of Ahr1 and Tup1 on the expression of *ECE1* and other CFR genes, a mutated *SSN3* (*SSN3_m*) was transformed into the *ADH1* locus of the wild type. Additionally, it was transformed into the *ahr1* Δ and the *tup1* Δ background to analyze whether the lack of any of these transcriptional regulators had an impact on the influence of *SSN3_m*. Furthermore, *SSN3_m* was transformed into the *cph1* Δ /*efg1* Δ mutant. For microscopy, *ECE1* promotor driven GFP strains were used to visualize *ECE1* expression in wild type and the *ahr1* Δ and *tup1* Δ mutants (strain no. 127, 128, 132, 364, 218, 267, 104 and 109, Tab. 1). Fig. 26A shows micrographs of the strains taken after 4 h growth in SDG with or without 10% human serum at 37°C. Mutation of *SSN3* already induced a GFP signal in some cells in the wild type background under yeast growth conditions (Fig. 26A). The same was true for the *ahr1* Δ mutant, although the GFP signal was not as strong as in the *SSN3_m* mutant in the wild type background (Fig. 26A). A transformation of *SSN3_m* into the *ADH1* locus of *tup1* Δ , resulted in a bright GFP fluorescence under yeast and hyphal growth conditions, shown in Fig. 26A. The mutation of *SSN3* did not have an influence on yeast growth of the *cph1* Δ /*efg1* Δ mutant under non-inducing conditions. Under hyphal growth conditions, wild type hyphae showed a bright GFP fluorescence, which was a little brighter in the *SSN3_m* strain (Fig. 26A). The *SSN3* mutation in the *ahr1* Δ background resulted in a bright GFP fluorescence of some, but not all hyphae. As already known (Wartenberg *et al.*, 2014), *SSN3_m* led to hyphal formation of in the *cph1* Δ /*efg1* Δ background after serum-induction. Again, due to a lack of selection markers the GFP reporter system could not be transformed into the *cph1* Δ /*efg1* Δ mutant.

For RT-qPCR analyses, strains without GFP reporter system were analysed (strain no. 1, 271, 14, 104, 106, 109, 460 and 461, Tab. 1). Fig. 26B illustrates the relative expression of *ECE1*

3. Results

after 4 h growth in SDG with or without 10% human serum in wild type and the *ahr1* Δ , the *tup1* Δ and the *cph1* Δ /*efg1* Δ mutants with and without mutated *SSN3*. The *SSN3_m* significantly increased *ECE1* expression in the wild type and all mutants under both growth conditions, which correlated to the microscopic findings in Fig. 26A. Under hyphal growth conditions, this increase in the *tup1* Δ background was quite small and, in contrast to the expression in the *ahr1* Δ and the *cph1* Δ /*efg1* Δ mutants with mutated *SSN3*, not able to reach wild-type hyphae level. This

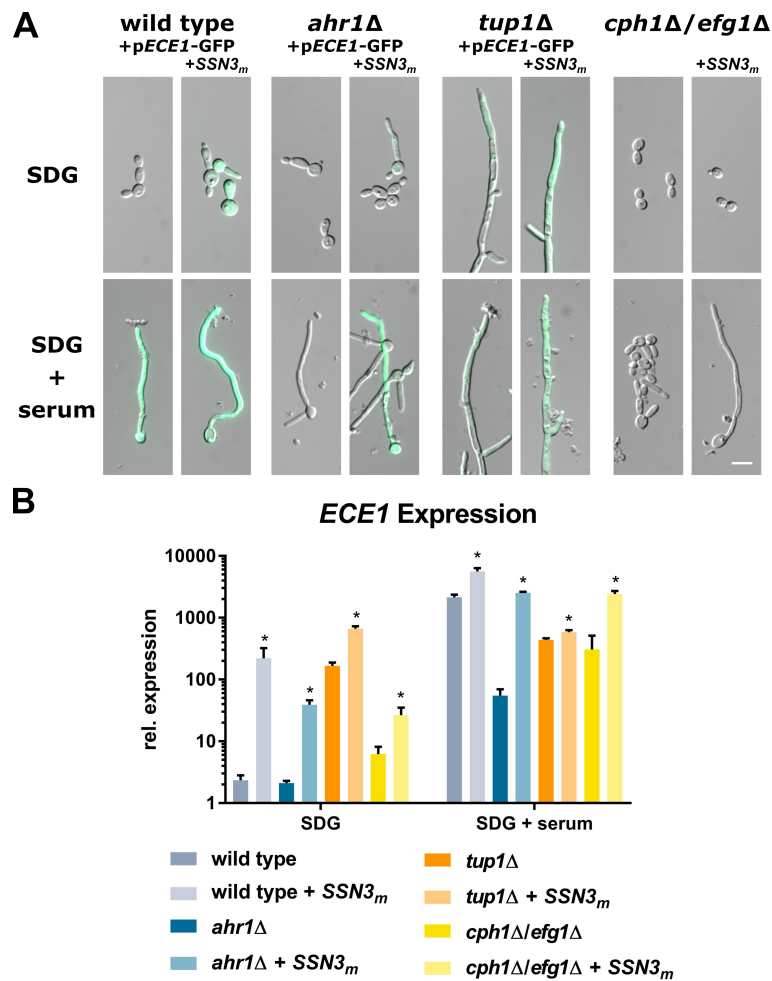


Fig. 26: Mutated *SSN3* allele (*SSN3_m*) induces *ECE1* expression in the wild type and the *ahr1* Δ , the *tup1* Δ and the *cph1* Δ /*efg1* Δ mutants.

A The wild type and the *ahr1* Δ , the *tup1* Δ and the *cph1* Δ /*efg1* Δ mutants with and without *SSN3_m* transformed into the *ADH1* locus. For wild type, *ahr1* Δ and *tup1* Δ mutants, the *ECE1* promoter driven GFP reporter system could additionally be employed. Micrographs were taken after 4 h growth in SDG with or without 10% human serum at 37°C. DIC and GFP channel images were merged. Bar=10 μ m.

B Total RNA of the wild type and the *ahr1* Δ , the *tup1* Δ and the *cph1* Δ /*efg1* Δ mutants with and without *SSN3_m* was isolated after 4 h growth in SDG with and without 10% human serum in biological triplicates. 100 ng/ μ l of this RNA was used for RT-qPCR to determine the relative gene expression of *ECE1*. Data was normalized to a control RNA (wild type, 6 h YPD, 37°C) and the housekeeping gene *ACT1*. Asterisks mark significant differences of *SSN3_m* mutants compared to the respective parental strain (* $p \leq 0.05$, two tailed, unpaired student's t-test).

shows that *SSN3_m* was able to induce *ECE1* expression not only independent of Cph1 and Efg1 and cues for hyphal formation (which was already known), but also independent of Ahr1 and partly independent of Tup1.

3.7.2. Mutated *SSN3* allele induces *ALS3* expression and Als3 localization on cell surfaces

Subsequently, the role of *SSN3_m* in *ALS3* expression and Als3 localization on the cell surfaces was investigated. The RT-qPCR analyses, displayed in Fig. 27 A, show relative *ALS3* expression in the wild type and the *ahr1* Δ , the *tup1* Δ and the *cph1* Δ /*efg1* Δ mutants with and without *SSN3_m* after 4 h growth in SDG with or without 10% human serum (strain no. 1, 271, 14, 104, 106, 109, 460 and 461, Tab. 1). The mutation of *SSN3* resulted in significantly increased levels of *ALS3* expression in the wild type, the *ahr1* Δ and the *tup1* Δ backgrounds compared to the respective parenteral strains, already under non-inducing conditions. However, in the *ahr1* Δ background this increase was only intermediate in yeast growth conditions. For the *cph1* Δ /*efg1* Δ double mutant a mutated *SSN3* allele did not increase the *ALS3* expression under these conditions. After 4 h serum induction, a significant increase in *ALS3* expression was visible for the wild type and all mutants (Fig. 27A). Fig. 27 B shows Als3 staining performed on the strains mentioned above. In the wild type background *SSN3* mutation led to the formation of hyphae displaying an Als3 signal already under yeast growth conditions (Fig. 27B). While the *ahr1* Δ mutant only rarely formed filaments under these conditions, the *ahr1* Δ mutant with *SSN3_m* formed filaments, showing a faint Als3 signal, more frequently. Under yeast growth conditions, the *tup1* Δ mutant did not show an Als3 signal. However, *SSN3_m* induced an Als3 signal of the filament tips of the *tup1* Δ mutant under these conditions (Fig. 27B). There was no visible difference between the *cph1* Δ /*efg1* Δ mutants with or without *SSN3_m* in terms of Als3 localization under yeast growth conditions. Both mutants remained in yeast form without a notable Als3 signal, as depicted in Fig. 27B.

Unfortunately, due to a change in the serum-batch the induction of hyphal growth and Als3 localization was weaker in this assay compared to previous Als3 staining experiments. After 5 h serum induction, an Als3 signal which increased towards the hyphal tips could be seen in the wild type. Due to the mutation of the *SSN3* allele, this signal could be slightly increased (Fig. 27B). While the *ahr1* Δ hyphae did only rarely display an Als3 signal, *SSN3_m* led to an induction of Als3 localization on the filaments' surfaces, which increased towards the tips (Fig. 27A). The Als3 signal of the *tup1* Δ mutant concentrated on the very tips of the filaments under hyphal growth conditions. This signal could be increased due to *SSN3_m*, as shown in Fig. 27A. As already mentioned earlier (cf Fig. 25), the *cph1* Δ /*efg1* Δ double mutant remained in yeast form after serum-induction, which did not show an Als3 signal. The mutation of the *SSN3* allele was able to rescue the mutants ability to form hyphae under serum-inducing conditions. These hyphae showed an Als3 signal similar to the wild type hyphae (Fig. 27B). Taken together, the SNP mutation of *SSN3* was able to induce *ALS3* expression and localization on the cell walls independent of Ahr1, Tup1 and Cph1/Efg1.

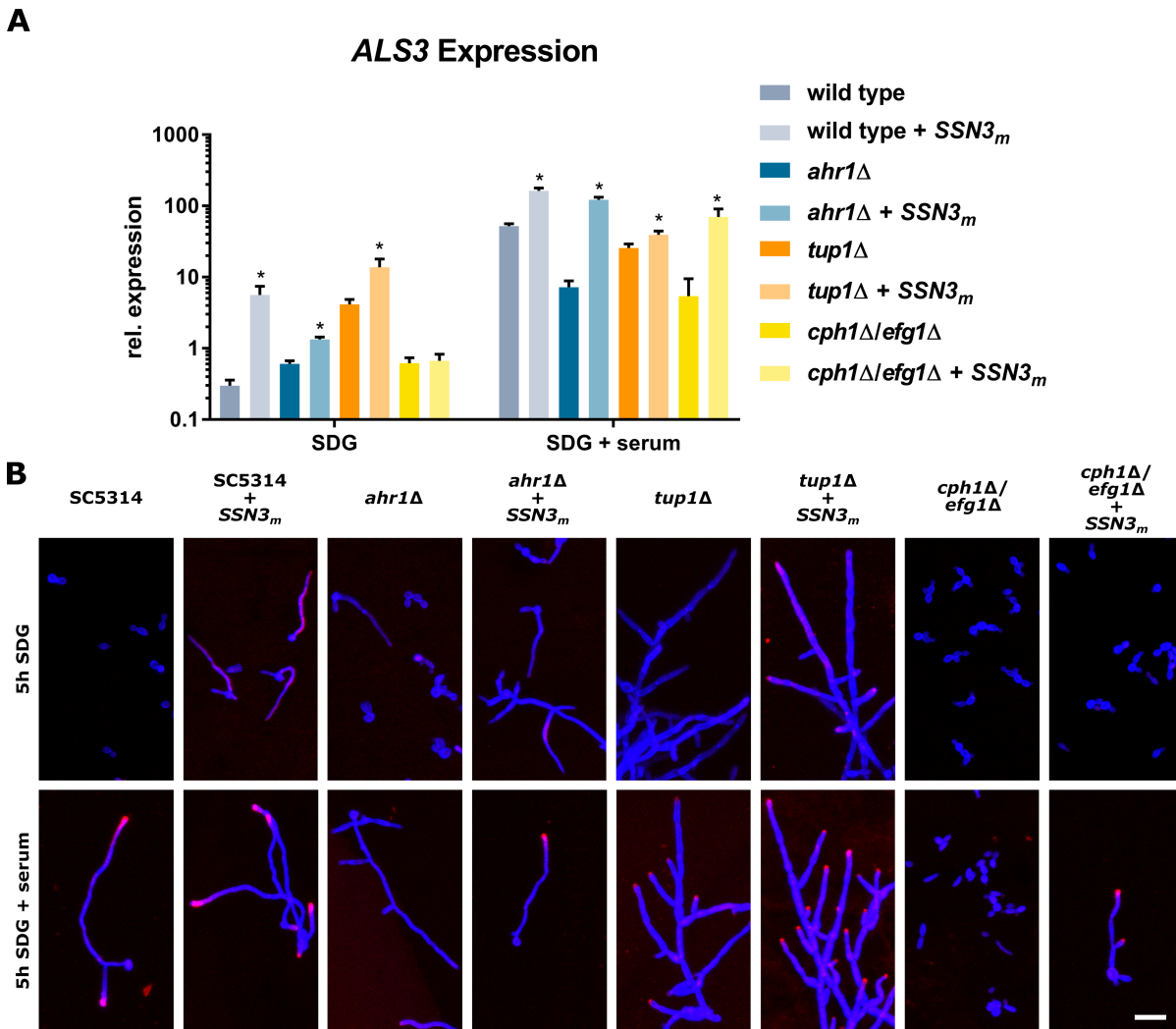


Fig. 27: Mutated *SSN3* allele (*SSN3_m*) induces *ALS3* expression and Als3 localization on cell surface.

A Total RNA of the wild type and the *ahr1* Δ, the *tup1* Δ and the *cph1* Δ/*efg1* Δ mutants with and without *SSN3_m* was isolated after 4 h growth in SDG with and without 10% human serum in biological triplicates. 100 ng/μl of this RNA was used for RT-qPCR to determine the relative gene expression of *ALS3*. Data was normalized to a control RNA (wild type, 6 h YPD, 37°C) and the housekeeping gene *ACT1*. Asterisks mark significant differences of *SSN3_m* mutants compared to the respective parental strain (* $p \leq 0.05$, two tailed, unpaired student's t-test).

B The wild type and the *ahr1* Δ, the *tup1* Δ and the *cph1* Δ/*efg1* Δ mutants with and without *SSN3_m* were grown for 5 h in SDG with or without 10% human serum at 37°C on μDishes. Subsequently, cells were stained with an anti Als3-antibody (secondary antibody: goat-anti-Rabbit-488-IgG (red)), fixed with Histofix and stained with calcofluor white (blue). An overlay of the DAPI and the A488 channel is depicted. Bar=20 μm.

3.7.3. Mutated *SSN3* allele induces the expression of other CFR genes

The influence of the mutated *SSN3* (*SSN3_m*) allele on the expression of the other CFR genes was assessed via RT-qPCR. Therefore RNA from the wild type and the *ahr1* Δ, the *cph1* Δ/*efg1* Δ and the *tup1* Δ mutants with or without *SSN3_m* was extracted after 4 h growth in SDG with or

without 10% human serum (strain no. 1, 271, 14, 104, 106, 109, 460 and 461, Tab. 1). Fig. 28 displays the determined relative expressions of *IHD1*, *HWP1*, *HGT2*, *DCK1*, *orf19.2457* and *RBT1* of these strains. The mutation of *SSN3* was able to significantly increase the expression of *IHD1* in the wild type and the *ahr1* Δ background under non-inducing and inducing conditions compared to the respective parental strains (Fig. 28).

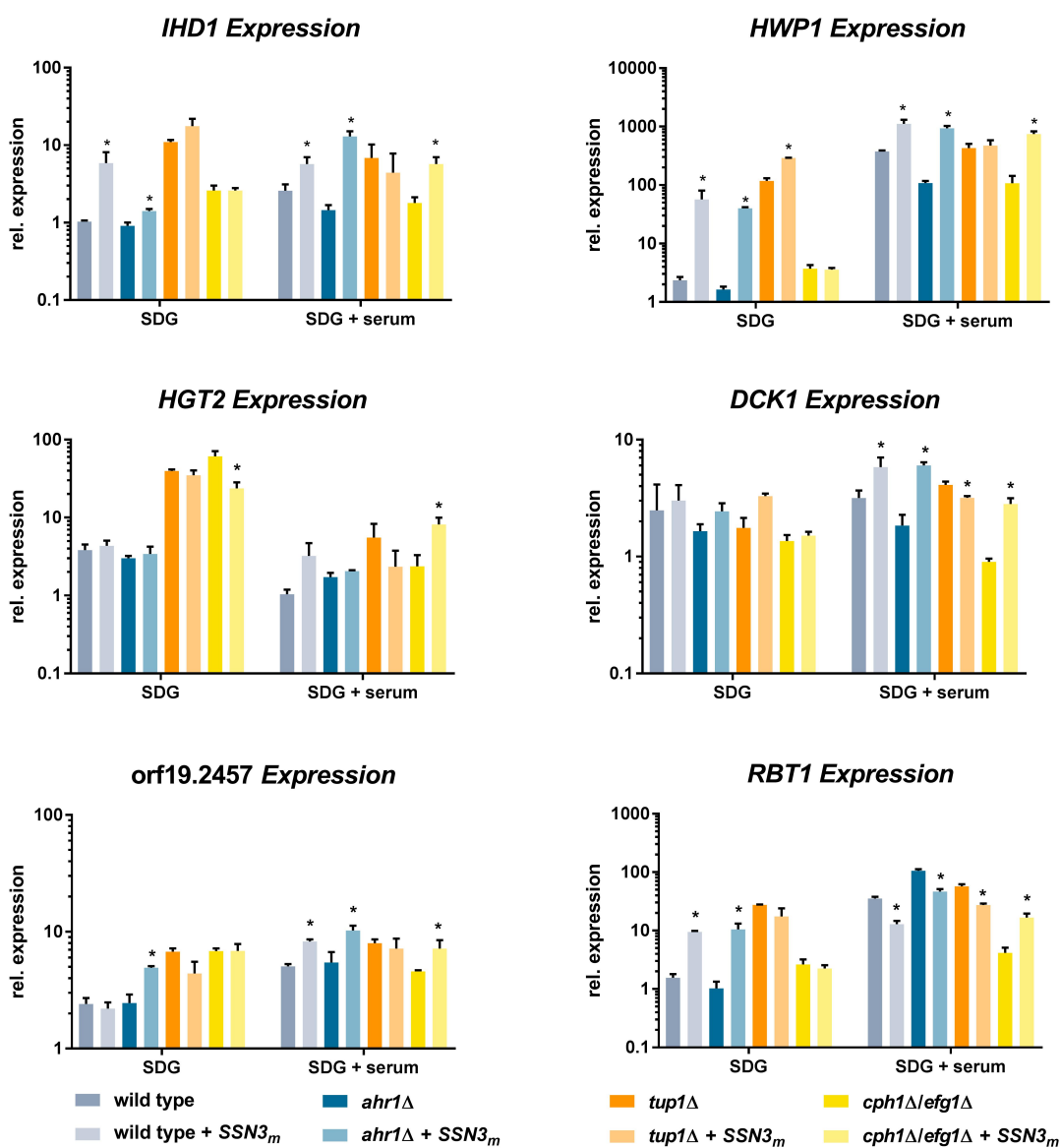


Fig. 28: Mutated *SSN3* allele (*SSN3_m*) influences the expression of CFR genes.

Total RNA of the wild type and *ahr1* Δ , the *tup1* Δ and the *cph1* Δ /*efg1* Δ mutants with and without *SSN3_m* was isolated after 4 h growth in SDG with and without 10% human serum in biological triplicates. 100 ng/ μ l of this RNA was used for RT-qPCR to determine the relative gene expression of *IHD1*, *HWP1*, *HGT2*, *DCK1*, *orf19.2457* and *RBT1*. Data was normalized to a control RNA (wild type, 6 h YPD, 37°C) and the housekeeping gene *ACT1*. Asterisks mark significant differences of *SSN3_m* mutants compared to the respective parental strain (* $p \leq 0.05$, two tailed, unpaired student's t-test).

Additionally, a significant increase in *IHD1* in the *cph1* Δ /*efg1* Δ mutant with *SSN3_m* after serum-induction could be observed, as depicted in Fig. 28. Under yeast growth conditions, a significant increase in *HWP1* expression due to *SSN3_m* could be noted in the wild type background and the *ahr1* Δ and the *tup1* Δ mutants compared to their parental strains. After serum-induction, this was true for the wild type background, and the *ahr1* Δ and the *cph1* Δ /*efg1* Δ mutants. Fig. 28 shows that *HGT2* expression was significantly reduced in the *cph1* Δ /*efg1* Δ mutant with *SSN3_m* compared to its parental strain under non-inducing conditions. However, under hyphae-inducing conditions, it was significantly increased. For the other strains, no significant differences in expression could be noted (Figure 28). While there were no significant changes in *DCK1* expression noted under non-inducing conditions, a mutated *SSN3* allele was able to significantly increase *DCK1* expression in the wild type and the *ahr1* Δ and the *cph1* Δ /*efg1* Δ mutants under hyphae-inducing conditions. Interestingly, as shown in Fig. 28, *SSN3_m* in the *tup1* Δ mutant led to a significant decrease in *DCK1* expression after serum-induction. The expression of orf19.2457 was significantly increased in the *ahr1* Δ mutant with *SSN3_m* compared to its parental strain under non-inducing conditions. Under hyphae-inducing conditions *SSN3_m* resulted in a significant upregulation of orf19.2457 expression in the wild type background and the *ahr1* Δ and the *cph1* Δ /*efg1* Δ mutants, as depicted in Figure 28. While *SSN3_m* in the wild type background and the *ahr1* Δ mutant led to a significant increase in *RBT1* expression under non-inducing conditions, a significant decrease under hyphae-inducing conditions of these strains could be observed compared to their respective parental strains (Fig. 28). Additionally, *RBT1* expression was also significantly decreased in the *tup1* Δ mutant with *SSN3_m*, while a significant increase in *RBT1* expression in the *cph1* Δ /*efg1* Δ mutant with *SSN3_m* could be observed (Fig. 28).

3.7.4. Deletion of *SSN3* induces expression of *ECE1* and *ALS3* and other CFR genes

A mutated allele *SSN3* led to the upregulation of *ECE1* and *ALS3* in the wild type background, which was largely independent of Ahr1, Tup1 and Cph1/Efg1 (Fig. 26 and 27). Subsequently, it is possible that the deletion of *SSN3* has a negative effect on the expression of these genes and that a hyperactive Ahr1 may be able to rescue this defect.

To test for *ECE1* expression, the GFP reporter system was transformed into the *ssn3* Δ mutants with and without hyperactive Ahr1 (strain no. 522, 552, Tab. 1). Subsequently, strains were grown in SDG with and without 10% human serum for 4 h and microscopic images were taken. Interestingly, both mutants formed hyphae already under yeast growth conditions and exhibited a bright GFP signal, which was a little brighter in the mutant with the hyperactive Ahr1 (Fig. 29A). Fig. 32 in Sec. VII shows that this was not the case in other yeast-inducing conditions such as growth at 37°C in YPD and M199 (pH 4) or at 30°C in SDG, where the wild type and the *ssn3* Δ mutant formed non-fluorescing yeast cells. For RT-qPCR confirmation, wild type and the *ssn3* Δ strains were grown under the same conditions mentioned above and RNA was isolated (strain no. 1, 250, 279, Tab. 1). Relative expression of *ECE1* confirmed the microscopic data. Compared to the wild type, *ECE1* expression was significantly increased in *ssn3* Δ with and without hyperactive Ahr1 under yeast growth conditions (Fig. 29A). Similar results were obtained concerning the expression of *ALS3*, depicted in Fig. 29B.

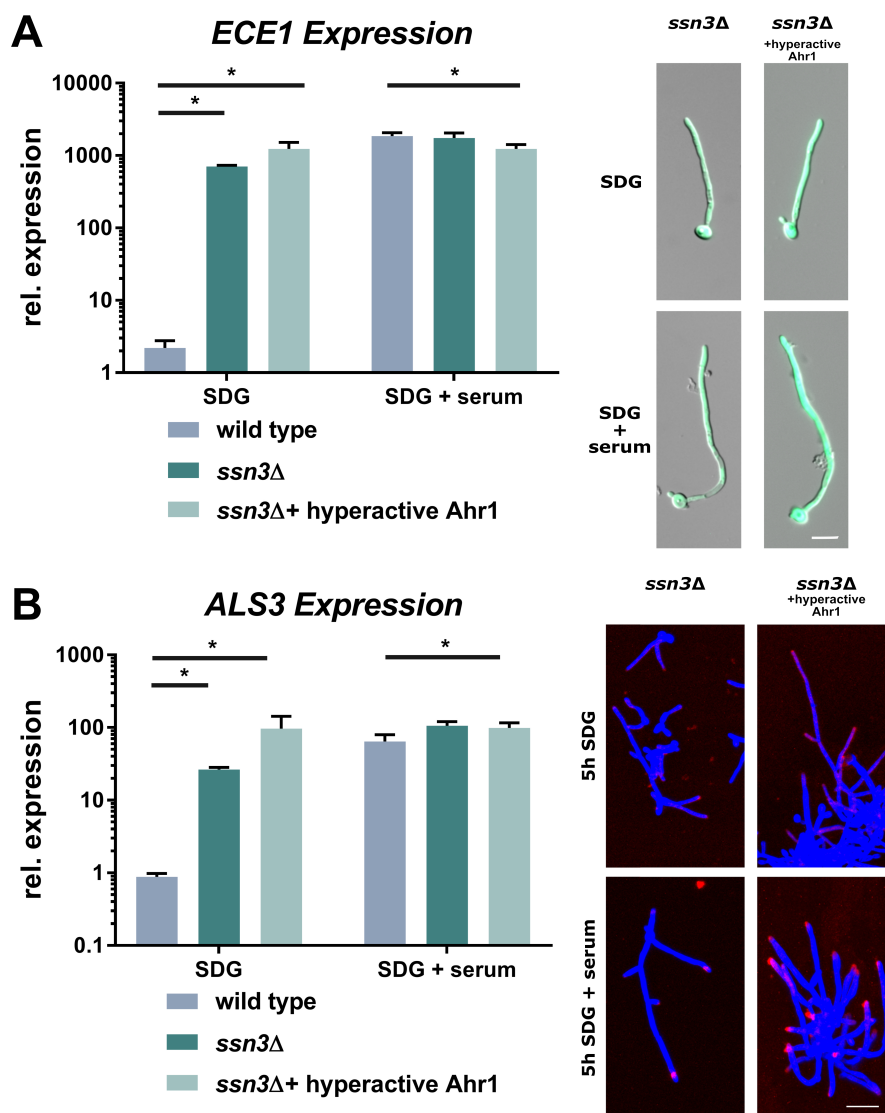


Fig. 29: Deletion of *SSN3* induces expression of *ECE1* and *ALS3* and Als3 localization on filament surface.

Total RNA of the wild type and the *ssn3Δ* mutants with and without hyperactive Ahr1 was isolated after 4 h growth in SDG with and without 10% human serum in biological triplicates. 100 ng/ μ l of this RNA was used for RT-qPCR to determine the relative gene expression of *ECE1* (A) and *ALS3* (B). Data was normalized to a control RNA (wild type, 6 h YPD, 37°C) and the housekeeping gene *ACT1*. Asterisks mark significant differences between strains (* $p \leq 0.05$, two tailed, unpaired student's t-test).

A right panel: The *ECE1* promoter driven GFP reporter system was transformed into the *ssn3Δ* mutants with and without hyperactive Ahr1. Micrographs of these strains were taken after 4 h growth in SDG with or without 10% human serum at 37°C. Depicted are overlays of the DIC and GFP channels. Bar=10 μ m.

B left panel: The *ssn3Δ* mutant with and without hyperactive Ahr1 were grown for 5 h in SDG with or without 10% human serum at 37°C on μ Dishes. Subsequently, cells were stained with an anti Als3-antibody (secondary antibody: goat-anti-Rabbit-488-IgG (red)), fixed with Histofix and stained with calcofluor white (blue). An overlay of the DAPI and the A488 channel is depicted. Bar= 20 μ m.

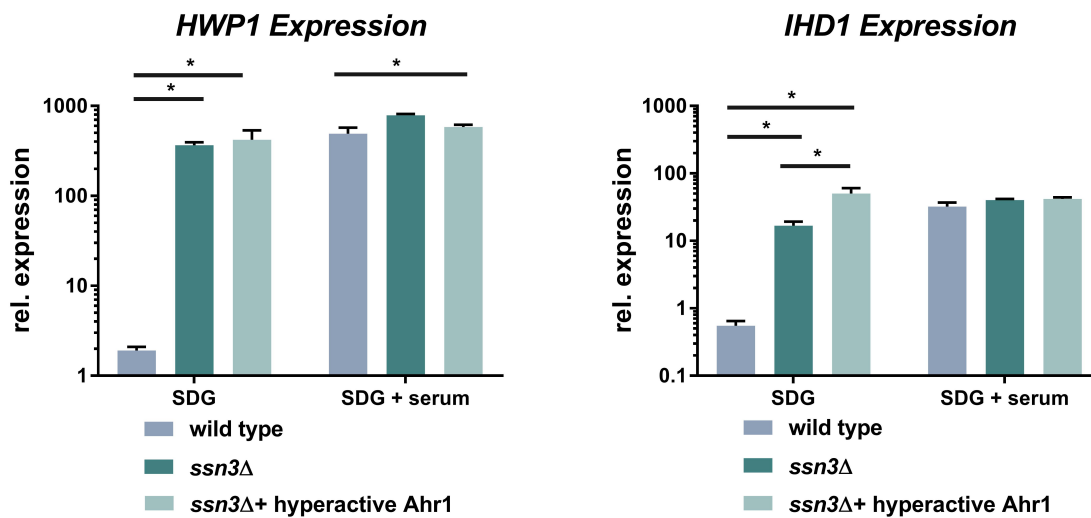


Fig. 30: **Deletion of *SSN3* induces expression of *HWP1* and *IHD1*.**

Total RNA of the wild type and the *ssn3Δ* mutants with and without hyperactive Ahr1 was isolated after 4 h growth in SDG with and without 10% human serum in biological triplicates. 100 ng/ μ l of this RNA was used for RT-qPCR to determine the relative gene expression of *IHD1* and *HWP1*. Data was normalized to a control RNA (wild type, 6 h YPD, 37°C) and the housekeeping gene *ACT1*. Asterisks mark significant differences (* $p \leq 0.05$, two tailed, unpaired student's t-test).

To ascertain whether this upregulation of *ALS3* correlated to increased Als3 localization on *C. albicans* hyphae, Als3 staining with the *ssn3Δ* mutant with or without hyperactive Ahr1 was performed (strain no. 250, 279, Tab. 1). Under yeast growth conditions, only little Als3 could be spotted in the *ssn3Δ* mutant, while the mutant with the hyperactive Ahr1 showed an Als3 signal along the hyphal tips (Fig. 29B). Unfortunately, a change in the serum-batch resulted in a reduction of hyphal formation, which had an influence on the Als3 localization of the wild type. This should be kept in mind when comparing the images shown in this section with earlier images of Als3 staining. After serum induction, Als3 on *ssn3Δ* mutant cells concentrated on the very tips of the hyphae. This was similar for the *ssn3Δ* mutant with a hyperactive Ahr1, where the Als3 signal was generally stronger than in the parental strain, as displayed in Fig. 29. Since, *SSN3* deletion had an effect on *ECE1* and *ALS3* expression, also the relative expression of *HWP1* and *IHD1* was analyzed. Through the deletion of *SSN3* the relative expressions of *HWP1* and *IHD1* were significantly increased under yeast growth conditions (Fig. 30). This increase was a little higher in the mutant with a hyperactive Ahr1. The influence of *SSN3* deletion on the expression of these genes was not observed under hyphae-inducing conditions.

4. Discussion

The ability of *C. albicans* to undergo reversible yeast-to-hyphae transition is crucial for its virulence. This morphological change, induced by various environmental stimuli, correlates with the upregulation of different hypha-specific genes. One of the most transcribed genes in hyphae is *ECE1*, which is not essential for hyphae formation but for the virulence of the fungus (Birse *et al.*, 1993; Moyes *et al.*, 2016). Once translated, the Ece1 protein is further processed by the protein kinases Kex1 and Kex2 into eight peptides which are secreted from hyphae (Bader *et al.*, 2008; Moyes *et al.*, 2016). One of these peptides, Candidalysin, is a toxin and crucial for the induction of host cell cytotoxicity (Moyes *et al.*, 2016; Richardson *et al.*, 2018b; Swidergall *et al.*, 2019). Homologs of Candidalysin were so far only identified in the closest relatives of *C. albicans*, *C. dubliniensis* and *C. tropicalis* (Richardson *et al.*, 2019). The virulence of *C. albicans* and probably also the other *Candida* species expressing *ECE1* homologs seems to be strongly dependent on the ability to form Candidalysin. Due to its importance for fungal virulence, insights into the regulation of *ECE1* can contribute to the comprehension of the fungal pathogenicity mechanisms.

4.1. The transcription factor Ahr1 is required for high-level expression of *ECE1* and Candidalysin secretion

So far, several transcriptional regulators were shown to play a role in *ECE1* expression in *C. albicans*. However, deletion mutants of these regulators usually exhibited hyphal growth defects, leading to the question if *ECE1* transcription is low due to the absent binding of transcription factors or due to the defects in hyphal formation. For example, deletion of *EFG1* leads to a yeast-locked phenotype with low *ECE1* expression levels under hyphal growth conditions (Braun and Johnson, 2000). Other transcription factors with a positive influence on *ECE1* expression are Ume6 and Ndt80 (Zeidler *et al.*, 2008; Carlisle *et al.*, 2009; Sellam *et al.*, 2010). But mutants lacking these regulators have defects in hyphal maintenance or growth (Banerjee *et al.*, 2008; Sellam *et al.*, 2010). In yeast cells, expression of *ECE1*, *ALS3* and *HWP1* is repressed by Nrg1, which, together with its co-factor Tup1, binds to the promoters of hypha-specific genes (Garcia-Sanchez *et al.*, 2005; Murad *et al.*, 2001a,b). Upon hyphal induction, Nrg1 is quickly downregulated and degraded (Martin *et al.*, 2013; Lu *et al.*, 2011). During hyphal elongation, Brg1 recruits Hda1 to promoters of these hypha-specific genes (Lu *et al.*, 2012). This causes nucleosome repositioning which leads to a Brg1-mediated suppression of Nrg1 binding (Lu *et al.*, 2012). Consequently, deletion of *BRG1* results in defective hyphal elongation (Lu *et al.*, 2012). In contrast, the expression of *ECE1* is derepressed in the pseudohyphal *tup1*Δ mutant, but still lower than in wild type hyphae (Braun and Johnson, 2000; Braun *et al.*, 2001). All of the above mentioned deletion mutants are reduced in their virulence (Lo *et al.*, 1997; Banerjee *et al.*, 2008; Yang *et al.*, 2012; Sellam *et al.*, 2010; Braun *et al.*, 2000; Allert *et al.*, 2018). Aside the morphological defects, a low or only intermediate *ECE1* expression and consequently lower Candidalysin production could be an explanation for this. Due to this, this study focused on determining which transcription factors regulate *ECE1* expression in the hyphal morphology of *C. albicans*. Findings from this study concur that during serum induction at 37°C (one of the strongest in-

ducers for hyphal formation), a reduction of *ECE1* expression through the deletion of target transcription factors usually coincided with a hyphal growth defect. The sole exemption was a mutant lacking the *AHR1* gene. It was the only mutant in the screen able to form wild type-like hyphae, while expressing significantly less *ECE1* compared to wild type hyphae. Furthermore, the *ahr1* Δ mutant was already shown to exhibit reduced virulence in systemic infection in mice (Askew *et al.*, 2011) and in an intestinal epithelial infection model (Allert *et al.*, 2018). In addition, it was already described that the mutant has a decreased ability to lyse macrophages and to induce IL-1 β secretion of macrophages, despite forming normal hyphae (Wellington *et al.*, 2014, 2012). Similar characteristics were also observed in *C. albicans* mutants lacking the gene encoding for Candidalysin (Moyes *et al.*, 2016; Swidergall *et al.*, 2019; Verma *et al.*, 2017; Kasper *et al.*, 2018). In the current study, the only intermediate *ECE1* expression of the *ahr1* Δ hyphae correlated to a reduced secretion of Candidalysin. This might be an explanation for the low virulence of the *ahr1* Δ mutant.

4.2. A hyperactive Ahr1 induces high-level *ECE1* expression independent of Cph1 and Efg1

The integration of a hyperactive *AHR1* allele into the wild type, led to a significant increase of *ECE1* expression even under yeast growth conditions. However, this upregulation did not result in enhanced Candidalysin secretion, indicating that hyphal morphology and associated processes are essential for the secretion of the peptide. The mechanistic reason remained unresolved within this study. It might be that the alterations in the fungal cell during the yeast to hyphae transition are required for the effective secretion of Candidalysin. It is also possible that the processing of the Ece1 propeptide requires so far unknown hyphae-associated steps. Another possibility is that the procession of Ece1 by Kex1 and Kex2 is defective in the yeast cell morphology. Kex2 is a membrane bound serine protease which processes proteins for secretion in the golgi. For its activation, the N-terminus of the enzyme undergoes several posttranslational processing steps. During these steps the inactive endoplasmatic-reticulum-bound Kex2 matures to the active enzyme which relocates to the golgi apparatus (for review on Kex2 see Rockwell and Thorner (2004)). It is possible that in *C. albicans* yeast cells the maturation of Kex2 or its ability to recognize Ece1 as target protein could be inhibited. To analyze this, intracellular levels of Candidalysin and the other Ece1 peptides in mutants with a hyperactive Ahr1 under yeast growth conditions should be measured.

A striking observation for the hyperactive Ahr1 was the upregulation of *ECE1* in the non-filamentous *cph1* Δ /*efg1* Δ double mutant even under yeast growth conditions. First, this underlines the central role of Ahr1 for the expression of *ECE1*, second it reveals a so far unknown possibility to bypass the absence of Cph1 and Efg1 and third, it confirmed the observation that upregulation of the *ECE1* gene alone does not necessarily lead to the secretion of Candidalysin. Like for the wild type background, it was observed that the double mutant with the hyperactive Ahr1 was not secreting Candidalysin under yeast growth conditions, even though *ECE1* expression was similar to that of wild type hyphae. Under hyphal growth conditions, the secretion of the peptide was comparable to wild type hyphae, although the *cph1* Δ /*efg1* Δ mutant with hyperactive Ahr1 did not grow strictly in hyphae, but more in a mixture of yeast cells, pseu-

dohyphae and hyphae. Nevertheless, the cytotoxicity towards epithelial cells stayed unchanged. According to Moyes *et al.* (2016), invading *C. albicans* hyphae secrete Candidalysin into invasion pockets in epithelial cells where it accumulates. Once a lytic concentration of Candidalysin is reached, membranes are damaged and LDH is released. These invasion pockets are stretching the epithelial membranes and probably facilitate the intercalation and damage induction of Candidalysin. Thus, non-hyphae-forming mutants like the *cph1* Δ /*efg1* Δ double mutant might exhibit a reduced virulence even though Candidalysin secretion is wild type like. Moyes *et al.* (2016) also showed, that the Ece1-III peptide alone is already sufficient to induce damage, which speaks against the prerequisite of hyphae and invasion pocket formation. However, they employed 70 μ M of the peptide, which may be much higher than the actual physiological concentration that can be reached during interaction between *C. albicans* and mammalian cells.

The data presented here show that the action of the hyperactive Ahr1 concerning *ECE1* expression is independent from Cph1 and Efg1 and thus the MAPK and the cAMP-PKA pathways but subsequent damage induction via Candidalysin relies on hyphae formation.

4.3. A hyperactive Ahr1 binds upstream of *ECE1*, *ALS3* and other core filamentation response genes and activates their expression

A hyperactive Ahr1 induces the expression of *ECE1*. Similar results were found for the core filamentation response genes *ALS3*, *HWP1* and *IHD1*. All three of them were only expressed at intermediate levels in the *ahr1* Δ mutant and upregulated after the integration of a hyperactive *AHR1* allele into the wild type and the *cph1* Δ /*efg1* Δ background. *ALS3* is encoding for a multifunctional protein which is involved in adhesion to and invasion of human host cells (Hoyer *et al.*, 2008; Phan *et al.*, 2007). It is also crucial for fungal iron acquisition in infected host cells, as it mediates the binding of ferritin of *C. albicans* (Almeida *et al.*, 2008). Intermediate *ALS3* expression was not sufficient for the localization of the Als3 protein on *ahr1* Δ hyphae. In contrast, a hyperactive Ahr1 led to an increased expression of this gene in the wild type background as well as in the *cph1* Δ /*efg1* Δ mutant. Consequently, it could be shown that the localization of Als3 increased due these increased transcription levels. As there are no functional assays for Hwp1 and Ihd1, it can only be speculated that the low expression of these genes in the *ahr1* Δ mutant results in decreased protein function. In the future, the presence of these proteins in the *ahr1* Δ mutant could be investigated. The expression data for *ECE1* and *ALS3* raised the question if Ahr1 regulates these genes directly or indirectly. To answer this, ChIP-Seq analyses with a hyperactive HA₃-tagged Ahr1 were performed. These experiments were conducted under yeast growth conditions and indeed proved a physical binding of hyperactive Ahr1 to the promoters of *ALS3*, *ECE1*, *HWP1* and *IHD1*. For future experiments, it should be kept in mind that the hyperactive Ahr1 is an artificial system and that clues about the possible role in gene regulation gained via ChIP-Seq and other experiments, may not coincide with the actual behavior of the transcription factor *in vivo*. However, hyperactivation of a zinc-cluster transcription factor has been shown to be a good tool for identifying regulators of virulence-associated features in the past (Schillig and Morschhäuser, 2013). Especially, since the deletion of genes encoding for transcription factors does not always lead to a certain phenotype that gives hints about the role of the gene. For more accurate results, tagging of Ahr1 and possible interactions partners should

be performed in the native loci. The ChIP-Seq data was used to identify the binding motif of the hyperactive Ahr1. This motif was identical to an already published one, where Ahr1 was myc-tagged in its native locus (Hernday *et al.*, 2013), which speaks for the validity of this study's results gathered with the hyperactive Ahr1.

Within the 5' intergenic region of *ECE1* three main binding sites of the hyperactive Ahr1 at positions 2721, 2012, and 996 bp upstream of the start codon were identified. Two of these binding sites at positions 996 and 2012 bp upstream the start codon are situated in the Crick strand and therefore in the same orientation as the *ECE1* ORF itself. Due to this, the gathered results are a valuable data set to further study the influence of Ahr1 on the expression of *ECE1*. To assess the necessity of these sites for Ahr1 binding, each binding site or a combination of binding sites could be deleted or changed by site-directed mutagenesis. A logical application tool would be the established GFP reporter system as it provides a fast and uncomplicated visualization for *ECE1* expression. Alternatively, these binding sites could be deleted in their native locus, e. g. by established CRISPR-Cas9 protocols (Nødvig *et al.*, 2015). Afterwards, *ECE1* expression and (if desired) Candidalysin secretion could be examined. In addition, a ChIP PCR-based approach could prove, if a binding of Ahr1 still occurs or not. It is also feasible that sequential binding to all binding sites occurs. ChIP-PCR at different time points could clarify dynamic Ahr1 occupancy at the *ECE1* promotor.

The same procedures could be performed to analyze the influence of Ahr1 onto the expression of *ALS3*, *HWP1* and *IHD1*, since data shows a binding of the hyperactive Ahr1 upstream of these genes. As already mentioned, the described ChIP Seq results were obtained with a hyperactive Ahr1. Working with a native Ahr1 might be more complicated due to lower expression rates and lower protein levels, but could deliver more realistic results in terms of promoter binding and transcription rates of the target genes. This would be especially important for answering the question when Ahr1 binds to the *ECE1* promotor after the initiation of hyphal growth. As mentioned earlier, *C. dubliniensis* and *C. tropicalis* also synthesize Candidalysin. Since Ahr1 homologs can also be found in both species, the regulatory mechanism described here may be conserved in other *Candida* species.

4.4. A hyperactive Ahr1 regulates other important transcriptional regulators

Aside the binding of the hyperactive Ahr1 to the promoters of *ECE1* and *ALS3*, ChIP-Seq data revealed, that the hyperactive Ahr1 bound upstream of several other genes, including those encoding for the transcription factors Bcr1, Brg1, Efg1, Tec1 and Ume6. As shown by RT-qPCR analyses, this binding also significantly increased the expression of these transcription factors already under yeast growth conditions. This effect might mean that Ahr1 controls a wide range of hyphae-associated processes. It is not clear if the binding upstream of these transcription factors also has additional effects on the transcription of *ALS3* and *ECE1*, since these transcription factors also possess possible binding sites upstream of the *ECE1* ORF. In deletion mutants of these transcription factors *ECE1* expression was reduced after serum-induction, indicating a role of these regulators in *ECE1* expression. However, integration of a hyperactive Ahr1 induced high-level expression of *ECE1* independent of Brg1, Ndt80, Tec1 and Ume6, which questions their importance for the activation of the gene. Interestingly, analyses indicate that Ahr1 does

not bind upstream of *NRG1* or is involved in the negative regulation of *NRG1*. It is possible that the aforementioned induction of *BRG1* expression via hyperactive Ahr1 suppresses binding of Nrg1 on target promoters already in yeast cells. This removal would allow the binding of Ahr1 to the promoters of *ALS3*, *ECE1* and other target genes. Another option is that the hyperactive Ahr1 itself suppresses Nrg1 promoter-binding in *C. albicans* yeast cells. Speaking for this possible mechanism is the fact that the hyperactive Ahr1 induces high-level expression of *ECE1* independently from *BRG1*.

The presented study focused on the regulation of *ECE1* and other core filamentation response genes. However, the ChIP-Seq data provide a lot of information about new targets of the Ahr1 transcription factor. As already mentioned, a hyperactive Ahr1 binds to the promoters and upregulates the expression of genes, which are involved in hyphal initiation and maintenance, biofilm formation and adhesion. This opens up the possibility of a complex regulatory network with Ahr1 in its center, which has yet to be examined.

Ahr1 also bound to its own upstream region, which coincides with already published data (Hernday *et al.*, 2013). This suggests the existence of an autoregulatory feedback loop. In this case expression of *AHR1* was increased due to a hyperactive Ahr1. Since the hyperactive Ahr1 construct was under the control of the *ADH1* promoter, self regulation can not completely account for increased messenger RNA levels.

Aside yeast-to-hyphae transition, *C. albicans* cells are also able to switch between the white and the opaque cell type (Slutsky *et al.*, 1987; Miller and Johnson, 2002). Ahr1, just like Efg1 and Czf1, was shown to play an important role in the white cell type (Wang *et al.*, 2011; Hernday *et al.*, 2013). Furthermore, data from this study indicates that Ahr1 plays a regulating role in hyphae, just like Efg1 in the cAMP-PKA pathway and Czf1 under embedded conditions (Sudbery, 2011; Brown Jr *et al.*, 1999). Due to this, it would be interesting to research, whether the other regulators of white-opaque-switching also play a role in *ECE1* and *ALS3* expression. Especially, since it was shown, that Ahr1 binds upstream of *WOR2* and *EFG1* in white cells and *CZF1*, *WOR2*, *WOR1*, *EFG1* and *WOR3* in opaque cells (Hernday *et al.*, 2013). In white cells Efg1 and Ahr1 bind upstream of *AHR1*. In opaque cells Wor1, Wor2 and Wor3 bind upstream of *AHR1* and regulate its expression (Hernday *et al.*, 2013). ChIP-analyses of the current study show that the hyperactive Ahr1 bound upstream of *WOR1*, *WOR2*, *WOR3*, *CZF1*, and *EFG1*. Due to this, future research could take a look at the role of Wor1, Wor2 and Wor3 during *ECE1* expression. It could for example be analyzed if a hyperactive Ahr1 is still able to induce *ECE1* and *ALS3* expression in the *wor1* Δ , *wor2* Δ , *wor3* Δ or *czf1* Δ mutants. Interestingly, Wang *et al.* (2011) identified that Ahr1 activates white cell formation but only if Efg1, a key regulator for white state maintenance is present. The data of this study show that for the regulation of several CFR genes, the hyperactive Ahr1 works independent of Efg1(/Cph1). Furthermore, transcriptional control of Wor1, the master regulator of the opaque cell type, is associated with Tup1, Ssn6 and Tcc1 (Alkafeef *et al.*, 2018). Here, Tup1 acts as major repressor of the opaque cell type, binding to the promoter of *WOR1* in white cells and repressing its expression (Alkafeef *et al.*, 2018).

4.5. A mutated *SSN3* allele induces *ECE1* and *ALS3* expression independent of *Ahr1* and *Tup1*

Of course, it would also be interesting to identify putative regulators of *Ahr1* which control its function in response to environmental stimuli. Phosphorylation might be a suitable subject for such further studies. For example, it was already shown that phosphorylation is important for the activation or deactivation of transcription factors like *Efg1* and *Cst6* (Bockmühl *et al.*, 2001; Pohlers *et al.*, 2017). In a previous study, it was shown that a point mutation in the *SSN3* gene induces filamentation and upregulation of genes like *ALS3* and *ECE1* in the *cpb1* Δ /*efg1* Δ double mutant (Wartenberg *et al.*, 2014), which is similar to the here presented results for hyperactive *Ahr1*. Therefore, a closer look at the role of the kinase *Ssn3* concerning the expression of hypha-specific genes has been taken. *Ssn3* (also known as *Cdk8* in humans) is part of the cyclin-dependent kinase (CDK) module of the mediator complex (Myers and Kornberg, 2000; Lewis and Reinberg, 2003). It is a kinase involved in the phosphorylation of the RNA polymerase II C-terminal domain and thus plays a role in regulating RNA polymerase II activity. The SNP mutation in *SSN3* described by Wartenberg *et al.* (2014) leads to an Arg³⁵²Gln substitution in the substrate recognition loop of *Ssn3*. Subsequently, it was speculated by the authors that due to reduced or impaired substrate recognition or phosphorylation activity of this kinase, positive regulators of filamentous growth were stabilized or a derepression of the genes involved in activation of filamentous growth was achieved (Wartenberg *et al.*, 2014). An example for this is that at high CO₂ concentrations, *Ssn3* is dephosphorylated by *Ptc2* which in turn reduces the phosphorylation of *Ume6* by *Ssn3* (Lu *et al.*, 2019). Subsequently, the degradation of *Ume6* is prevented and hyphal development is maintained (Lu *et al.*, 2019). In the current work and the study of Wartenberg *et al.* (2014) one mutated *SSN3* allele competed with the wild type allele(s) on a position in the mediator complex. Nevertheless, already one mutated allele alone was enough to promote the expression of hypha-specific genes (*ECE1*, *ALS3*, *HWP1*, *IHD1*). However, this was achieved independently of *Ahr1* and *Tup1*, indicating that an additional mechanism exists which induces the high-level transcription of *ECE1* and other core filamentation response genes. In *S. cerevisiae* it was previously shown that *Ssn3*, as part of the mediator complex, is involved in the repression of many genes in the presence of glucose, possibly as a target of *Tup1* (Balciunas and Ronne, 1995), since the catalytic activity of *Ssn3* contributes to the repression of a subset of *Tup1*-regulated genes (Kuchin *et al.*, 1995; Green and Johnson, 2004). This might explain other observations of this study, as *ECE1* upregulation is not only caused by the aforementioned mutated *SSN3* allele, but also after the deletion of the *SSN3* gene. A similar pattern was observed for *ALS3*, *HWP1* and *IHD1*. The upregulation of these genes correlated with hyphal formation in the glucose-containing SDG medium at 37°C, which usually only triggers yeast growth. However, *Ssn3* is probably not only involved in the repression of genes. In *S. cerevisiae* *Cdk8* (*Ssn3* ortholog) along with the mediator complex was shown to bind to sites of both activated and repressed genes (Andrau *et al.*, 2006). This demonstrates the complex nature of *Ssn3* regulation. However, the data provided here on *Ssn3* are only preliminary. Future studies should focus on the detailed regulation of target genes via *Ssn3*. The exact processes taking place at the respective promoters still need to be elucidated.

4.6. *MCM1* overexpression induces the expression of *ECE1* and *ALS3* in partly Ahr1-dependent manner

This study identified Ahr1 as an important regulator for CFR gene expression. As mentioned before, Ahr1 has so far been connected to the regulation of adhesion genes (Askew *et al.*, 2011), white-opaque switching (Wang *et al.*, 2011), amino acid utilization (Vylkova and Lorenz, 2017) and biofilm formation (Nobile and Johnson, 2015). Furthermore, Ahr1 was shown to recruit Mcm1 to promoters of adhesion genes where the Ahr1-Mcm1-complex activated the expression of *ALS1*, *ALS4*, *HWP1*, *EFG1* and *TEC1* (Askew *et al.*, 2011). Just like Ahr1, Mcm1 possesses possible binding sites upstream of the *ECE1* ORF and was already proven to bind upstream of *ECE1*, *ALS3* and *HWP1* in *C. albicans* hyphae (Lavoie *et al.*, 2008; Tuch *et al.*, 2008). Since *MCM1* is an essential gene, the effect of its deletion on *ECE1* expression could not be analyzed. Instead, a *MCM1* overexpression was used to study the influence of this regulatory gene on *ECE1* expression. Indeed, it induced an upregulation of *ECE1*, *ALS3*, *IHD1* and *HWP1*, similar to the patterns which were observed with the hyperactive Ahr1. This effect was less pronounced in a mutant lacking *AHR1*, showing that this mechanism is at least partially dependent on Ahr1. A possible interplay between Ahr1 and Mcm1 on the promoters of *ECE1* and *ALS3* and *IHD1* has not yet been reported.

4.7. High-level expression of *ECE1* and *ALS3* relies on Tup1

Interestingly, the *tup1* Δ mutant displayed a similar phenotype as the *ahr1* Δ mutant. The expression of *ECE1* was only intermediate in the *tup1* Δ mutant under hyphal growth conditions compared to the wild type (Fig. 10). This correlated to a low secretion of Candidalysin, which could be an explanation for the reduced cytotoxicity (Allert *et al.*, 2018) and avirulence (Braun *et al.*, 2000; Straffon *et al.*, 2001) of this filamentous mutant. The current study indicates that, just like in the *ahr1* Δ mutant, an intermediate expression of *ECE1* and subsequent intermediate levels of secreted Candidalysin are not enough to induce full virulence in the *tup1* Δ mutant. Neither a hyperactive Ahr1 nor the overexpression of *MCM1* could increase the transcription of *ECE1* or *ALS3* up to wild-type level in the *tup1* Δ mutant.

4.8. Model for Ahr1-dependent transcription of *ECE1* and *ALS3* in *C. albicans* hyphae

Based on all these observations, the following model for the transcriptional control of *ECE1* and *ALS3* in *C. albicans* yeast and hyphal cells is being proposed (Fig. 31):

In yeast cells, the complex of Tup1 and Nrg1 represses the expression of *ECE1* and *ALS3* (Murad *et al.*, 2001b; Braun *et al.*, 2001; Murad *et al.*, 2001a; Lu *et al.*, 2011). This repression is released after the initiation of hyphal growth (Martin *et al.*, 2013; Lu *et al.*, 2011; Kadosh and Johnson, 2005; Murad *et al.*, 2001a,b). The release is most likely mediated by degradation of the Nrg1 protein (Lu *et al.*, 2011). However, the fate of Tup1 was not studied so far. The data presented in this study indicate that Tup1 remains at the promoters and contributes to the Ahr1/Mcm1 mediated transcription of *ECE1* and *ALS3* in *C. albicans*' hyphae. However, it is neither clear if this interaction is direct or indirect nor where Tup1 is actually localized. In

contrast to Nrg1, Ahr1 and Mcm1, it does not contain a DNA binding domain. The proposed Ahr1-dependent activation of *ECE1* and *ALS3* expression works alternatively from the already mentioned MAPK and cAMP-PKA pathways where the activation of hypha-specific genes works mainly via Efg1 and Cph1. In this model, Brg1 recruitment of Hda1 to promoters of hypha-specific genes during hyphal elongation (Lu *et al.*, 2012) is not needed since it was shown that the action of the hyperactive Ahr1 is independent from Brg1.

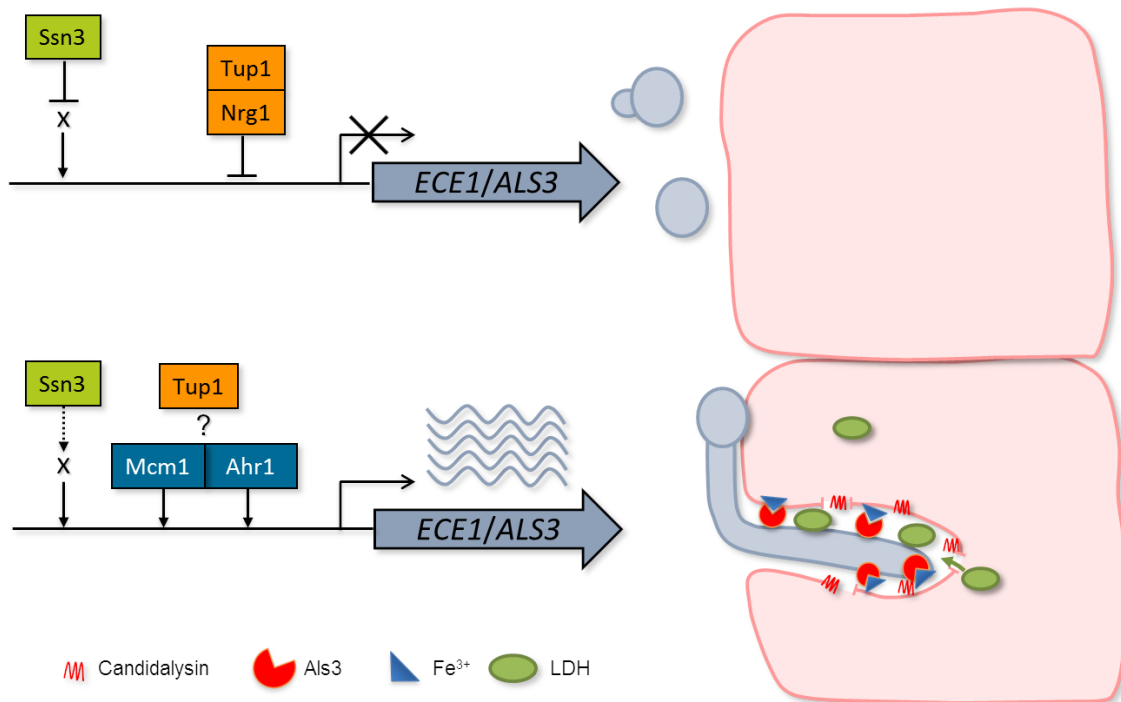


Fig. 31: **Model for the regulation of *ECE1* and *ALS3* in *C. albicans*' hyphae.**

Under yeast growth conditions the expression of *ECE1* and *ALS3* is repressed by Tup1-Nrg1. In parallel, Ssn3 prevents the expression of these genes via a so far unknown mechanism or factor. Upon hyphal induction Ssn3 is deactivated and hypha-specific genes are expressed. Independently, Ahr1 binds to the promoters of *ECE1* and *ALS3* and interacts with Tup1 and Mcm1 to activate the expression. Subsequent high-level gene expression leads to a functional level of Candidalysin and Als3. This model may also be valid for other virulence and hypha-specific genes.

The hypothesis that Tup1 plays a central role in the proposed model is supported by the fact that Als3 localization on cell surfaces and Candidalysin amounts secreted from *ahr1* Δ and *tup1* Δ under hyphal growth conditions were reduced. The exact mechanism by which Ssn3 inactivates and activates the transcription of *ECE1* and *ALS3* in yeast and hyphae, respectively, is so far unknown. However, a possible link to Ume6 has already been described (Lu *et al.*, 2019). This study proves that neither Ahr1 nor Tup1 are necessary for the expression of these genes via the mutated *SSN3*.

Speaking for a regulating role of Tup1 in *C. albicans* hyphae is that a Tup1-Tup1 interaction (Tup1 forms tetramers with itself (Varanasi *et al.*, 1996; Spargue *et al.*, 2000)) was observed after 1 h serum induction using a split-GFP system by Garbe (2016). With the same system, a dissolution of the Tup1-Nrg1 interaction was observed after the initiation of hyphal growth

(Garbe, 2016). For the proposed model, it would be necessary to examine possible physical interactions between Tup1, Mcm1 and especially Ahr1 in future experiment. If it exists, such an interaction could be proven by either a split-GFP approach or by co-immunoprecipitation. Although both assays might prove an interaction between Tup1 and Ahr1, they are both limited in the resolution of time. To show when exactly both regulators interact with each other, the more dynamic Förster resonance energy transfer (FRET) assay could be applied. A more general approach to prove an interaction would be a pull-down assay with Ahr1 and/ or Tup1.

The proposed model includes only Tup1, Ahr1 and Mcm1. However, there might be more factors involved, including those which are known interaction partners of Tup1, especially Tcc1 and Ssn6 (Kaneko *et al.*, 2006; Smith and Johnson, 2000). Like Tup1, Ssn6 contributes at least partially to hyphal growth and associated gene expression (Hwang *et al.*, 2003; Lee *et al.*, 2015). Its homolog in *S. cerevisiae*, Cyc8 was already shown to contribute to repression and activation of gene expression, always together with its co-factor Tup1 (Smith and Johnson, 2000; Courey and Jia, 2001; Papamichos-Chronakis *et al.*, 2002; Mennella *et al.*, 2003). In contrast, the role of Tcc1 is rather unknown. A pull-down assay with Ahr1 might show, if it interacts with one of these co-factors. Interestingly, the ChIP-Seq data of this study showed that hyperactive Ahr1 could bind to the promoter of *TCC1* and induces its expression. This might be a hint to a possible interaction. Another fascinating approach would be the usage of ChIP with selective isolation of chromatin-associated proteins (ChIP-SICAP) followed by mass spectrometry (MS) (Rafiee *et al.*, 2016; van Wijlick *et al.*, 2019). This method could be used to show an interaction between Tup1 and Ahr1/Mcm1 on hyphal chromatin, e.g. of the *ECE1* promoter.

According to expression and ChIP-seq data from this study, the proposed model could also be valid for *HWP1* and *IHD1*. Furthermore, a binding of Mcm1 to the promoter of *Hwp1* has already been observed by others (Lavoie *et al.*, 2008). Also further virulence and hypha-specific genes could be regulated in an Ahr1-dependent manner. The hyperactive Ahr1 for example bound 807, 1144 and 833 bp upstream the hypha-specific genes *SAP4*, *SAP5* and *SAP6*, respectively. Sap4-6 are secreted aspartyl proteinases and facilitate the liberation of nutrients from host cells and play a role in the destruction and active penetration of tissue (Felk *et al.*, 2002) and immune cell evasion (Borg-von Zepelin *et al.*, 1998). Furthermore, ChIP binding profiles suggests that the hyperactive Ahr1 regulates *SOD5* expression. Sod5 is a superoxide dismutase and important for the survival of *C. albicans* in blood (Fradin *et al.*, 2005).

In summary, this study introduced Ahr1 as a novel key contributor of the regulation of hypha- and virulence-associated genes. Its beneficial role for the activation of *ALS3* and *ECE1* expression depends on the presence of Tup1, indicating that the latter is not only important for repression, but also activation of these genes, and might involve its interacting partner Mcm1. This adds another mechanism to the overall complex regulation of the two virulence-associated genes in *C. albicans* hyphae.

VI. Literature

- KH Abu-Elteen, AZ Elkarmi, and M Hamad. Characterization of Phenotype-Based Pathogenic Determinants of Various *Candida albicans* strains in Jordan. *Jpn. J. Infect. Dis.*, 54:229–236, 2001.
- A Ahlquist Cleveland, LH Harrison, MM Farley, R Hollick, B Stein, TM Chiller, SR Lockhart, and BJ Park. Declining incidence of candidemia and the shifting epidemiology of *Candida* resistance in two US metropolitan areas, 2008-2013: Results from population-based surveillance. *PLoS One*, 10(3):2008–2013, 2015.
- SS Alkafeef, C Yu, L Huang, and H Liu. Wor1 establishes opaque cell fate through inhibition of the general co-repressor Tup1 in *Candida albicans*. *PLoS Genet*, 14(1):e1007176, 2018.
- S Allert, T Förster, C-M Svensson, JP Richardson, T Pawlik, B Hebecker, S Rudolphi, M Juraschitz, M Schaller, M Blagojevic, J Morschhäuser, T Figge, ID Jacobsen, JR Naglik, L Kasper, S Mogavero, and B Hube. *Candida albicans* -Induced Epithelial Damage Mediates Translocation through Intestinal Barriers. *MBio*, 9(3):e00915–18, 2018.
- RS. Almeida, S Brunke, A Albrecht, S Thewes, M Laue, JE. Edwards, SG. Filler, and B Hube. The hyphal-associated adhesin and invasin Als3 of *Candida albicans* mediates iron acquisition from host ferritin. *PLoS Pathog.*, 4(11):1–17, 2008.
- R Alonso Monge, E Román, C Nombela, and J Pla. The MAP kinase signal transduction network in *Candida albicans*. *Microbiology*, 152(4):905–912, 2006.
- FJ Alvarez and JB Konopka. Identification of an N-Acetylglucosamine Transporter That Mediates Hyphal Induction in *Candida albicans*. *Mol. Biol. Cell*, 18:965–975, 2007.
- JC Andrau, L van de Pasch, P Lijnzaad, T Bijma, M Groot Koerkamp, J van de Peppel, M Werner, and FCP Holstege. Genome-Wide Location of the Coactivator Mediator: Binding without Activation and Transient Cdk8 Interaction on DNA. *Mol. Cell*, 22(2):179–192, 2006.
- M Arendrup, T Horn, and N Frimodt-Møller. In vivo pathogenicity of eight medically relevant *Candida* species in an animal model. *Infection*, 30(5):286–291, 2002.
- MC Arendrup. Epidemiology of invasive candidiasis. *Curr. Opin. Crit. Care*, 16(5):445–452, 2010.
- S Argimón, JA Wishart, R Leng, S Macaskill, Mavor, T Alexandris, S Nicholls, AW Knight, B Enjalbert, R Walmsley, FC Odds, NAR Gow, and AJP Brown. Developmental regulation of an adhesin gene during cellular morphogenesis in the fungal pathogen *Candida albicans*. *Eukaryot. Cell*, 6(4):682–692, 2007.
- C Askew, A Sellam, E Epp, J Mallick, H Hogues, A Mullick, A Nantel, and M Whiteway. The zinc cluster transcription factor Ahr1p directs Mcm1p regulation of *Candida albicans* adhesion. *Mol. Microbiol.*, 79(4):940–953, 2011.

- O Bader, Y Krauke, and B Hube. Processing of predicted substrates of fungal Kex2 proteinases from *Candida albicans*, *C. glabrata*, *Saccharomyces cerevisiae* and *Pichia pastoris*. *BMC Microbiol.*, 8:1–16, 2008.
- YS Bahn and FA Mühlshlegel. CO₂ sensing in fungi and beyond. *Curr. Opin. Microbiol.*, 9(6): 572–578, 2006.
- DA Bailey, PJF Feldmann, M Bovey, NAR Gow, and AIP Brown. The *Candida albicans* HYR1 gene, which is activated in response to hyphal development, belongs to a gene family encoding yeast cell wall proteins. *J. Bacteriol.*, 178(18):5353–5360, 1996.
- D Balciunas and H Ronne. Three subunits of the RNA polymerase II mediator complex are involved in glucose repression. *Nucleic Acids Res.*, 23(21):4426–4433, 1995.
- CW Baldridge and RW Gerard. The Extra Respiration of Phagocytosis. *Am. J. Physiol.*, 103(1):235–236, 1932.
- M Banerjee, DS Thompson, A Lazzell, PL Carlisle, C Pierce, C Monteagudo, JL López-Ribot, and D Kadosh. UME6, a Novel Filament-specific Regulator of *Candida albicans* Hyphal Extension and Virulence. *Mol. Biol. Cell*, 19:1354–1365, 2008.
- KJ Barwell, JH Boysen, W Xu, and AP Mitchell. Relationship of DFG16 to the Rim101p pH response pathway in *Saccharomyces cerevisiae* and *Candida albicans*. *Eukaryot. Cell*, 4(5): 890–899, 2005.
- M Bassilana, J Blyth, and RA Arkowitz. Cdc24, the GDP-GTP exchange factor for Cdc42, is required for invasive hyphal growth of *Candida albicans*. *Eukaryot. Cell*, 2(1):9–18, 2003.
- V Basso, C D’Enfert, S Znaidi, and S Bachellier-Bassi. From Genes to Networks: The Regulatory Circuitry Controlling *Candida albicans* Morphogenesis. *Curr. Top. Microbiol. Immunol.*, 433: 61–99, 2019.
- J Bauer and J Wendland. *Candida albicans* Sfl1 suppresses flocculation and filamentation. *Eukaryot. Cell*, 6(10):1736–1744, 2007.
- K Bedard and KH Krause. The NOX family of ROS-generating NADPH oxidases: Physiology and Pathophysiology. *Physiol. Rev.*, 87(1):245–313, 2007.
- ES Bensen, SG Filler, and J Berman. A forkhead transcription factor is important for true hyphal as well as yeast morphogenesis in *Candida albicans*. *Eukaryot. Cell*, 1(5):787–798, 2002.
- ES Bensen, SJ Martin, M Li, J Berman, and DA Davis. Transcriptional profiling in *Candida albicans* reveals new adaptive responses to extracellular pH and functions for Rim101p. *Mol. Microbiol.*, 54(5):1335–1351, 2004.
- J Berman and PE Sudbery. *Candida albicans*: A molecular revolution built on lessons from budding yeast. *Nat. Rev. Genet.*, 3(12):918–930, 2002.

- CE Birse, MY Irwin, WA Fonzi, and PS Sypherd. Cloning and characterization of ECE1, a gene expressed in association with Cell Elongation of the Dimorphic Pathogen *Candida albicans*. *Infect. Immun.*, 61(9):3648–3655, 1993.
- K Biswas and J Morschhäuser. The Mep2p ammonium permease controls nitrogen starvation-induced filamentous growth in *Candida albicans*. *Mol. Microbiol.*, 56(3):649–669, 2005.
- DP Bockmühl and JF Ernst. A potential phosphorylation site for an A-Type kinase in the Efg1 regulator protein contributes to hyphal morphogenesis of *Candida albicans*. *Genetics*, 157(4):1523–1530, 2001.
- DP Bockmühl, S Krishnamurthy, M Gerads, A Sonneborn, and JF Ernst. Distinct and redundant roles of the two protein kinase A isoforms Tpk1p and Tpk2p in morphogenesis and growth of *Candida albicans*. *Mol. Microbiol.*, 42(5):1243–1257, 2001.
- M Borg-von Zepelin, S Beggah, K Boggian, D Sanglard, and M Monod. The expression of the secreted aspartyl proteinases Sap4 to Sap6 from *Candida albicans* in murine macrophages. *Mol. Microbiol.*, 28(3):543–554, 1998.
- A Boveris. *Production of superoxide anion and hydrogen peroxide in yeast mitochondria*. In: *Biochemistry and Genetics of Yeast*. New York: Academic Press, biochemist edition, 1978.
- BR Braun and AD Johnson. Control of filament formation in *Candida albicans* by the transcriptional repressor TUP1. *Science (80-.)*, 277(5322):105–109, 1997.
- BR Braun and AD Johnson. TUP1, CPH1 and EFG1 make independent Contributions to Filamentation in *Candida albicans*. *Genetics*, 155:57–67, 2000.
- BR Braun, WS Head, MX Wang, and AD Johnson. Identification and characterization of TUP1-regulated genes in *Candida albicans*. *Genetics*, 156:31–44, 2000.
- BR Braun, D Kadosh, and AD Johnson. NRG1, a repressor of filamentous growth in *C. albicans*, is down-regulated during filament induction. *EMBO J.*, 20(17):4753–4761, 2001.
- GD Brown, DW Denning, NAR Gow, SM Levitz, MG Netea, and TC White. Hidden killers: Human fungal infections. *Sci. Transl. Med.*, 4(165):1–9, 2012.
- DH Brown Jr, AD Giusani, X Chen, and CA Kumamoto. Filamentous growth of *Candida albicans* in response to physical environmental cues and its regulation by the unique CZF1 gene. *Mol. Microbiol.*, 34(4):651–662, 1999.
- J Buffo, MA Herman, and DR Soll. A characterization of pH-regulated dimorphism in *Candida albicans*. *Mycopathologia*, 85(1-2):21–30, 1984.
- F Cao, S Lane, PP Raniga, Y Lu, Z Zhou, K Ramon, J Chen, and H Liu. The Flo8 Transcription Factor Is Essential for Hyphal Development and Virulence in *Candida albicans*. *Mol. Biol. Cell*, 17:295–307, 2006.

- PL Carlisle and D Kadosh. *Candida albicans* Ume6, a filament-specific transcriptional regulator, directs hyphal growth via a pathway involving Hgc1 cyclin-related protein. *Eukaryot. Cell*, 9(9):1320–1328, 2010.
- PL Carlisle, M Banerjee, A Lazzell, C Monteagudo, JL López-Ribot, and D Kadosh. Expression levels of a filament-specific transcriptional regulator are sufficient to determine *Candida albicans* morphology and virulence. *Proc. Natl. Acad. Sci. U. S. A.*, 106(2):599–604, 2009.
- L Casteilla, M Rigoulet, and L Pénicaud. Mitochondrial ROS metabolism: Modulation by uncoupling proteins. *IUBMB Life*, 52(3-5):181–188, 2002.
- C-G Chen, Y-L Yang, H-I Shih, C-L Su, and H-J Lo. CaNdt80 is involved in drug resistance in *Candida albicans* by regulating CDR1. *Antimicrob. Agents Chemother.*, 48(12):4505–4512, 2004.
- H Chu, Y Duan, S Lang, L Jiang, Y Wang, C Llorente, J Liu, S Mogavero, F Bosques-Padilla, JG Abraldes, V Vargas, XM Tu, L Yang, X Hou, B Hube, P Stärkel, and B Schnabl. The *Candida albicans* exotoxin Candidalysin promotes alcohol-associated liver disease. *J. Hepatol.*, 72(3):391–400, 2019.
- IA Cleary, SM Reinhard, AL Lazzell, C Monteagudo, DP Thomas, JL Lopez-Ribot, and SP Saville. Examination of the pathogenic potential of *Candida albicans* filamentous cells in an animal model of haematogenously disseminated candidiasis. *FEMS Yeast Res.*, 16(2):1–10, 2016.
- AJ Courey and S Jia. Transcriptional repression: The long and the short of it. *Genes Dev.*, 9(6):2786–2796, 2001.
- PWJ de Groot, O Bader, AD de Boer, M Weig, and N Chauhan. Adhesins in human fungal pathogens: Glue with plenty of stick. *Eukaryot. Cell*, 12(4):470–481, 2013.
- PA De Viragh, D Sanglard, G Togni, R Falchetto, and M Monod. Cloning and sequencing of two *Candida parapsilosis* genes encoding acid proteases. *J. Gen. Microbiol.*, 139(2):335–342, 1993.
- DW Denning. Echinocandins: a new class of antifungal. *J. Antimicrob. Chemother.*, 49(6):889–891, 2002.
- H Du, G Guan, J Xie, F Cottier, Y Sun, W Jia, FA Mühlischlegel, and G Huang. The transcription factor Flo8 mediates CO₂ sensing in the human fungal pathogen *Candida albicans*. *Mol. Biol. Cell*, 23(14):2692–2701, 2012.
- JF Ernst. Transcription factors in *Candida albicans*-environmental control of morphogenesis. *Microbiology*, 146(8):1763–1774, 2000.
- LP Erwig and NAR Gow. Interactions of fungal pathogens with phagocytes. *Nat. Rev. Microbiol.*, pages 163–176, 2016.

- HM Fang and Y Wang. RA domain-mediated interaction of Cdc35 with Ras1 is essential for increasing cellular cAMP level for *Candida albicans* hyphal development. *Mol. Microbiol.*, 61(2):484–496, 2006.
- A Felk, M Kretschmar, A Albrecht, M Schaller, S Beinhauer, T Nichterlein, D Sanglard, HC Korting, W Schäfer, and B Hube. *Candida albicans* hyphal formation and the expression of the Efg1-regulated proteinases Sap4 to Sap6 are required for the invasion of parenchymal organs. *Infect. Immun.*, 70(7):3689–3700, 2002.
- PL Fidel. *Candida*-host interactions in HIV disease: implications for oropharyngeal candidiasis. *Adv. Dent. Res.*, 23(1):45–49, 2011.
- C Fradin, P De Groot, D MacCallum, M Schaller, F Klis, FC Odds, and B Hube. Granulocytes govern the transcriptional response, morphology and proliferation of *Candida albicans* in human blood. *Mol. Microbiol.*, 56(2):397–415, 2005.
- E Garbe. *Characterization of the Candida albicans ECE1 promoter*. PhD thesis, Friedrich-Schiller-Universität Jena, 2016.
- S Garcia-Sanchez, AL Mavor, CL Russell, S Argimon, P Dennison, B Enjalbert, and AJP Brown. Global Roles of Ssn6 in Tup1- and Nrg1-dependent Gene Regulation in the Fungal Pathogen, *Candida albicans*. *Mol. Biol. Cell*, 16(June):2913–2925, 2005.
- GD Gilfillan, DJ Sullivan, K Haynes, T Parkinson, DC Coleman, and NAR Gow. *Candida dubliniensis*: Phylogeny and putative virulence factors. *Microbiology*, 144(4):829–838, 1998.
- AM Gillum, EYH Tsay, and DR Kirsch. Isolation of the *Candida albicans* gene for orotidine-5'-phosphate decarboxylase by complementation of *S. cerevisiae* *ura3* and *E. coli* *pyrF* mutations. *Mol. Gen. Genet.*, 198(1):179–182, 1984.
- J Gomez-Raja and DA Davis. The beta-arrestin-like protein Rim8 is hyperphosphorylated and complexes with Rim21 and Rim101 to promote adaptation to neutral-alkaline pH. *Eukaryot. Cell*, 11(5):683–693, 2012.
- KC Gray, DS Palacios, I Dailey, MM Endo, BE Uno, BC Wilcock, and MD Burke. Amphotericin primarily kills yeast by simply binding ergosterol. *Proc. Natl. Acad. Sci.*, 109(7):2234–2239, 2012.
- SR Green and AD Johnson. Promoter-dependent Roles for the Srb10 Cyclin-dependent Kinase and the Hda1 Deacetylase in Tup1-mediated Repression in *Saccharomyces cerevisiae*. *Mol. Biol. Cell*, 15:4191–4202, 2004.
- JA Greig, IM Sudbery, JP Richardson, JR Naglik, Y Wang, and PE Sudbery. Cell cycle-independent phospho-regulation of Fkh2 during hyphal growth regulates *Candida albicans* pathogenesis. *PLoS Pathog.*, 11(1):e1004630, 2015.

- CT Harbison, DB Gordon, TI Lee, NJ Rinaldi, KD Macisaac, TW Danford, NM Hannett, JB Tagne, DB Reynolds, J Yoo, EG Jennings, J Zeitlinger, DK Pokholok, M Kellis, PA Rolfe, KT Takusagawa, ES Lander, DK Gifford, E Fraenkel, and RA Young. Transcriptional regulatory code of a eukaryotic genome. *Nature*, 431:99–104, 2004.
- D Marcus, A Nantel, A Marcil, T Rigby, and M Whiteway. Transcription Profiling of Cyclic AMP Signaling in *Candida albicans*. *Mol. Biol. Cell*, 15:4490–4499, 2004.
- AD Hernday, MB Lohse, PM Fordyce, CJ Nobile, JL Derisi, and AD Johnson. Structure of the transcriptional network controlling white-opaque switching in *Candida albicans*. *Mol. Microbiol.*, 90(1):22–35, 2013.
- J Ho, X Yang, SA Nikou, N Kichik, A Donkin, NO Ponde, JP Richardson, RL Gratacap, LS Archambault, CP Zwirner, C Murciano, R Henley-Smith, S Thavaraaj, CJ Tynan, SL Gaffen, B Hube, RT Wheeler, DL Moyes, and JR Naglik. Candidalysin activates innate epithelial immune responses via epidermal growth factor receptor. *Nat. Commun.*, 10(1), 2019.
- NJ Holton, TJD Goodwin, MI Butler, and RTM Poulter. An active retrotransposon in *Candida albicans*. *Nucleic Acids Res.*, 29(19):4014–4024, 2001.
- OR Homann and AD Johnson. MochiView: Versatile software for genome browsing and DNA motif analysis. *BMC Biol.*, 8(49), 2010.
- OR Homann, J Dea, SM Noble, and AD Johnson. A phenotypic profile of the *Candida albicans* regulatory network. *PLoS Genet*, 5(12), 2009.
- H Hope, C Schmauch, RA Arkowitz, and M Bassilana. The *Candida albicans* ELMO homologue functions together with Rac1 and Dck1, upstream of the MAP Kinase Cek1, in invasive filamentous growth. *Mol. Microbiol.*, 76(6):1572–1590, 2010.
- LL Hoyer, TL Payne, M Bell, AM Myers, and S Scherer. *Candida albicans* ALS3 and insights into the nature of the ALS gene family. *Curr. Genet.*, 33(6):451–459, 1998.
- LL Hoyer, Cl Green, S-h Oh, and X Zhao. Discovering the secrets of the *Candida albicans* agglutinin-like sequence (ALS) gene family - a sticky pursuit. *Med. Mycol.*, 46(February): 1–15, 2008.
- B Hube, M Monod, DA Schofield, AJP Brown, and NAR Gow. Expression of seven members of the gene family encoding secretory aspartyl proteinases in *Candida albicans*. *Mol. Microbiol.*, 14(1):87–99, 1994.
- B Hube, D Sanglard, FC Odds, D Hess, M Monod, W Schäfer, AJP Brown, and NAR Gow. Disruption of Each of the Secreted Aspartyl Proteinase Genes Attenuates Virulence. *Infect. Immun.*, 65(9):3529–3538, 1997.
- CS Hwang, GE Rhie, JH Oh, WK Huh, HS Yim, and SO Kang. Copper- and zinc-containing superoxide dismutase (Cu/ZnSOD) is required for the protection of *Candida albicans* against oxidative stresses and the expression of its full. *Microbiology*, 148:3705–3713, 2002.

- CS Hwang, JH Oh, WK Huh, HS Yim, and SO Kang. Ssn6, an important factor of morphological conversion and virulence in *Candida albicans*. *Mol. Microbiol.*, 47(4):1029–1043, 2003.
- ID Jacobsen, D Wilson, B Wächtler, S Brunke, JR Naglik, and B Hube. *Candida albicans* dimorphism as therapeutic target. *Expert Rev. Anti Infect. Ther.*, 10(1):85–93, 2012.
- WH Jung and LI Stateva. The cAMP phosphodiesterase encoded by CaPDE2 is required for hyphal development in *Candida albicans*. *Microbiology*, 149(10):2961–2976, 2003.
- D Kadosh and AD Johnson. Induction of the *Candida albicans* Filamentous Growth Program by Relief of Transcriptional Repression: A Genome-wide Analysis. *Mol. Biol. Cell*, 16:2903–2912, 2005.
- A Kaneko, T Umeyama, Y Utena-Abe, S Yamagoe, M Niimi, and Y Uehara. Tcc1p, a novel protein containing the tetratricopeptide repeat motif, interacts with Tup1p to regulate morphological transition and virulence in *Candida albicans*. *Eukaryot. Cell*, 2006.
- L Kasper, A König, P-A Koenig, MS Gresnigt, J Westman, RA Drummond, MS Lionakis, O Groß, J Ruland, JR Naglik, and B Hube. The fungal peptide toxin Candidalysin activates the NLRP3 inflammasome and causes cytolysis in mononuclear phagocytes. *Nat. Commun.*, 9(1):4260, 2018.
- T Klengel, WJ Liang, J Chaloupka, C Ruoff, K Schröppel, JR Naglik, SE Eckert, E Gewiss Mogensen, K Haynes, MF Tuite, LR Levin, J Buck, and FA Mühlischlegel. Fungal adenylyl cyclase integrates CO₂ sensing with cAMP signaling and virulence. *Curr. Biol.*, 15(22):2021–2026, 2005.
- EM Kojic and RO Darouiche. *Candida* Infections of Medical Devices. *Clin. Microbiol. Rev.*, 17(2):255–267, 2004.
- S Kuchin, P Yeghiayan, and M Carlson. Cyclin-dependent protein kinase and cyclin homologs SSN3 and SSN8 contribute to transcriptional control in yeast. *Proc. Natl. Acad. Sci. U. S. A.*, 92(9):4006–4010, 1995.
- BJ Kullberg and MC Arendrup. Invasive Candidiasis. *Infect. Dis. Clin. North Am.*, pages 1445–1456, 2016.
- RV Lalla, MC Latortue, CH Hong, A Ariyawardana, S D’Amato-Palumbo, DJ Fischer, A Martof, LL Patton, O Nicolatou-Galitis, LS Elting, FKL Spijkervet, and MT Brennan. A systematic review of oral fungal infections in patients receiving cancer therapy. *Support Care Cancer*, 18(8):985–992, 2010.
- C Lamarre, J-D Lemay, N Deslauriers, and Y Bourbonnais. *Candida albicans* Expresses an Unusual Cytoplasmic Manganese-containing Superoxide Dismutase (SOD3 Gene Product) upon the Entry and during the Stationary Phase. *J. Biol. Chem.*, 276(47):43784–43791, 2001.
- H Lavoie, A Sellam, C Askew, A Nantel, and M Whiteway. A toolbox for epitope-tagging and genome-wide location analysis in *Candida albicans*. *BMC Genomics*, 9:578, 2008.

- E Leberer, D H Marcus, D Dignard, L Johnson, S Ushinsky, DY Thomas, and K Schröppel. Ras links cellular morphogenesis to virulence by regulation of the MAP kinase and cAMP signalling pathways in the pathogenic fungus *Candida albicans*. *Mol. Microbiol.*, 42(3):673–687, 2001.
- JE Lee, JH Oh, M Ku, J Kim, JS Lee, and SO Kang. Ssn6 has dual roles in *Candida albicans* filament development through the interaction with Rpd31. *FEBS Lett.*, 589(4):513–520, 2015.
- KL Lee, HR Buckley, and CC Campbell. An amino acid liquid synthetic medium for the development of mycelial and yeast forms of *Candida albicans*. *Sabouraudia*, 13(2):148–153, 1975.
- A Lemke, AF Kiderlen, and O Kayser. Amphotericin B. *Appl. Microbiol. Biotechnol.*, 68(2):151–162, 2005.
- P Leng, PR Lee, H Wu, and AJP Brown. Efg1, a Morphogenetic Regulator in *Candida albicans*, Is a Sequence-Specific DNA Binding Protein. *J. Bacteriol.*, 183(13):4090–4093, 2001.
- BA Lewis and D Reinberg. The mediator coactivator complex: Functional and physical roles in transcriptional regulation. *J. Cell Sci.*, 116(18):3667–3675, 2003.
- F Li and Sean P. Palecek. EAP1, a *Candida albicans* Gene Involved in Binding Human Epithelial Cells. *Eukaryot. Cell*, 2(6):1266–1273, 2003.
- H Liu. Transcriptional control of dimorphism in *Candida albicans*. *Curr. Opin. Biol. Chem.*, 4:728–735, 2001.
- H Liu, J Köhler, and GR Fink. Suppression of hyphal formation in *Candida albicans* by mutation of a STE12 homolog. *Science (80-.)*, 266(5191):1723–1726, 1994.
- HJ Lo, JR Kohler, B Didomenico, D Loebenberg, A Cacciapuoti, and GR Fink. Non-filamentous *C. albicans* mutants are avirulent. *Cell*, 90:939–949, 1997.
- MC Lorenz, JA Bender, and GR Fink. Transcriptional response of *Candida albicans* upon internalization by macrophages. *Eukaryot. Cell*, 3(5):1076–1087, 2004.
- O Lortholary, C Renaudat, K Sitbon, Y Madec, L Denoeud-Ndam, M Wolff, A Fontanet, S Bretagne, and F Dromer. Worrisome trends in incidence and mortality of candidemia in intensive care units (Paris area, 2002-2010). *Intensive Care Med.*, 40(9):1303–1312, 2014.
- Y Lu, C Su, A Wang, and H Liu. Hyphal development in *Candida albicans* requires two temporally linked changes in promoter chromatin for initiation and maintenance. *PLoS Biol.*, 9(7):e1001105, 2011.
- Y Lu, C Su, and H Liu. A GATA transcription factor recruits Hda1 in response to reduced Tor1 signaling to establish a hyphal chromatin state in *Candida albicans*. *PLoS Pathog.*, 8(4), 2012.
- Y Lu, C Su, NV Solis, SG Filler, and H Liu. Synergistic regulation of hyphal elongation by hypoxia, CO₂, and nutrient conditions controls the virulence of *Candida albicans*. *Cell Host Microbe*, 14(5):499–509, 2013.

- Y Lu, C Su, S Ray, Y Yuan, and H Liu. CO₂ Signaling through the Ptc2-Ssn3 Axis Governs Sustained Hyphal Development of *Candida albicans* by Reducing Ume6 Phosphorylation and Degradation. *MBio*, 10(1):e02320–18, 2019.
- P Machanick and TL Bailey. MEME-ChIP: Motif analysis of large DNA datasets. *Bioinformatics*, 27(12):1696–1697, 2011.
- JA Maertens. History of the development of azole derivatives. *Clin. Microbiol. Infect.*, 10(Suppl. 1):1–10, 2004.
- D Mardon, E Balish, and AW Phillips. Control of dimorphism in a biochemical variant of *Candida albicans*. *J. Bacteriol.*, 100(2):701–707, 1969.
- M Martchenko, A-M Alarco, D Harcus, and M Whiteway. Superoxide Dismutases in *Candida albicans*: Transcriptional Regulation and Functional Characterization of the Hyphal-induced SOD5 Gene. *Mol. Biol. Cell*, 15:456–467, 2004.
- R Martin, GP Moran, ID Jacobsen, A Heyken, J Domey, DJ Sullivan, O Kurzai, and B Hube. The *Candida albicans*-specific gene EED1 encodes a key regulator of hyphal extension. *PLoS One*, 6(4):e18394, 2011.
- R Martin, D Albrecht-Eckardt, S Brunke, B Hube, K Hünninger, and O Kurzai. A Core Filamentation Response Network in *Candida albicans* Is Restricted to Eight Genes. *PLoS One*, 8(3):e58613, 2013.
- CJ McInerny, JF Partridge, GE Mikesell, DP Creemer, and LL Breeden. A novel Mcm1-dependent element in the SWI4, CLN3, CDC6, and CDC47 promoters activates M/G1-specific transcription. *Genes Dev.*, 11(10):1277–1288, 1997.
- CGJ McKenzie, U Koser, LE Lewis, JM Bain, HM Mora-Montes, RN Barker, NAR Gow, and LP Erwig. Contribution of *Candida albicans* cell wall components to recognition by and escape from murine macrophages. *Infect. Immun.*, 78(4):1650–1658, 2010.
- TA Mennella, LG Klinkenberg, and RS Zitomer. Recruitment of Tup1-Ssn6 by Yeast Hypoxic Genes and Chromatin-Independent Exclusion of TATA Binding Protein. *Eukaryot. Cell*, 2(6):1288–1303, 2003.
- E Meyer, C Geffers, P Gastmeier, and F Schwab. No increase in primary nosocomial candidemia in 682 German intensive care units during 2006 to 2011. *Eurosurveillance*, 18(24):1–8, 2013.
- MG Miller and AD Johnson. White-opaque switching in *Candida albicans* is controlled by mating-type locus homeodomain proteins and allows efficient mating. *Cell*, 110(3):293–302, 2002.
- M Monod, G Togni, B Hube, and D Sanglard. Multiplicity of genes encoding secreted aspartic proteinases in *Candida* species. *Mol. Microbiol.*, 13(2):357–368, 1994.
- EC Moore, AA Padiglione, J Wasiak, E Paul, and H Cleland. *Candida* in Burns: Risk Factors and Outcomes. *J. Burn Care Res.*, 31(2):257–263, 2010.

- DL Moyes, D Wilson, JP Richardson, S Mogavero, SX Tang, J Wernecke, S Höfs, RL Gratacap, J Robbins, M Runglall, C Murciano, M Blagojevic, S Thavaraj, TM Förster, B Hebecker, L Kasper, G Vizcay, SI Iancu, N Kichik, A Häder, O Kurzai, T Luo, T Krüger, O Kniemeyer, E Cota, O Bader, RT Wheeler, T Gutschmann, B Hube, and JR Naglik. Candidalysin is a fungal peptide toxin critical for mucosal infection. *Nature*, 532:64–68, 2016.
- AMA Murad, C D’Enfert, C Gaillardin, H Tournu, F Tekaia, D Talibi, D Marechal, V Marchais, J Cottin, and AJP Brown. Transcript profiling in *Candida albicans* reveals new cellular functions for the transcriptional repressors CaTup1, CaMig1 and CaNrg1. *Mol. Microbiol.*, 42(4): 981–993, 2001a.
- AMA Murad, Pi Leng, M Straffon, J Wishart, S Macaskill, DM MacCallum, N Schnell, D Talibi, D Marechal, F Tekaia, C D’Enfert, C Gaillardin, FC Odds, and AJP Brown. NRG1 represses yeast-hypha morphogenesis and hypha-specific gene expression in *Candida albicans*. *EMBO J.*, 20(17):4742–4752, 2001b.
- LC Myers and RD Kornberg. Mediator of Transcriptional Regulation. *Annu. Rev. Biochem.*, 69: 729–49, 2000.
- JR Naglik, SJ Challacombe, and B Hube. *Candida albicans* Secreted Aspartyl Proteinases in Virulence and Pathogenesis. *Microbiol. Mol. Biol. Rev.*, 67(3):400–428, 2003.
- JR Naglik, SL Gaffen, and B Hube. Candidalysin: discovery and function in *Candida albicans* infections. *Curr. Opin. Microbiol.*, 52:100–109, 2019.
- CJ Nobile and AD Johnson. *Candida albicans* Biofilms and Human Disease. *Annu. Rev. Microbiol.*, 69:71–92, 2015.
- CJ Nobile and AP Mitchell. Regulation of cell-surface genes and biofilm formation by the *C. albicans* transcription factor Bcr1p. *Curr. Biol.*, 15(12):1150–1155, 2005.
- CJ Nobile, DR Andes, JE Nett, FJ Smith, F Yue, QT Phan, JE Edwards, SG Filler, and AP Mitchell. Critical role of Bcr1-dependent adhesins in *C. albicans* biofilm formation in vitro and in vivo. *PLoS Pathog.*, 2(7):0636–0649, 2006.
- CJ Nobile, EP Fox, JE Nett, TR Sorrells, QM Mitrovich, AD Hernday, BB Tuch, DR Andes, and AD Johnson. A recently evolved transcriptional network controls biofilm development in *Candida albicans*. *Cell*, 148(1-2):126–138, 2012.
- SM Noble, S French, LA Kohn, V Chen, and AD Johnson. Systematic screens of a *Candida albicans* homozygous deletion library decouple morphogenetic switching and pathogenicity. *Nat. Genet.*, 42(7):590–8, 2010.
- CS Nødvig, JB Nielsen, ME Kogle, and UH Mortensen. A CRISPR-Cas9 system for genetic engineering of filamentous fungi. *PLoS One*, 10(7):1–18, 2015.
- FC Odds. Morphogenesis in *Candida*, with special reference to *C. albicans*. In *Candida Candidosis. A Rev. Bibliogr.*, pages 42–59. 1988.

- SH Oh, G Cheng, JA Nuessen, R Jajko, KM Yeater, X Zhao, C Pujol, DR Soll, and LL Hoyer. Functional specificity of *Candida albicans* Als3p proteins and clade specificity of ALS3 alleles discriminated by the number of copies of the tandem repeat sequence in the central domain. *Microbiology*, 151(3):673–681, 2005.
- M Papamichos-Chronakis, T Petrakis, E Ktistaki, I Topalidou, and D Tzamarias. Cti6, a PHD domain protein, bridges the Cyc8-Tup1 corepressor and the SAGA coactivator to overcome repression at GAL1. *Mol. Cell*, 9:1297–1305, 2002.
- J Perleth, B Choi, and B Spellberg. Nosocomial fungal infections: epidemiology, diagnosis, and treatment. *Med. Mycol.*, 45(4):321–346, 2007.
- MW Pfaffl. A new mathematical model for relative quantification in real-time RT-PCR. *Nucleic Acids Res.*, 29(9), 2001.
- MA Pfaller and DJ Diekema. Epidemiology of invasive candidiasis: A persistent public health problem. *Clin. Microbiol. Rev.*, 20(1):133–163, 2007.
- MA Pfaller and DJ Diekema. *Epidemiology of invasive mycoses in North America*, volume 36. 2010.
- QT Phan, CL Myers, Y Fu, DC Sheppard, MR Yeaman, WH Welch, AS Ibrahim, JE Edwards, and SG Filler. Als3 is a *Candida albicans* invasin that binds to cadherins and induces endocytosis by host cells. *PLoS Biol.*, 5(3):0543–0557, 2007.
- EG Playford, GR Nimmo, M Tilse, and TC Sorrell. Increasing incidence of candidaemia: Long-term epidemiological trends, Queensland, Australia, 1999-2008. *J. Hosp. Infect.*, 76(1):46–51, 2010.
- S Pohlers, R Martin, D Hellwig, O Knienmeyer, HP Saluz, P van Dijck, JF Ernst, A Brakhage, and O Kurzai. Lipid Signaling via Pkh1/2 Regulates Fungal CO₂ Sensing through the Kinase Sch9. *MBio*, 8(1):e02211–16, 2017.
- M Polke, B Hube, and ID Jacobsen. *Candida Survival Strategies*, volume 91. 2015.
- MR Rafiee, C Girardot, G Sigismondo, and J Krijgsveld. Expanding the Circuitry of Pluripotency by Selective Isolation of Chromatin-Associated Proteins. *Mol. Cell*, 64(3):624–635, 2016.
- J Rhodes and MC Fisher. Global epidemiology of emerging *Candida auris*. *Curr. Opin. Microbiol.*, 52:84–89, 2019.
- JP Richardson, S Mogavero, DL Moyes, M Blagojevic, T Krüger, AH Verma, BM Coleman, J De La Cruz Diaz, D Schulz, NO Ponde, G Carrano, O Knienmeyer, D Wilson, O Bader, SI Enoiu, J Ho, N Kichik, SL Gaffen, B Hube, and JR Naglik. Processing of *Candida albicans* Ece1p Is Critical for Candidalysin Maturation and Fungal Virulence. *MBio*, 9(1):1–16, 2018a.
- JP Richardson, HME Willems, DL Moyes, S Shoaie, KS Barker, SL Tan, GE Palmer, B Hube, JR Naglik, and BM Peters. Candidalysin Drives Epithelial Signaling, Neutrophil Recruitment, and Immunopathology at the Vaginal Mucosa. *Infect. Immun.*, 86(2):1–15, 2018b.

- JP Richardson, R Brown, A Turkova, I Kabelka, G Carrano, N Kichik, S Tang, D Moyes, D Wilson, B Hube, R Vacha, and JR Naglik. The candidalysins are a family of cytolytic fungal toxins. *Poster HFP La Colle-sur-Loupe*, 2019.
- CR Rocha, K Schröppel, D Harcus, A Marcil, D Dignard, BN Taylor, DY Thomas, M Whiteway, and E Leberer. Signaling through adenylyl cyclase is essential for hyphal growth and virulence in the pathogenic fungus *Candida albicans*. *Mol. Biol. Cell*, 12(11):3631–3643, 2001.
- NC Rockwell and JW Thorner. The kindest cuts of all: Crystal structures of Kex2 and furin reveal secrets of precursor processing. *Trends Biochem. Sci.*, 29(2):80–87, 2004.
- M Rottmann, S Dieter, H Brunner, and S Rupp. A screen in *Saccharomyces cerevisiae* identified CaMCM1, an essential gene in *Candida albicans* crucial for morphogenesis. *Mol. Microbiol.*, 47(4):943–959, 2003.
- M Ruhnke, AH Groll, P Mayser, AJ Ullmann, W Mendling, H Hof, and DW Denning. Estimated burden of fungal infections in Germany. *Mycoses*, 58:22–28, 2015.
- C Salerno, M Pascale, M Contaldo, V Esposito, M Busciolano, L Milillo, A Guida, M Petruzzi, and R Serpico. *Candida*-associated denture stomatitis. *Med Oral Patol Oral Cir Bucal*, 16(2):e139–43, 2011.
- D Sanglard, B Hube, M Monod, FC Odds, and NAR Gow. A triple deletion of the secreted aspartyl proteinase genes SAP4, SAP5, and SAP6 of *Candida albicans* causes attenuated virulence. *Infect. Immun.*, 65(9):3539–3546, 1997.
- C Sasse, R Schillig, F Dierolf, M Weyler, S Schneider, S Mogavero, PD Rogers, and J Morschhäuser. The transcription factor Ndt80 does not contribute to Mrr1-, Tac1-, and Upc2-mediated fluconazole resistance in *Candida albicans*. *PLoS One*, 6(9):e25623, 2011.
- K Satoh, K Makimura, Y Hasumi, Y Nishiyama, K Uchida, and H Yamaguchi. *Candida auris* sp. nov., a novel ascomycetous yeast isolated from the external ear canal of an inpatient in a Japanese hospital. *Microbiol. Immunol.*, 53(1):41–44, 2009.
- SP Saville, AL Lazzell, C Monteagudo, and JL Lopez-Ribot. Engineered Control of Cell Morphology In Vivo Reveals Distinct Roles for Yeast and Filamentous Forms of. *Society*, 2(5):1053–1060, 2003.
- SP Saville, AL Lazzell, AP Bryant, A Fretzen, A Monreal, EO Solberg, C Monteagudo, JL Lopez-Ribot, and G. T Milne. Inhibition of filamentation can be used to treat disseminated candidiasis. *Antimicrob. Agents Chemother.*, 50(10):3312–3316, 2006.
- R Schillig and J Morschhäuser. Analysis of a fungus-specific transcription factor family, the *Candida albicans* zinc cluster proteins, by artificial activation. *Mol. Microbiol.*, 89(5):1003–1017, 2013.
- A Schweizer, S Rupp, BN Taylor, M Röllinghoff, and K Schröppel. The TEA/ATTS transcription factor CaTec1p regulates hyphal development and virulence in *Candida albicans*. *Mol. Microbiol.*, 38(3):435–445, 2003.

- A Sellam, F Tebbji, and A Nantel. Role of Ndt80p in sterol metabolism regulation and azole resistance in *Candida albicans*. *Eukaryot. Cell*, 8(8):1174–1183, 2009.
- A Sellam, C Askew, E Epp, F Tebbji, A Mullick, M Whiteway, and A Nantel. Role of transcription factor CaNdt80p in cell separation, hyphal growth, and virulence in *Candida albicans*. *Eukaryot. Cell*, 9(4):634–644, 2010.
- RS Shapiro, P Uppuluri, AK Zaas, C Collins, H Senn, JR Perfect, J Heitman, and LE Cowen. Hsp90 Orchestrates Temperature-Dependent *Candida albicans* Morphogenesis via Ras1-PKA Signaling. *Curr. Biol.*, 19(8):621–629, 2009.
- RS Shapiro, N Robbins, and LE Cowen. Regulatory circuitry governing fungal development, drug resistance, and disease. *Microbiol. Mol. Biol. Rev.*, 75(2):213–267, 2011.
- N Simonetti, V Strippoli, and A Cassone. Yeast-mycelial conversion induced by N-acetyl-D-glucosamine in *Candida albicans*. *Nature*, 250(464):344–346, 1974.
- B Slutsky, M Staebell, J Anderson, L Risen, M Pfaller, and DR Soll. ‘White-opaque transition’: A second high-frequency switching system in *Candida albicans*. *J. Bacteriol.*, 169(1):189–197, 1987.
- RL Smith and AD Johnson. Turning genes off by Ssn6–Tup1: a conserved system of transcriptional repression in eukaryotes. *TIBS*, 25, 2000.
- JD Sobel. Vaginitis. *N. Engl. J. Med.*, 337:1896–1903, 1997.
- ER Spargue, MJ Redd, AD Johnson, and C Wolberger. Structure of the C-terminal domain of Tup1, a corepressor of transcription in yeast. *EMBO J.*, 19(12):3016–3027, 2000.
- VR Stoldt, A Sonneborn, CE Leuker, and JF Ernst. Efg1p, an essential regulator of morphogenesis of the human pathogen *Candida albicans*, is a member of a conserved class of bHLH proteins regulating morphogenetic processes in fungi. *EMBO J.*, 16(8):1982–1991, 1997.
- M Straffon, J Wishart, S Macaskill, D Maccallum, FC Odds, and AJP Brown. NRG1 represses yeast-hypha morphogenesis and hypha-specific gene expression in *Candida albicans*. *EMBO J.*, 20(17):4742–4751, 2001.
- PE Sudbery. Growth of *Candida albicans* hyphae. *Nat. Rev. Microbiol.*, 9:737–748, 2011.
- M Swidergall, M Khalaji, NV Solis, DL Moyes, RA Drummond, B Hube, MS Lionakis, C Murdoch, SG Filler, and JR Naglik. Candidalysin Is Required for Neutrophil Recruitment and Virulence During Systemic *Candida albicans* Infection. *J. Infect. Dis.*, 220(9):1477–1488, 2019.
- CL Taschdjian, JJ Burchall, and PJ Kozinn. Rapid Identification of *Candida Albicans* by Filamentation on Serum and Serum Substitutes. *AMA Am J Dis Child*, 99(2):212–215, 1960.
- BB Tuch, DJ Galgoczy, AD Hernday, H Li, and AD Johnson. The evolution of combinatorial gene regulation in fungi. *PLoS Biol.*, 6(2):0352–0364, 2008.

- SC Ushinsky, D Harcus, J Ash, D Dignard, A Marcil, J Morchhauser, DY Thomas, M Whiteway, and E Leberer. CDC42 is required for polarized growth in human pathogen *Candida albicans*. *Eukaryot. Cell*, 1(1):95–104, 2002.
- N Uwamahoro, J Verma-Gaur, HH Shen, Y Qu, R Lewis, J Lu, K Bambery, SL Masters, JE Vince, T Naderer, and A Traven. The pathogen *Candida albicans* hijacks pyroptosis for escape from macrophages. *MBio*, 5(2):1–11, 2014.
- L van Wijlick, S Znaidi, S Bachellier-Bassi, and C D’Enfert. Regulatory networks controlling pathogenesis in the fungal pathogen *Candida albicans*. *Poster HFP Adv. Lect. Course, La Colle sur Loup*, 2019.
- US Varanasi, M Klis, PB Mikesell, and RJ Trumbly. The Cyc8 (Ssn6)-Tup1 corepressor complex is composed of one Cyc8 and four Tup1 subunits. *Mol. Cell. Biol.*, 16(12):6707–6714, 1996.
- AH Verma, JP Richardson, C Zhou, BM Coleman, DL Moyes, J Ho, AR Huppler, K Ramani, MJ McGeachy, IA Mufazalov, A Waisman, LP Kane, PS Biswas, B Hube, JR Naglik, and SL Gaffen. Oral epithelial cells orchestrate innate type 17 responses to *Candida albicans* through the virulence factor candidalysin. *Sci. Immunol.*, 2(17):eaam8834, 2017.
- J-L Vincent, J Rello, J Marshall, E Silva, A Anzueto, CD Martin, Rui Moreno, J Lipman, C Gomersall, Y Sakr, and K Reinhart. International Study of the Prevalence and Outcomes of Infection in Intensive Care Units. *JAMA*, 302(21):2323–2329, 2009.
- C Viscoli, C Girmenia, A Marinus, L Collette, P Martino, B Vandercam, C Doyen, B Lebeau, D Spence, V Krcmery, B De Pauw, and F Meunier. Candidemia in Cancer Patients: A Prospective, Multicenter Surveillance Study by the Invasive Fungal Infection Group (IFIG) of the European Organization for Research and Treatment of Cancer (EORTC). *Clin. Infect. Dis.*, 28(5):1071–1079, 1999.
- S Vylkova and MC Lorenz. Modulation of Phagosomal pH by *Candida albicans* Promotes Hyphal Morphogenesis and Requires Stp2p, a Regulator of Amino Acid Transport. *PLoS Pathog.*, 10(3), 2014.
- S Vylkova and MC Lorenz. Phagosomal Neutralization by the Fungal Pathogen *Candida albicans* Induces Macrophage Pyroptosis. *Infect. Immun.*, 85(2):e00832–16, 2017.
- S Vylkova, AJ Carman, HA Danhof, JR Collette, H Zhou, and MC Lorenz. The fungal pathogen *Candida albicans* autoinduces hyphal morphogenesis by raising extracellular pH. *MBio*, 2(3), 2011.
- A Walther and J Wendland. An improved transformation protocol for the human fungal pathogen *Candida albicans*. *Curr. Genet.*, 42:339–343, 2003.
- H Wang, W Song, G Huang, Z Zhou, Y Ding, and J Chen. *Candida albicans* Zcf37, a zinc finger protein, is required for stabilization of the white state. *FEBS Lett.*, 585:797–802, 2011.
- Y Wang, H Zou, HM Fang, and Y Zhu. Linking cellular actin status with cAMP signaling in *Candida albicans*. *Virulence*, 1(3):202–205, 2010.

- A Wartenberg, J Linde, R Martin, M Schreiner, F Horn, ID Jacobsen, S Jenull, T Wolf, K Kuchler, R Guthke, O Kurzai, A Forche, C D'Enfert, S Brunke, and B Hube. Microevolution of *Candida albicans* in Macrophages Restores Filamentation in a Nonfilamentous Mutant. *PLoS Genet*, 10(12):e1004824, 2014.
- M Wellington, K Koselny, and DJ Krysan. *Candida albicans* morphogenesis is not required for macrophage interleukin 1beta production. *MBio*, 4(1), 2012.
- M Wellington, K Koselny, FS Sutterwala, and DJ Krysan. *Candida albicans* triggers NLRP3-mediated pyroptosis in macrophages. *Eukaryot. Cell*, 13(2):329–340, 2014.
- H Wisplinghoff, SM Tallent, H Seifert, T Bischoff, RP Wenzel, and MB Edmond. Nosocomial Bloodstream Infections in US Hospitals: Analysis of 24,179 Cases from a Prospective Nationwide Surveillance Study. *Clin. Infect. Dis.*, 39(3):309–317, 2004.
- W Xu and AP Mitchell. Yeast PalA / AIP1 / Alix Homolog Rim20p Associates with a PEST-Like Region and Is Required for Its Proteolytic Cleavage. *J. Bacteriol.*, 183(23):6917–6923, 2001.
- YL Yang, CW Wang, SN Leaw, TP Chang, IC Wang, CG Chen, JC Fan, KY Tseng, SH Huang, CY Chen, TY Hsiao, CA Hsiung, CT Chen, CD Hsiao, and HJ Lo. R432 is a key residue for the multiple functions of Ndt80p in *Candida albicans*. *Cell. Mol. Life Sci.*, 69(6):1011–1023, 2012.
- N Yapar. Epidemiology and risk factors for invasive candidiasis. *Ther. Clin. Risk Manag.*, 10(1):95–105, 2014.
- K Zakikhany, JR Naglik, A Schmidt-Westhausen, G Holland, M Schaller, and B Hube. In vivo transcript profiling of *Candida albicans* identifies a gene essential for interepithelial dissemination. *Cell. Microbiol.*, 9(12):2938–2954, 2007.
- C Zaugg, M Borg-Von Zepelin, U Reichard, D Sanglard, and M Monod. Secreted aspartic proteinase family of *Candida tropicalis*. *Infect. Immun.*, 69(1):405–412, 2001.
- U Zeidler, T Lettner, C Lassnig, M Müller, R Lajko, H Hintner, M Breitenbach, and A Bitto. UME6 is a crucial downstream target of other transcriptional regulators of true hyphal development in *Candida albicans*. *FEMS Yeast Res.*, 9:126–142, 2008.
- X Zhao, SH Oh, G Cheng, CB Green, JA Nuessen, K Yeater, RP Leng, AJP Brown, and LL Hoyer. ALS3 and ALS8 represent a single locus that encodes a *Candida albicans* adhesin; functional comparisons between Als3p and Als1p. *Microbiology*, 150(7):2415–2428, 2004.
- X Zheng, Y Wang, and Y Wang. Hgc1, a novel hypha-specific G1 cyclin-related protein regulates *Candida albicans* hyphal morphogenesis. *Embo J*, 23(8):1845–1856, 2004.
- C Zhu, KJRP Byers, R Patton McCord, Z Shi, MF Berger, DE Newburger, K Saulrieta, Z Smith, MV Shah, M Radhakrishnan, AA Philippakis, Y Hu, F De Masi, M Pacek, A Rolfs, T Murthy, J Labaer, and ML Bulyk. High-resolution DNA-binding specificity analysis of yeast transcription factors. *Genome Res.*, 19(4):556–566, 2009.

VII. Appendix

Tab. 6: **Possible transcription factor binding sites upstream of the *ECE1* ORF.**

Transcription factor binding motifs from the literature were identified in the *ECE1* 5' intergenic region. The exact sequences and positions upstream the start codon are displayed.

Transcription Factor Binding Motif	Motif	Start Position (bp upstream start codon)	Sequence	Notes
Ahr1_1	HGBBWAWVHTDHH	-2748	AGTTTATTCTTATC	The perfect site would be TCGNYWAWWSTTGCC Hernday <i>et al.</i> (2013)
Ahr1_2	HGBBWAWVHTDHH	-2094	AGGCTAAAAATGCT	
Ahr1_3	HGBBWAWVHTDHH	-352	CGCCTAAACTTGTA	
Bcr1	TAMATRCAY	-107	TAAATACAT	Perfect site: TACATRCAYRWM Nobile <i>et al.</i> (2012)
Brg1_1	MGGTAM	-2735	CGGTAA	Nobile <i>et al.</i> (2012)
Brg1_2	MGGTAM	-1252	AGGTAC	
Brg1_3	MGGTAM	-810	AGGTAA	
Cph1	TGAAACA	-1521	TGAAACA	According to <i>S. cerevisiae</i> Ste12 Harbison <i>et al.</i> (2004)
Efg1_1	RYGCATRD	-1631	ATGCATG	Nobile <i>et al.</i> (2012)
Efg1_2	CANNTG	-2559	CATCTG	Argimón <i>et al.</i> (2007)
Efg1_3	CANNTG	-2143	CAACTG	
Efg1_4	CANNTG	-1609	CAATTG	
Efg1_5	CANNTG	-1591	CAAGTG	
Efg1_6	CANNTG	-1103	CAAATG	
Efg1_7	CANNTG	-1053	CAAATG	
Efg1_8	CANNTG	-764	CAATTG	
Efg1_9	CANNTG	-498	CATTTG	
Efg1_10	CANNTG	-314	CAGGTG	
Efg1_11	CANNTG	-204	CAATTG	
Efg1_12	TGCAT	-2976	TGCAT	
Efg1_13	TGCAT	-2830	TGCAT	
Efg1_14	TGCAT	-2116	TGCAT	
Efg1_15	TGCAT	-1630	TGCAT	
Fkh2_1	KTAAAYAAA	-1243	TAAACAAA	According to <i>S. cerevisiae</i> Fkh2 Zhu <i>et al.</i> (2009)
Fkh2_2	KTAAAYAAA	-1080	GTAACAAA	
Mcm1_1	WCGNNWAWVVTNCY	-2736	TCGGTAATTCTTCCC	Tuch <i>et al.</i> (2008)
Mcm1_2	CCNNNNNNGG	-1139	CCTAACTCGG	According to <i>S. cerevisiae</i> Mcm1 McInerney <i>et al.</i> (1997)
Mcm1_3	CCNNNNNNGG	-2480	CCATAGTTGG	

VII. Appendix

Transcription Factor Binding Motif	Motif	Start Position (bp up- stream start codon)	Sequence	Notes
Ndt80_1	CRCAA	-2704	CACAAA	Chen <i>et al.</i> (2004); Yang <i>et al.</i> (2012)
Ndt80_2	CRCAA	-1989	CGCAA	
Ndt80_3	CRCAA	-1810	CACAAA	
Ndt80_4	CRCAA	-404	CACAAA	
Ndt80_5	CRCAA	-379	CGCAA	
Ndt80_6	CRCAA	-329	CACAAA	
Tec1	WRCATTCYH	-2872	TACATTCTT	Nobile <i>et al.</i> (2012)
Ume6_1	GCGG	-2430	GCGG	Lu <i>et al.</i> (2013)
Ume6_2	GCGG	-2020	GCGG	
Ume6_3	GCGG	-971	GCGG	

Tab. 7: Secretion of Candidalysin of the wild type (SC514) and the *cph1Δ/efg1Δ* and the *ahr1Δ* mutants.

Strains were incubated for 18 h under yeast growth conditions (YNBS pH 4, 37°C) and/or hyphal growth conditions (YNBS pH 7.2, 37°C). Candidalysin was extracted from supernatant and measured by LC/MS-MS. Red font indicates the Ece1-III peptide. PSM= peptide spectrum matches.

	Yeast-inducing conditions	PSM	Hyphae-inducing conditions	PSM
SC5314	SIIGIIMGILGNIPQVIQIIMSIVKAFKGNKR	0	SIIGIIMGILGNIPQVIQIIMSIVKAFKGNKR	345
			SIIGIIMGILGNIPQVIQIIMSIVKAFKGNK	291
			SIIGIIMGILGNIPQVIQIIMSIVKAFKGN	25
			SIIGIIMGILGNIPQVIQIIM	11
			SIIGIIMGILGNIPQVIQII	5
			EFNTAITKRSIIGIIMGILGNIPQVIQIIMSIVKAFKGNK	4
			ITKRSIIGIIMGILGNIPQVIQIIMSIVKAFKGNK	1
			GILGNIPQVIQIIMSIVKAFKGNK	1
SC5314 + hyperactive Ahr1	SIIGIIMGILGNIPQVIQIIMSIVKAFKGNKR	0	SIIGIIMGILGNIPQVIQIIMSIVKAFKGNKR	612
			SIIGIIMGILGNIPQVIQIIMSIVKAFKGNK	480
			SIIGIIMGILGNIPQVIQIIMSIVKAFKGN	53
			SIIGIIMGILGNIPQVIQIIMSIVKA	22
			SIIGIIMGILGNIPQVIQIIMSIVKAFKG	16
			SIIGIIMGILGNIPQVIQIIMSIVKAFK	14
			SIIGIIMGILGNIPQVIQIIMSIVK	14
			SIIGIIMGILGNIPQVIQIIM	6
			SIIGIIMGILGNIPQVIQIIMSIVKAF	2
			SIIGIIMGILGNIPQVIQII	2
			SIIGIIMGILGNIPQVIQI	1
			SIIGIIMGILGNIPQVIQ	1
			ITKRSIIGIIMGILGNIPQVIQIIMSIVKAFKGNK	1
<i>cph1Δ/efg1Δ</i>	SIIGIIMGILGNIPQVIQIIMSIVKAFKGNKR	37	SIIGIIMGILGNIPQVIQIIMSIVKAFKGNKR	0
	SIIGIIMGILGNIPQVIQIIMSIVKAFKGNK	36		
	SIIGIIMGILGNIPQVIQIIMSIVKAFKGN	1		
<i>cph1Δ/efg1Δ</i> + hyperactive Ahr1	SIIGIIMGILGNIPQVIQIIMSIVKAFKGNKR	52	SIIGIIMGILGNIPQVIQIIMSIVKAFKGNKR	352
	SIIGIIMGILGNIPQVIQIIMSIVKAFKGNK	40	SIIGIIMGILGNIPQVIQIIMSIVKAFKGNK	286
	SIIGIIMGILGNIPQVIQIIMSIVKAFKGN	9	SIIGIIMGILGNIPQVIQIIMSIVKA	26
	SIIGIIMGILGNIPQVIQIIM	3	SIIGIIMGILGNIPQVIQIIMSIVKAFKGN	23
			SIIGIIMGILGNIPQVIQIIMSIVK	8
			SIIGIIMGILGNIPQVIQIIM	4
			SIIGIIMGILGNIPQVIQIIMSIVKAFKG	2
			SIIGIIMGILGNIPQVIQIIMSIVKAFK	2
		SIIGIIMGILGNIPQVIQ	1	
<i>ahr1Δ</i>			SIIGIIMGILGNIPQVIQIIMSIVKAFKGNKR	68
			SIIGIIMGILGNIPQVIQIIMSIVKAFKGNK	68

Tab. 8: **Identified binding motifs of hyperactive Ahr1 on intergenic regions of sought out genes.**

Sought out genes are displayed with their position in the *C. albicans* genome, the height of the peak identified (the more reads were mapped to this region, the higher the corresponding peak) and the position of the motif identified including the motif score. The higher the motif score the more the sequence concurs to the identified binding motif (lowest score is 0, highest score is 6.58, cf. Fig. 20). Asterisks mark identified motifs that correspond to local peak summits and thus probably represent a true binding site.

Gene Name	orf19 Name	Gene Str.	Chr.	Peak Height	Distance between Motif and Gene (bp)	Motif Str.	Motif Score	Motif Sequence
AHR1	orf19.7381	+	chr3	791	6258	-	2,1	CACAAC TAATAACGA
AHR1	orf19.7381	+	chr3	791	6218	-	2,8	TGATATTTTAAGCGA
AHR1*	orf19.7381	+	chr3	791	5929	+	5,0	TGCAAGTATAACCGG
AHR1*	orf19.7381	+	chr3	791	5586	-	5,4	GGCAACAATTACCGG
AHR1	orf19.7381	+	chr3	791	5584	+	3,9	GGTAATTGTTGCCGG
AHR1	orf19.7381	+	chr3	791	4903	+	3,3	AGAAATAACACCCGA
AHR1	orf19.7381	+	chr3	1050	2905	-	3,6	GTCAACTCAAACCGA
AHR1	orf19.7381	+	chr3	1050	2453	-	2,6	GGAAATAATGAACGA
AHR1*	orf19.7381	+	chr3	1050	2397	+	3,5	AGCAACTATAACCTT
AHR1	orf19.7381	+	chr3	1050	2177	-	2,6	TTAATCAATAACCGA
AHR1*	orf19.7381	+	chr3	1050	1669	-	4,9	AGCAAGTTTAACCGT
ALS1*	orf19.5741	+	chr6	2089	2570	+	2,3	GGTAAGATAATGCGA
ALS1	orf19.5741	+	chr6	2089	1548	-	2,3	TTCAAGTAGAACAGA
ALS1*	orf19.5741	+	chr6	2089	1390	-	4,6	GGAAACTTCAAACGA
ALS1	orf19.5741	+	chr6	2089	1293	-	3,8	AACAAGTTCTAGCGA
ALS1*	orf19.5741	+	chr6	2089	336	-	3,9	TGCAAGTTAAAACGA
ALS3*	orf19.1816	-	chrR	1478	340	+	4,5	TGCAAGTTAAACCGA
ALS3	orf19.1816	-	chrR	1478	1118	+	3,4	AACAAGTGCTAGCGA
ALS3*	orf19.1816	-	chrR	1478	1209	+	3,5	GGAAACTTTGAACGA
ALS3*	orf19.1816	-	chrR	1478	1921	-	2,6	GGTTTTTTTAACCGA
ALS4	orf19.4555	-	chr6	1140	1128	+	4,1	GGCAAGTTCTAACGT
ALS4*	orf19.4555	-	chr6	1140	1649	-	3,4	CACAAGTGTAAGCGA
BCR1*	orf19.723	-	chrR	676	2178	-	2,8	AGAAAGGAAAAGCGA
BCR1	orf19.723	-	chrR	676	2232	+	2,1	GGAAACAATGGGAGA
BCR1	orf19.723	-	chrR	676	2517	+	3,7	AGAAAGAAAAGCGA
BRG1	orf19.4056	+	chr1	544	5837	-	3,7	TGCAATTATAACAGA
BRG1*	orf19.4056	+	chr1	544	5765	+	5,1	TGCAAGAATTACCGA
BRG1	orf19.4056	+	chr1	683	2470	-	2,3	CAAAAGATTAAACGA
BRG1	orf19.4056	+	chr1	683	2161	-	3,3	AACAAGAAAAGCCGA
BRG1*	orf19.4056	+	chr1	683	2129	-	4,5	GGAATGAATAGCCGA
CDR1	orf19.6000	+	chr3	696	1419	+	3,0	GGTGTGTTTAACCGA
CDR1*	orf19.6000	+	chr3	696	1337	+	4,7	ATCAACTATTGCCGA
CDR1	orf19.6000	+	chr3	696	1282	-	2,5	AAGAAGTTGAGGCGA
CDR1*	orf19.6000	+	chr3	696	569	-	2,8	TTCAGTTTTAAGCGA
CZF1*	orf19.3127	-	chr4	681	4304	-	2,4	TGCAGTGTAACCGA
DCK1	orf19.815	-	chr2	327	124	-	2,3	GGAAATAAAAAGAGA
DCK1*	orf19.815	-	chr2	327	506	+	4,5	GGAAAGTATAGTCGA
EAP1	orf19.1401	+	chr2	551	5622	+	2,3	TGAAATTTTAAACTA
EAP1	orf19.1401	+	chr2	551	5225	+	3,4	GGTAAATACAAGCGA
EAP1	orf19.1401	+	chr2	551	4773	-	2,7	AACTATTTTAGCCGA
EAP1	orf19.1401	+	chr2	551	4701	-	3,2	AGCAGCTGCAAACGA
EAP1	orf19.1401	+	chr2	1093	1843	+	3,1	AACAACAACAACCGG

Gene Name	orf19 Name	Gene Str.	Chr.	Peak Height	Distance between Motif and Gene (bp)	Motif Str.	Motif Score	Motif Sequence
EAP1	orf19.1401	+	chr2	1093	1326	-	4,5	TGCAACATTTTCGCGA
EAP1*	orf19.1401	+	chr2	1093	1204	+	4,5	GGGAAGTTCAAGCGA
EAP1	orf19.1401	+	chr2	1093	1008	+	4,1	TACAACATTTTGGCGA
ECE1*	orf19.3374	-	chr4	1676	996	-	4,2	TTCAAGTATTAGCGA
ECE1	orf19.3374	-	chr4	1676	1103	+	2,8	GCCAACAACAGGCGT
ECE1	orf19.3374	-	chr4	1676	1670	-	2,4	TTTATGTATTAGCGA
ECE1*	orf19.3374	-	chr4	1676	2015	-	2,9	CACAACATTTTAGCGG
ECE1	orf19.3374	-	chr4	1676	2079	+	2,8	AGCATTTTTTAGCCTA
ECE1*	orf19.3374	-	chr4	1676	2721	+	4,8	GGGAAGAATTACCGA
ECE1	orf19.3374	-	chr4	1676	2773	+	2,3	GACAATTCTTGAGAGA
EED1	orf19.7561	+	chrR	673	2196	+	2,3	AAGAAGATTTGCCGG
EED1	orf19.7561	+	chrR	673	2129	+	3,1	AGTAAGAATAAGAGA
EED1*	orf19.7561	+	chrR	673	1719	-	4,0	GTCAACTTCTGACGA
EED1	orf19.7561	+	chrR	673	1674	+	2,7	GGCATCTTTACCCTC
EED1	orf19.7561	+	chrR	673	1349	+	2,5	TGTATTTTTTAACGA
EED1	orf19.7561	+	chrR	673	1243	-	3,5	GCCATTTTTTAGCCGA
EED1	orf19.7561	+	chrR	673	1078	-	3,3	TACAACATAATACCGA
EED1	orf19.7561	+	chrR	673	495	-	4,0	GGAAATTAGAAACGA
EED1	orf19.7561	+	chrR	673	110	-	2,2	TGAAAGTTAAAGCTA
EFG1	orf19.610	+	chrR	648	7506	+	2,6	GGAAATATGAGCAGA
EFG1	orf19.610	+	chrR	648	7227	-	3,7	GTCAATAATTGCCGG
EFG1*	orf19.610	+	chrR	648	7225	+	4,3	GGCAATTATTGACGT
EFG1	orf19.610	+	chrR	648	6589	+	2,0	AGTAGTTTTTAGCAGA
EFG1	orf19.610	+	chrR	648	6501	-	2,6	AGCATGTAGAACCTA
EFG1	orf19.610	+	chrR	2583	5867	+	2,2	GGCAAGTTAAAGATA
EFG1	orf19.610	+	chrR	2583	4362	+	2,5	TACAACAACAACCGT
EFG1	orf19.610	+	chrR	2583	3403	-	3,4	AGCAACTTTACTCGG
EFG1*	orf19.610	+	chrR	2583	3301	-	3,8	GTCAACTTTAAGAGA
EFG1	orf19.610	+	chrR	2583	3199	+	2,8	GGAAAGTGAAAGAGA
EFG1	orf19.610	+	chrR	2583	2946	-	2,8	AACAACAATAGGAGA
EFG1	orf19.610	+	chrR	2583	2498	-	2,8	GGAATGAATTAGAGA
EFG1*	orf19.610	+	chrR	2583	2311	+	5,0	TGCAACTACAACCGA
FLO8*	orf19.1093	-	chr6	1435	2066	-	3,5	GGCAAGAAGTAGAGA
HGC1	orf19.6028	-	chr1	886	10767	-	2,7	AACAATTAGTACCGG
HGC1*	orf19.6028	-	chr1	886	11187	-	3,3	GTAAACTATAGCCTA
HGC1	orf19.6028	-	chr1	886	11590	-	2,3	AGTAATTCTAGCCTA
HGC1*	orf19.6028	-	chr1	886	11647	-	4,3	GGAAAGTGGTAGCGA
HGC1	orf19.6028	-	chr1	886	11678	+	2,3	ATCAATTATTTGCGA
HGT2	orf19.3668	-	chr1	1632	2254	-	2,9	GGGAACAATACACGT
HGT2	orf19.3668	-	chr1	1632	2500	-	2,7	AAAAACTTTAATCGA
HGT2*	orf19.3668	-	chr1	1632	2952	+	3,5	AGCAACTTCTAGAGA
HGT2*	orf19.3668	-	chr1	1632	3442	+	4,9	TGCAACTATTCGCGA
HGT2	orf19.3668	-	chr1	1632	3495	+	3,9	AGCAACAATACACGG
HGT2	orf19.3668	-	chr1	1632	4076	+	2,3	AACAACATCAAACGC
HGT2	orf19.3668	-	chr1	1632	4087	-	2,6	AGAAATAACAGGCGT
HGT2*	orf19.3668	-	chr1	701	5644	-	2,2	AGCATTTTTTTGAAGA
HWP1	orf19.1321	+	chr4	790	1875	-	2,1	ATAAACAATTACCTA
HWP1	orf19.1321	+	chr4	790	1619	-	2,1	GGATTTTTTTTGACGA
HWP1*	orf19.1321	+	chr4	790	1225	-	3,9	GGCAAGTTTATCCGC
HWP1	orf19.1321	+	chr4	790	1106	-	3,2	GGCAACTCTTACCTT
HWP1	orf19.1321	+	chr4	790	1104	+	3,2	GGTAAGAGTTGCCTA
HWP1	orf19.1321	+	chr4	790	1083	+	2,1	GAAAATAATAGGCTA

VII. Appendix

Gene Name	orf19 Name	Gene Str.	Chr.	Peak Height	Distance between Motif and Gene (bp)	Motif Str.	Motif Score	Motif Sequence
HWP1	orf19.1321	+	chr4	790	1030	+	2,3	AAAAGTTATTAGCGA
HWP1	orf19.1321	+	chr4	790	6	-	3,2	CGAAACTAAAAGCGA
HYR1*	orf19.4975	+	chr1	538	6303	-	4,7	AGCAACAAGAACCGA
HYR1*	orf19.4975	+	chr1	1787	1938	+	4,8	AGCAATATTAGGCGA
HYR1	orf19.4975	+	chr1	1787	1346	-	2,9	AGAAACAAAAACCGT
HYR1	orf19.4975	+	chr1	1787	928	-	2,2	AGTAAGAATTGGCTG
HYR1	orf19.4975	+	chr1	1787	792	+	3,0	TGAAATCCCAAGCGA
HYR1*	orf19.4975	+	chr1	1787	536	-	4,2	AACAATTTTAACCGA
HYR1*	orf19.4975	+	chr1	1787	186	-	4,7	GGAAAGTATTCACGA
IHD1*	orf19.5760	-	chr6	2931	-1534	+	4,1	GGAAAGTTGAACCGT
IHD1	orf19.5760	-	chr6	2931	-1237	+	2,7	AGAATTTAAAACCGA
IHD1	orf19.5760	-	chr6	2931	764	+	2,8	TACATTTTTTGCCGA
IHD1*	orf19.5760	-	chr6	2931	861	+	5,1	TGCAACAATTACCGA
IHD1	orf19.5760	-	chr6	2931	979	-	3,7	AGAAAGAAAAAGCGA
IHD1	orf19.5760	-	chr6	2931	1649	+	2,4	TGTAAGTAGAAACGT
LMO1	orf19.5147	+	chr7	466	457	-	2,8	TTTATGTATAACCGA
LMO1*	orf19.5147	+	chr7	466	179	+	4,4	AGAAATTTTTAGCGA
MDR1	orf19.5604	-	chr6	743	-124	-	2,2	GAAATATTTAGCCGA
MDR1	orf19.5604	-	chr6	743	381	+	2,9	GGCAAGGAAAAACGG
MDR1*	orf19.5604	-	chr6	743	537	-	5,4	GGTAACTATTGGCGA
NDT80*	orf19.2119	+	chr2	854	1567	-	5,1	GGCAAGTTTAATCGA
RBT1*	orf19.1327	-	chr4	739	98	-	4,4	GGTAAGATTTACCGG
RIM101*	orf19.7247	-	chr1	490	664	-	5,1	AGCAAGTAGAGCCGA
RIM101	orf19.7247	-	chr1	490	679	+	2,1	TGAAAGAAGTGACGT
RIM101	orf19.7247	-	chr1	490	1079	+	2,3	ATAAAATGTAACCGA
RIM101	orf19.7247	-	chr1	490	1157	-	3,6	CGCAACTATAGCAGA
SAP4	orf19.5716	-	chr6	680	217	-	2,7	AGGAATCCTTGACGA
SAP4	orf19.5716	-	chr6	680	651	+	2,0	GGGAAATAGAGGCGC
SAP4*	orf19.5716	-	chr6	680	807	-	3,8	AGCAATTTTAAGAGA
SAP5	orf19.5585	+	chr6	543	1665	+	2,5	GGCAATAAATCTCGA
SAP5*	orf19.5585	+	chr6	543	1144	+	4,3	GGCAATTTTAAGAGA
SAP5*	orf19.5585	+	chr6	543	858	-	4,0	GTCAACTGGTACCGA
SAP5	orf19.5585	+	chr6	543	837	-	2,5	GACAGGTATATGCGA
SAP5*	orf19.5585	+	chr6	543	470	+	3,6	GGAAAGAAAAACGG
SAP6	orf19.5542	-	chr6	712	249	-	2,4	TGGAATCCTTGACGA
SAP6	orf19.5542	-	chr6	712	448	-	2,6	AGAAAGAAAAAACGG
SAP6*	orf19.5542	-	chr6	712	833	-	3,5	GGTAATTTTAAGAGA
SAP6	orf19.5542	-	chr6	712	1349	-	2,5	GGCAATAAATCTCGA
SFL1	orf19.454	-	chrR	1065	5727	+	3,0	GGAAGGAATAGACGC
SFL1	orf19.454	-	chrR	1065	6188	+	5,5	GGCAAGTTTTGGCGG
SFL1*	orf19.454	-	chrR	1065	6551	-	5,1	GGAAACTATTACCGG
SFL1	orf19.454	-	chrR	1065	6823	-	2,6	GTTATGATTAAACGA
SFL1*	orf19.454	-	chrR	1065	7489	+	3,3	GGCAGTTGTTAGCGT
SFL1	orf19.454	-	chrR	1065	8169	-	2,6	GATAATTTCTAACGA
SFL1	orf19.454	-	chrR	597	9428	+	4,1	GGTAAGAAATACCGA
SFL1	orf19.454	-	chrR	591	12499	+	2,3	GTAACAGAAGACGA
SFL1	orf19.454	-	chrR	591	12671	+	4,0	AACAAC TATTACCGG
SFL1	orf19.454	-	chrR	591	12772	-	2,1	AATAATAATAACCGT
SFL2*	orf19.3969	+	chr5	666	7759	+	3,2	ATCAAGAAAAAGCGA
SFL2*	orf19.3969	+	chr5	666	7235	+	3,6	GTAAC TATTCACGA
SFL2*	orf19.3969	+	chr5	1609	6157	+	3,7	AGTATCAATAGCCGA
SFL2	orf19.3969	+	chr5	1609	5779	+	2,4	TGAAACTAGTAGCTA

Gene Name	orf19 Name	Gene Str.	Chr.	Peak Height	Distance between Motif and Gene (bp)	Motif Str.	Motif Score	Motif Sequence
SFL2	orf19.3969	+	chr5	1609	5523	+	2,5	TCAAACAATAGACGA
SFL2*	orf19.3969	+	chr5	1609	5242	-	3,8	GGAAACTGAAAACGA
SFL2	orf19.3969	+	chr5	1609	4840	-	2,7	ATAAACAATAAGCGT
SFL2	orf19.3969	+	chr5	605	2833	+	2,1	AGTATTTTGAAACGA
SFL2*	orf19.3969	+	chr5	605	2733	+	4,0	AACAAGTAGAGCCGA
SFL2	orf19.3969	+	chr5	605	2614	+	4,1	AGCAAATATTGGCGA
SFL2	orf19.3969	+	chr5	605	2604	+	2,2	GGCGAAAGTTGGCGA
SFL2	orf19.3969	+	chr5	605	2594	+	2,2	GGCGAAAGTTGGCGA
SOD5	orf19.2060	-	chr2	711	520	-	2,0	GGCAATTGATTACGA
SOD5	orf19.2060	-	chr2	711	522	+	2,3	GTAATCAATTGCCGT
SOD5	orf19.2060	-	chr2	711	755	+	3,8	TTCAATTTTTACCGA
SOD5*	orf19.2060	-	chr2	711	888	+	4,9	GGCATCTTTTCCCGA
SOD5	orf19.2060	-	chr2	711	996	+	2,0	AAAAATAACAAACGA
SOD5	orf19.2060	-	chr2	711	1042	-	2,7	GTTAAGTTCTCACGA
SOD5*	orf19.2060	-	chr2	711	1512	+	4,9	GGAAAGTTGAAGCGA
SOD5	orf19.2060	-	chr2	711	1791	-	2,0	ACTAACTATTGCAGA
SOD5*	orf19.2060	-	chr2	711	1839	-	4,2	AGCAATTATTACCGA
SOD5	orf19.2060	-	chr2	711	1993	-	2,4	ATCAGCTAATAGCGA
STP2*	orf19.4961	+	chr1	639	1496	-	2,2	GGTAAAAATAAGAGA
STP2*	orf19.4961	+	chr1	639	915	+	2,9	TGCAAGACTTGCAGA
STP2	orf19.4961	+	chr1	639	419	+	2,6	GGAAAGAGGAGGAGA
TCC1*	orf19.6734	+	chr3	705	8002	+	3,2	AGTAACTTCAAACGG
TCC1	orf19.6734	+	chr3	705	7945	+	3,8	AGCAATAAAAAGCGA
TCC1*	orf19.6734	+	chr3	705	7019	+	2,1	ATCATCATCAACCGG
TCC1	orf19.6734	+	chr3	705	6624	-	4,6	GACAAGTTTTGACGA
TCC1*	orf19.6734	+	chr3	705	6528	-	2,1	GGATAGTTTTAAAGA
TCC1	orf19.6734	+	chr3	854	1486	-	2,6	AGCAATATTAATCGT
TCC1*	orf19.6734	+	chr3	854	1475	+	3,2	TGCTAGTATTAGCGG
TEC1	orf19.5908	-	chr3	628	1109	+	2,1	GTATACTAATACCGA
TEC1*	orf19.5908	-	chr3	628	1477	-	2,4	GGTAGTTATTAGAGA
TEC1	orf19.5908	-	chr3	1754	3461	+	2,1	GTCATTTGTTAACGG
TEC1*	orf19.5908	-	chr3	1754	3943	-	3,5	GACAAGATTACGCGC
TEC1*	orf19.5908	-	chr3	1754	4383	-	3,0	GTTAATTCTTAGCGA
TEC1	orf19.5908	-	chr3	1754	4874	+	2,8	GTCAAGAAAAAGCGT
TEC1*	orf19.5908	-	chr3	1754	5005	-	4,8	GGCAAGTATAAGCTA
TEC1	orf19.5908	-	chr3	1754	6065	-	2,9	TGCAAGACTAGGAGA
TEC1	orf19.5908	-	chr3	1754	6187	-	2,8	TGGAACAAATACCGA
TEC1	orf19.5908	-	chr3	1754	6247	-	2,2	GGATGTTATAACGA
TEC1*	orf19.5908	-	chr3	1754	6281	-	3,3	GTAAAGAATTACCGT
TEC1	orf19.5908	-	chr3	1754	6553	+	4,0	GGAAAGTATAACCAGA
UME6	orf19.1822	-	chr1	1108	6881	+	2,1	AACAAGTACAAAAGA
UME6	orf19.1822	-	chr1	1108	7204	+	3,6	GGAAATTATTAGAGA
UME6*	orf19.1822	-	chr1	1108	7283	-	3,7	GTAAAGTAAAACCGA
UME6	orf19.1822	-	chr1	1108	7577	-	2,7	AGAAATTATAGAAGA
UME6*	orf19.1822	-	chr1	1108	7675	+	2,9	TTCAGGAATTACCGA
UME6*	orf19.1822	-	chr1	1108	8177	+	2,9	AGCATGAATAGGAGA
UME6	orf19.1822	-	chr1	1108	8219	+	2,7	ATCAATTTTAGCCTA
UME6	orf19.1822	-	chr1	1108	8259	-	2,1	AAAAACATTTGCAGA
UME6	orf19.1822	-	chr1	1108	8285	-	2,1	TGCATGTGTTACGCT
UME6	orf19.1822	-	chr1	539	12233	-	3,1	AGTAAGAATAAGAGA
UME6	orf19.1822	-	chr1	539	12864	-	2,4	TGTATGTATAACAGA
UME6	orf19.1822	-	chr1	1082	14343	-	2,2	GGCAACAATTACATC

VII. Appendix

Gene Name	orf19 Name	Gene Str.	Chr.	Peak Height	Distance between Motif and Gene (bp)	Motif Str.	Motif Score	Motif Sequence
UME6	orf19.1822	-	chr1	1082	15221	+	2,8	GGCAGGAATAACGGA
UME6	orf19.1822	-	chr1	1082	15515	-	4,1	GGCAAGAATAAAAAGA
UME6*	orf19.1822	-	chr1	1082	15928	+	4,2	AACAACCTTTAAACGA
UME6	orf19.1822	-	chr1	1082	16066	+	3,3	ATCAAATTTAGCCGA
WOR1*	orf19.4884	+	chr1	647	6170	-	4,2	TGCAACTTGAAACGA
WOR1*	orf19.4884	+	chr1	647	5648	-	5,0	AGCAAGTATAGCCGT
WOR1	orf19.4884	+	chr1	647	5047	+	2,9	AGTAAGTGTGGAGA
WOR2*	orf19.5992	+	chr3	1407	9450	+	4,8	GTCAACATTAAGCGA
WOR2	orf19.5992	+	chr3	1878	4252	+	3,5	AGCAAGTTGTATCGA
WOR2	orf19.5992	+	chr3	1878	4116	-	2,1	ATAAAATTTAAACGA
WOR2	orf19.5992	+	chr3	1878	3548	-	2,8	GGTAACTTTGCACGA
WOR2	orf19.5992	+	chr3	1878	3504	-	2,5	TGCTACTGTAAACGA
WOR2	orf19.5992	+	chr3	1878	3170	-	3,8	GGCAAGAATGAACGA
WOR2	orf19.5992	+	chr3	1878	2813	-	3,3	AGTAAGTTGAACCGT
WOR2*	orf19.5992	+	chr3	1878	2755	-	4,3	GTCAATGTTGCCGA
WOR2	orf19.5992	+	chr3	1878	2610	+	2,2	AGCAAGTTTAATAGC
WOR2	orf19.5992	+	chr3	1878	2444	+	3,3	GGGAAATATTCCCGA
WOR2*	orf19.5992	+	chr3	1878	1834	+	5,0	GGCATCAATTACCGA
WOR2	orf19.5992	+	chr3	1878	1115	+	2,4	GGGAAGATGAGACGT

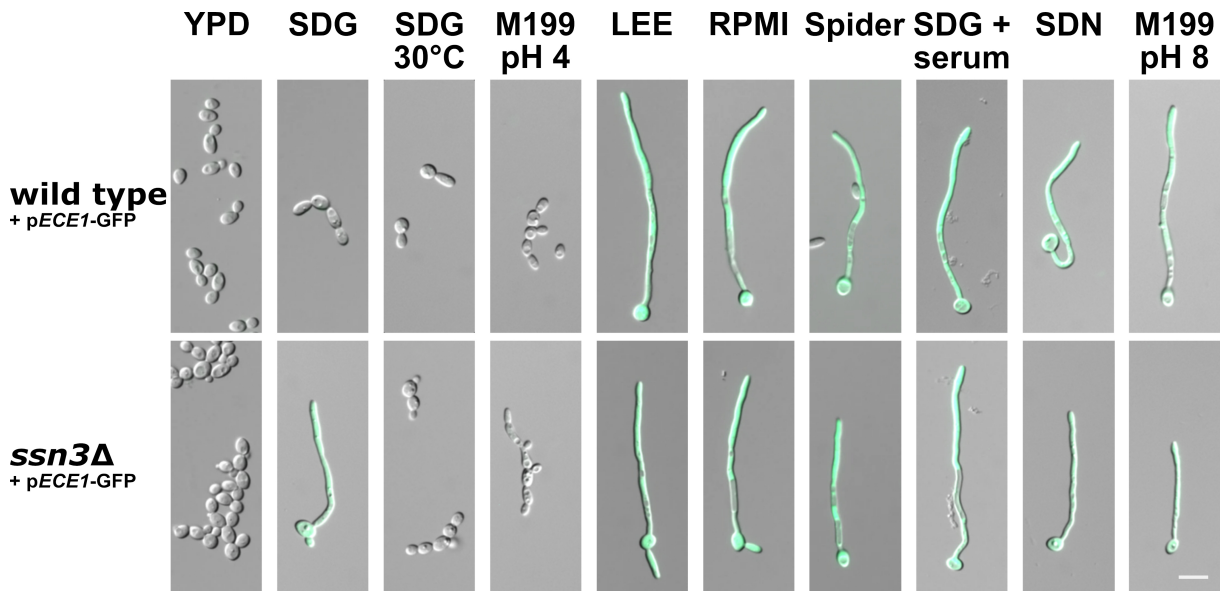


Fig. 32: Deletion of *SSN3* induces the expression of *ECE1* in SDG medium at 37°C. Wild type and the *ssn3Δ* mutant with *ECE1*-promotor driven GFP-reporter systems (*pECE1-GFP*) were grown for 4 h in indicated yeast and hyphal inducing media at 37°C if not noted otherwise. An overlay of the DIC and GFP channel is presented. Scale bar= 10 μm.

VIII. List of publications

Publications

Sophia Ruben, Enrico Garbe, Selene Mogavero, Daniela Albrecht-Eckardt, Daniela Hellwig, Antje Haeder, Thomas Krüger, Katrin Gerth, Ilse D. Jacobsen, Sascha Brunke, Kerstin Hünninger, Olaf Kniemeyer, Axel A. Brakhage, Slavena Vylkova, Joachim Morschhäuser, Bernhard Hube, Oliver Kurzai and Ronny Martin

Ahr1 and Tup1 contribute to the transcriptional control of virulence-associated genes in *Candida albicans*. (under review)

Presentations

S. Ruben, J. Morschhäuser, B. Hube, R. Martin, O. Kurzai (2019) The transcription factor Ahr1 is important for high-level expression of *ECE1* and Candidalysin secretion in *Candida albicans*. Status-workshop Eucaryotic Pathogens, Innsbruck, Austria (**travel grant**)

S. Ruben, J. Morschhäuser, B. Hube, R. Martin, O. Kurzai (2019) The central repressor Tup1 is required for high level expression of *ALS3* and *ECE1* in *Candida albicans*. Human Fungal Pathogens Advanced Lecture Course, La Colle-sur-Loup, France

S. Ruben, R. Martin, O. Kurzai (2019) Ahr1 and Mcm1 contribute to the regulation of *ECE1*, *ALS3* and other hyphae-specific genes in *Candida albicans*. 12th ILRS Symposium/Joint Meeting with Graduiertenkolleg KoInfekt, Lutherstadt Wittenberg, Germany

S. Ruben, R. Martin, O. Kurzai (2018) Ahr1 and Tup1 contribute to the regulation of the *ECE1* gene in *Candida albicans*. 11th ILRS Symposium, Jena, Germany (**presentation prize**)

S. Ruben, R. Martin, O. Kurzai (2018) The expression of *ECE1* in *Candida albicans* is regulated by the transcription factor Ahr1. 70th Annual Meeting of the DGHM e. V., Bochum, Germany

Posters

S. Ruben, R. Martin, O. Kurzai (2018) The transcription factor Ahr1 is required for high-level transcription of *ECE1*. 7th International Conference on Microbial Communication for Young Scientists, Jena, Germany

S. Ruben, R. Martin, O. Kurzai (2018) Ahr1 and Tup1 contribute to the regulation of the *ECE1* gene in *Candida albicans*. 14th ASM Conference on Candida and Candidiasis, Providence, RI, USA (**travel grant**)

S. Ruben, J. Morschhäuser, R. Martin, O. Kurzai (2017) Ahr1 contributes to control of *ALS3* and *ECE1* expression in *Candida albicans*. Human Fungal Pathogens Advanced Lecture Course 2017, La Colle-sur-Loup, France (**travel grant**)

S. Ruben, R. Martin, O. Kurzai (2017) The role of the transcription factor Ahr1 in *ECE1* expression in *Candida albicans*. 10th ILRS Symposium, Jena, Germany (**poster prize**)

S. Ruben, R. Martin, O. Kurzai (2017) The role of the transcription factor Ahr1 in *ECE1* expression in *Candida albicans*. 8th International Conference on Microbial Communication for Young Scientists, Jena, Germany

S. Ruben, R. Martin, O. Kurzai (2017) Transcription factor Ahr1 regulates expression of *ECE1* in *Candida albicans*. 5th Joint Conference of DGHM e. V. and VAAM, Würzburg, Germany

IX. Acknowledgment

First and foremost I would like to thank Prof. Dr. Oliver Kurzai for giving me the opportunity to write my PhD thesis at the Fungal Septomics Group and for providing the necessary resources. I also would like to thank him for always being available for questions and giving great and helpful advice.

Secondly, I would like to thank Prof. Dr. Bernhard Hube for his supervision and the evaluation of this thesis. I am thankful for his ideas and the possibility to cooperate with members of the MPM group and for conducting experiments in the MPM laboratory.

Furthermore I would like to thank Dr. Ronny Martin for his supervision from Jena and Würzburg and for his patience and scientific advice throughout the whole course of my PhD. Thank you also for all your knowledge and preliminary research I could base my thesis on.

Thanks to Dr. Selene Mogavero and Dr. Thomas Krüger for processing Candidalysin secreted from culture supernatants and the subsequent LC/MS-MS measurements. I also thank Dr. Stefanie Allert and Rita Müller for their help performing the invasion and LDH assays in the laboratories of the MPM. I am thankful to Prof. Dr. Joachim Morschhäuser for providing the *pAHR1-GAD* plasmid. I would like to thank Scott Filler for providing the Als3 antibody that was used in this thesis.

A special thank goes out to the whole groups of Fungal Septomics and Host Fungal Interfaces for creating a very pleasant, friendly and cooperative working atmosphere in the offices and in the laboratories. They made it easy for me to settle in Jena and instantly became my friends. I will always remember all the events (Firmenlauf, Day Outs, Birthday and Christmas gatherings, Cake and Sekt time, Zumba Party, After Work Partys, Retreats,...) we enjoyed together. I want to thank Kerstin for her good moods and helpfulness and letting me operate the BBQ. I also want to thank her and Bettina for their help with the stubborn LSM. I want to give thanks to Enrico. I can not thank him enough for all the help he provided for me in the laboratory. I also want to thank my other dear colleagues Jenny, Antje, Ines, Amelia, Daniel, Silke, Katrin, Christin, Franzi, Cindy and Susi for their support and their cheerfulness. I loved working alongside with you and I will really miss you and our lunch breaks. The same is true for my office mates and lovely colleagues Lysett, Alessandra and Wolfgang. They were always there for me when I needed help and a welcome distraction when things in the lab did not work out. Thank you, Alessandra for all those spontaneous dinners that we had together after tough days at work. Wolfgang, thanks for making me laugh countless times even though going through a difficult time yourself. Over the years I also grew very fond of Dolly and Alessandro. I will never forget the game and cooking nights, the afternoons at the pool or the Schleichersee, the tours to the Bad Köseener Weinfest and the Wartburg, Ala's perfect bachelorette party and the incredible Wedding in Pozzouli!

Last but not least, I thank my family and Felix for always supporting and believing in me. My mom and grandmother in particular for supporting me financially throughout the many years I studied. Thank you Felix for distracting me (when needed) and for keeping me focused (when needed), especially towards the end of my PhD.

X. Ehrenwörtliche Erklärung

Hiermit teile ich ehrenwörtlich mit, dass mir die geltende Promotionsordnung der Friedrich-Schiller-Universität Jena bekannt ist.

Ich habe die vorliegende Dissertation selbstständig verfasst. Alle verwendeten Hilfsmittel, Quellen und persönliche Mitteilungen habe ich angegeben.

Personen, welche mir bei der Auswahl und Auswertung der Materialien geholfen haben, habe ich benannt und in der Danksagung erwähnt.

Alle Personen, die bei der Erstellung des Manuskripts geholfen haben, sind in der Publikationsliste aufgeführt.

Die Hilfe eines Promotionsberaters wurde nicht in Anspruch genommen.

Für meine Arbeiten, die im Zusammenhang mit dem Inhalt der vorgelegten Dissertation stehen, habe ich weder unmittelbar noch mittelbar geldwerte Leistungen erhalten.

Die vorliegende Arbeit wurde bisher weder an der Friedrich-Schiller-Universität Jena noch an einer anderen Hochschule als Dissertation oder in Form einer Prüfungsarbeit für eine staatliche oder andere wissenschaftliche Prüfung eingereicht.

Jena, April 2020

Sophia Ruben